APPLICATION OF ZIMONT'S TURBULENT FLAME SPEED CLOSURE FOR COMBUSTION MODELING OF A SINGLE CYLINDER SPARK IGNITION ENGINE

J.K. Lishan Eranga

168039V

Thesis/Dissertation submitted in partial fulfilment of the requirements for the degree of Master of Science

Department of Mechanical Engineering

University of Moratuwa

Sri Lanka

November 2018

ACKNOWLEDGEMENT

Author would like to acknowledge the support and guidance given by Dr. R.A.C.P. Ranasinghe who is the supervisor of the present study, National Research council on behalf of funding the research and the staff of University of Moratuwa for providing technical support and laboratory facilities to make this study a success.

Declaration

I declare that this is my own work and does not incorporate without acknowledgement any material previously submitted in a degree or diploma in any other university or institute of higher learning and to the best of my knowledge and belief it does not contain any material previously published or written by any other except where the acknowledgement is made in the text.

Also, I hereby grant to University of Moratuwa the non-exclusive right to reproduce and distribute my thesis, in whole or in part in print, electronic or other medium. I retain the right to use this content in whole or part in future works (such as articles or books).

Signature: Date:

J.K.L. Eranga

Above candidate has carried out research for the Master of Engineering under my supervision.

Signature of the supervisor: Date:

Dr. R.A.C.P. Ranasinghe,

University of Moratuwa

ABSTRACT

Increasing need to get the maximum power out from fuels while maintaining less amount of toxic emissions has created the requirement of making an optimum IC engine. Numerical simulations play a vital part in determining those design and operating parameters which make that idea of an optimum engine a reality. In the present work applicability of two well-known turbulent flame speed models: Namely Peters and Zimont in premixed charge gasoline spark ignition (SI) engines were evaluated. Their ability to predict the characteristics of premixed turbulent combustion process of an SI engine in the RANS context was first assessed and based on those results Zimont model was used to evaluate the applicability of Smagorinsky-Lilly Large eddy simulation (LES) model in engine simulations. Several simulations were done to identify and implement required modifications to get correct solutions from the LES model.

Combustion of the Ricardo E6 single cylinder test engine was modeled with the above two turbulent flame speed closure models implemented to a commercial computational fluid dynamics (CFD) code. Full cycle simulations, covering all four strokes including the valve motion, spark discharge, flame kernel development and fully developed combustion, were performed using different engine operating conditions. Engine was fueled with gasoline. Obtained results were compared with experimental values obtained using the same operating conditions of the E6 engine to evaluate the prediction ability of the different models. Accordingly, In-cylinder pressure variation and the combustion heat release rate versus crank angle were compared with measured values. In general, predictions, of both models were found to be in reasonable agreement with experiment values, but significant discrepancies could be observed in certain operating conditions.

Keywords: CFD; LES; premixed; RANS; SI engine; turbulent combustion.

TABLE OF CONTENTS

Acknowledgement i

Declaration ii

Abstract iii

List of figures vi

List of tables vii

1 Introduction 1

1.1 In cylinder flow 2

1.2 Combustion process and geometrical configuration 3

1.3 Objectives of the present study 4

2 Turbulent premixed combustion 6

2.1 Interaction between flow and reactions 6

2.2 Regimes of Premixed turbulent combustion 7

3 Modelling procedure: RANS 11

3.1 Reynolds averaged Navier-Stokes equations (RANS) 11

3.2 Conservation equations for reacting flows 13

3.3 C equation model 14

3.4 Turbulent flame speed models 15

3.4.1 Zimont model 15

3.4.2 Peter's model 18

3.5 Laminar flame speed 19

3.6 Gas density model 20

3.7 Turbulence model 22

3.7.1 K-epsilon model 22

3.8 Early flame propagation speed model 22

3.8.1 Laminar 24

3.8.2 Turbulent curvature 24

3.8.3 Herweg and Maly 24
3.8.4 Transition radius 25
3.8.5 Selection of numerical schemes 26
4 Simulations procedure 27
4.1 Preparation of the geometry 27
4.2 Meshing process 28
4.3 Test cases and engine parameters 30
5 Results and discussion: RANS 36
5.1 Flow inside the chamber 36
5.2 Heat release and pressure at spark 44
5.2.1 Initial radius 44
5.2.2 Early flame propagation speed model 45
5.3 Fully developed combustion (RANS) 47
6 Modelling procedure: LES 54
6.1 Large eddy simulation (LES) 54
6.1.1 Pros and cons of LES 55
6.2 Turbulent premixed combustion in LES context 57
6.2.1 Smagorinsky-Lilly Model 59
6.2.2 Zimont in LES 61
7 Results and discussion: LES 62
8 Conclusion and recommendations 76
9 References 78

LIST OF FIGURES

Figure 1- Regimes of the premixed combustion proposed by Peters. 8
Figure 2- Engine geometry before decomposition.....27
Figure 3- Engine geometry after decomposition 28
Figure 4- Meshed engine geometry 29
Figure 5- Sectioned view of the mesh.....29
Figure 6 - Valve motion profiles.....31
Figure 7- Meshed engine geometry 33
Figure 8- Ricardo E6 engine specifications [82] 34
Figure 9- Velocity contour plot with velocity vectors.....37
Figure 10- Velocity contour plot with velocity vectors at Z = 4.5 cm.....37
Figure 11- Velocity contour plot with velocity vectors at Z = 8.0 cm.....38
Figure 12- Velocity contour plot with velocity vectors at Z = 11.5 cm.....38
Figure 13- Velocity vectors at Z = 8.0 cm at crank angle.....39
Figure 14 - Swirling flow near the spark point.....40
Figure 15- velocity contours on cross sectional plane through the intake valve 40
Figure 16- Temperature variation near the spark point before ignition.....41
Figure 17- Velocity variation near the spark point before ignition 41
Figure 18- Turbulent kinetic energy variation near the spark point before ignition....42
Figure 19- Temperature variation near the spark point after ignition.....42
Figure 20- Velocity variation near the spark point after ignition 43
Figure 21- Turbulent kinetic energy variation.....43
Figure 22- Change in heat release rate vs. crank angle.....44
Figure 23- Heat release rate vs initial radius 46
Figure 24- Case 1 heat release rate comparison.....48
Figure 25- Case 2 heat release rate comparison.....48
Figure 26- Case 3 heat release rate comparison.....49
Figure 27- Case 4 heat release rate comparison.....49
Figure 28- Case 1 In cylinder pressure vs. crank angle comparison 50
Figure 29- Case2 In cylinder pressure vs. crank angle comparison 50
Figure 30- Case 3 In cylinder pressure vs. crank angle comparison 51
Figure 31- Case 4 In cylinder pressure vs. crank angle comparison 51
Figure 32- Comparison of velocity vectors from RANS and LES simulations.....56

Figure 33- Evolution of the flow in the cylinder 63
Figure 34- Flow in the cylinder during intake stroke 64
Figure 35 - Evolution of the flow in the cylinder during intake stroke 65
Figure 36- Flow structures inside the cylinder during compression stroke 66
Figure 37 - Variation of mixture fraction across the intake valve plane 67
Figure 38 – Variation of magnitude of velocity across the intake valve plane.....68
Figure 39– Variation of magnitude of velocity across a plane located closer to 69
Figure 40 - Variation of the sub grid scale flame radius with crank angle. 70
Figure 41 – Variation of heat release rate for 5 consecutive engine cycles.....74
Figure 42 - Variation of in cylinder pressure for 5 consecutive engine cycles.....75

LIST OF TABLES

Table 1- Values of coefficients 18
Table 2- Input parameters for spark model.....31
Table 3- Ricardo e6 engine specifications 32
Table 4- 4 Cases and their details 33

1 INTRODUCTION

Performance of Internal Combustion engines heavily depends on the flow and combustion characteristics inside the engine and their interactions with each other. Therefore, studying the flow and combustion in IC engines and developing techniques to simulate those processes have been a major research interest. Large number of studies focused on different aspects can be found on this topic [1, 2, 3] and yet there is more room for improvements due to the complex nature of the process [4] and the vast number of process controlling parameters [5]. The complexity comes with the physical and chemical processes involved in a reacting flow field. Some of the phenomena involving with a reacting flow have not even been fully understood [6, 7, 8]. Therefore, studying the behavior of such phenomena is extremely important [9].

Another factor to consider is the performance of the vehicles. It heavily depends on the performance of the engine [10], which is governed by the characteristics of combustion. Obtaining greater power and efficiency while reducing the emissions have become a must. Therefore, development of such engines requires thorough analysis of the process and underling physics. There are many traditional ways of optimizing an engine. They will require repetitive hardware modifications, excessive testing and exhaustive analysis of experimental data [11]. These processes are extremely slow, much costly and hardly yield the optimum conditions. Gathering data from those experiments where rapid changes of the controlling parameters occur and maintaining operating conditions uniform are nearly impossible [12]. Hence more successful methods must be found.

In recent decades, CFD techniques are being used widely as a supporting tool to predict the behavior of such flows. This has been encouraged by the substantial development in numerical methods and computing technology and resources. CFD analysis gives the access to useful results and data which cannot be accessed from physical experiments [13]. This gives the opportunity to understand the relationships between each parameter and provides much of a flexibility over design optimization process. However, it is very important to understand that the actual process happening inside a combustion chamber is very complex and highly turbulent in nature so that various number of simplifications and assumptions must be made to obtain results within acceptable time and cost.

This creates a requirement to develop comprehensive CFD model or models to capture all the flow and combustion related processes in detail, with great accuracy. Hence improvement of CFD modelling techniques requires very extensive research and fast computational techniques.

1.1 In cylinder flow

Flow inside an internal combustion (IC) engine is complex in nature with a swirling and tumbling of flow inside the cylinder occurring due to the geometry and inlet conditions of both intake and exhaust ports. Combustion characteristics are greatly influenced by the in-cylinder flow which is inherently turbulent as mentioned above, thus it has become an important aspect in CFD to resolve those flow properties to get an accurate detail of the flame. The reacting gases present inside the chamber will be mixed with the turbulent flow and this interaction between flame and the turbulent flow is complex and unsteady in nature [14]. That complexity comes mainly with the different behavior of the flame to the different levels of turbulence. There are merits and demerits of turbulence with respect to the propagation of flames. Low and moderate levels of turbulence affect combustion by wrinkling the flame front, whereby its surface area is increased and hence increased mixing of high temperature burned products with the fresh gas causing an acceleration of the combustion reactions. Premixed combustion is benefited with this. However high levels of turbulence will exert lot of strain on flame front thus it will be torn apart [15]. This will cause the flame to extinguish. Hence predicting the level of turbulence precisely inside the chamber and accurately capturing the interaction between flow and turbulence are some of the major targets in CFD.

Turbulence of the in-cylinder flow is governed by the rapid fluctuation of velocity in all three directions. The length and time scales which are involved in this process varies from very large values to very small values like from bore diameter to micrometers and from milliseconds to microseconds [16]. Perfect simulation will resolve for every size of eddies regardless of their length and time scales. Nowadays, even though equations acting as the foundation of thermo-fluid processes are well known, predicting the exact amount of turbulence in the configurations of an engine is still not achieved. Navier-Stokes equations [3] accurately describe the gas motion. Taking this into consideration, the safest approach would be solving the Navier-Stokes equations without any modelling, hence any numerical discretization.

This method, Direct Numerical Simulation (DNS), is considered as the least complicated and highly accurate. Still, even though with the present technological capabilities, a DNS of a realistic IC engine, would need several years of computing. Considering this, the above described method has been applied only for simple test cases or one-dimensional simulations. But, on the other hand, there are other procedures, Large Eddy Simulation (LES) and Reynolds Averaged Navier-Stokes equations (RANS), which partially resolve the turbulent spectrum or entirely model it by applying techniques of ensemble averaging or Favre averaging. In this work, those two approaches will be discussed in coming chapters and their applicability in IC engine context will be assessed.

1.2 Combustion process and geometrical configuration

Combustion inside IC engines can be described as a set of chemical reactions which are controlled by the in-cylinder turbulent flow. To simulate the combustion, it is a must to harmonize the governing fluid flow equations with a reaction rate model and a chemical reaction mechanism. The task of the reaction mechanism is to prescribe how fuel and oxidant react, what products are produced and the mutual relationship between them. Determining how fast the reactions are taking place is the responsibility of the reaction rate model. Since even the simplest of hydrocarbons undergo at least about 40 elementary reactions [17] during combustion, many models can be found with different complexities and accuracies [18]. Most complex models will use hundreds of different reaction steps and species to describe the reaction mechanism, while the simplest ones will represent the whole process in one reaction. It will transform the reactants into the burnt products in one step. The reactions rate can be modeled using either Arrhenius type expression [19], assuming the process is chemically driven or else using Phenomenological models. These Phenomenological models may be derived considering the physical aspects and experimental observations of flame propagation in a turbulent flow field. Accuracy of these types of models is subjective to the application. However, in general, phenomenological models are found to produce better predictions in premixed SI engine simulations [20].

Another important factor for determining the in-cylinder flow and combustion characteristics is the geometrical configuration particularly the intake port, valve assembly, vale lift profile and the combustion chamber. Even a small change to this may cause a large difference to the macro flow structure, swirl and tumble motion and combustion characteristics [21]. Micro flow structure is governed by the discharge gap at the valve throat (Turbulent intensity, Kolmogorov scale and integral scale). Those factors control the flame penetration rate [22]. Also, the residual mass fraction (fraction of mass of burnt gas remains inside the engine after exhaust stroke) is controlled by the wave action taking place at valve overlap. Therefore, it is evident that not only the combustion process, but the flow at valves and ports influence the characteristics of the in-cylinder flow.

1.3 Objectives of the present study

Premixed combustion modelling for RANS and LES is a considerable challenge. RANS and LES mesh sizes are usually bigger compared to the flame front reaction zone thickness. That is why, solving the flame front on grids like that is hard using traditional methods. Effects of sub-grid wrinkling occur due to the interaction between turbulent flow and flame need to be calculated accurately as far as resolved parameters are concerned. Majority of today LES combustion models are like RANS combustion models. At this phase, it is not clear whether these models have the ability to get the full use of the resolved flow field, even though providing a good starting point. Thus, strongest requisite in terms of engine simulation at present, is the proper re-evaluation of the actual methodology and enabling the necessary allowances to be applied into the LES models to get accurate results.

To overcome the issues mentioned above, Zimont with the help of others has developed a model [23, 24] taking turbulent flame speed closure as the basis. In this model, a single transport equation is solved for the progress variable and its source term is closed with turbulent flame speed (TFS). In this model, TFS, which is a parameter with a significant importance in premixed turbulent combustion, is calculated using scaling logics and theoretical considerations taking local turbulent parameters (wrinkling, thickening, straining of flame) and physio chemical properties into consideration. This is a very efficient approach for TFS closure since it only needs one additional governing equation other than in a non-reacting case and that equation

requires only less computational resources since it does not contain source terms for chemical reactions or integration over parametric PDFs. Also, the model itself is robust and efficient in a computational perspective making it a best match for the present study. Keeping all these factors in mind, following objectives for present work were outlined.

- To investigate the applicability of Zimont RANS formulation for turbulent flame speed to resolve the flow and combustion characteristics in spark ignited gasoline engines.
- Extension of the Zimont RANS turbulent flame speed model for LES.
- Investigating the applicability of Zimont LES formulation against experimental data.

2 TURBULENT PREMIXED COMBUSTION

2.1 Interaction between flow and reactions

Combustion inside IC engines can be described as a set of chemical reactions which are controlled by the in-cylinder turbulent flow. Chemical heat release and species production due to combustion are associated with governing equations by introducing source terms. These source terms can be found in both energy and species equations and determining them remains a huge challenge.

A significant role in the engine simulation is being played by the combustion model. RANS based reacting flow modelling has undergone notable progress in last decades. Regarding to flame front description and reaction rate estimation, there are different points of view. For instance, the Standard Arrhenius type models assume that the combustion process is completely chemically driven while the Eddy-Break-Up (EBU) type models assume that the combustion process is turbulence driven [25]. Instead, the models that are based on flamelet assumptions take into consideration chemical and turbulence effects altogether [11].

Anyways, especially in dealing with new designs or significantly different operating conditions, the common weaknesses of the most of models is that they should be tuned empirically to obtain satisfactory quantitative predictions. There are two main factors that contribute to this; there should be a consequence associated with the large number of simplifying modelling assumptions or due to the poor understanding of the actual phenomenon.

Taking as example, the flame surface density (FSD) model that is proposed by Bray-Moss-Libby (BML) [26] involves four model constants, meanwhile the balance equation proposed by Cant [27] for FSD contains three model constants [28]. If these constants were tuned in a flow simulation that is often required to obtain good predictions, it will be a time-consuming task. Another weakness of these models is the associated wall flame acceleration (i.e. predicting extremely high unphysical reaction rate near solid boundaries). The consequences EBU model issues have been reported in [29, 29] while those of BML model, in [30]. Because of the wall flame acceleration, these models are barely useful without modifications in wall bounded reacting flow modelling. Both models do assume isotropic homogeneous turbulence. Their application in the core region of the flame provides satisfactory results.

Meanwhile, if applied near solid boundaries, the homogeneous assumption does not stand because of the presence of a sharp gradient of turbulence flow properties. So, to achieve accurate results, it is necessary to accept sufficient allowances for special inhomogeneity in turbulence in the different regions of the problem domain. As a result, different elements of RANS based combustion models are yet to be researched. An important note is that, the combustion modelling concepts used in immerging LES modelling are themselves based on the ideas developed in RANS. Therefore, both the LES and RANS can be considered equally benefitted if further evaluation and improvements of RANS based combustion models is done.

2.2 Regimes of Premixed turbulent combustion

As described previously, interaction between turbulent flow and combustion control the behavior of the propagation of the flame and its characteristics. Level of turbulence and chemical kinetics work as limiting factors for the turbulence models in application. Hence selecting suitable turbulence and combustion models should be done by considering the application. To distinguish the combustion process depending on the intensity of interaction between turbulent flow and chemistry, the concept of combustion regimes has been introduced.

Eddies in a turbulent flow can have sizes from micrometers to meters. To represent an eddy of size radius, a time scale can be defined in following manner [31].

$$t(r) = \frac{l(r)}{u'(r)} \tag{1}$$

Here l and u' are the characteristics length and velocity scales of the eddy of size r and are functions of r [25]. To compare the relative magnitudes, chemical time scale is being defined using flame properties in following manner.

$$t_c = \frac{\delta_l}{u_l^0} \tag{2}$$

This scale depends on the laminar flame thickness δ_l and unstrained laminar burning velocity u_l^0 Ratio between these two scales is called as Damköhler number Da and is one of the basis of distinguishing combustion regimes.

$$Da(r) = \frac{t(r)}{t_c} \tag{3}$$

Yet, it is not clearly understood the most significant turbulence scale which controls the structure of the flame. Each range of turbulent scales affect the structure and propagation of the flame in different manner. At the Kolmogorov scale, reciprocal of the Damköhler number is called as Karlovitz number which depends on Kolmogorov length, time and velocity scales.

These scales are evaluated using kinematic viscosity ν and turbulent kinetic energy dissipation rate ϵ,

$$t_n = \left(\frac{\nu}{\epsilon}\right)^{0.5} , \qquad u_n = (\nu\,\epsilon)^{0.25} , \quad n = \left(\frac{\nu^3}{\epsilon}\right)^{0.25}$$

There are several combustion regime diagrams developed by various researchers [25]. Barrera [32], Bray [33], Borghi [34], Williams [35], Poinsot [19] and Peters [36] have come up with good diagrams and the regime diagram proposed by Peters is given below.

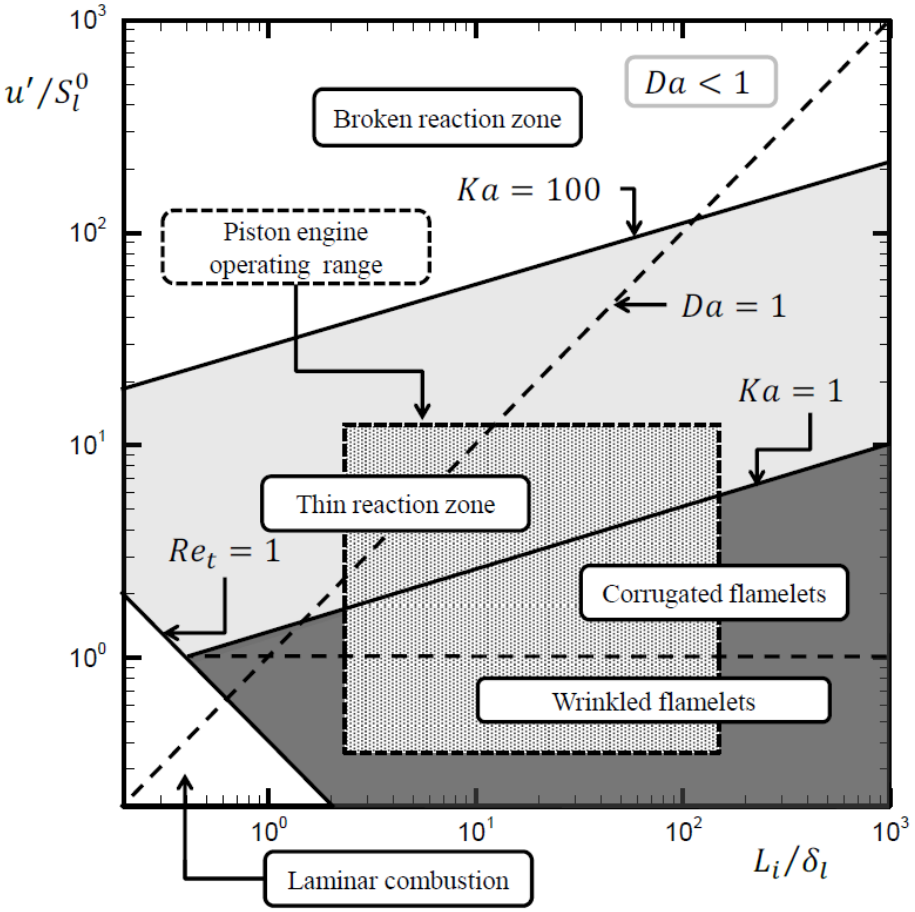

Figure 1- Regimes of the premixed combustion proposed by Peters. Squared region indicates the values where piston engine operates [37]

These boundaries of the regimes are derived based on the order of magnitude assumptions rather than implicit physical foundation. Also, isotropic homogeneous turbulence in all directions is assumed though it is highly unphysical.

In the diagram, there are four main regimes present while one regime is divided into two sub regimes. Ka =1, Ka = 100 and Re_t = 1 provides boundaries to these regimes and a dashed line for Da = 1 and the dashed square region where piston engines operate are given for the ease of explanation.

Laminar combustion regime: is located below $Re_t = 1$. In this regime, turbulence is not strong enough to interact with the flame, thus laminar flames can be observed.

Modelling of combustion in this regime is quite straightforward since no turbulence is involved. Laminar flame speed will govern the rate of heat release and formation of products.

When the Damköhler number is greater than 1, it implies that the chemical time scale is much smaller than the turbulent time scale. This means that the turbulent eddies cannot penetrate the inner flame structure causing a reduction of flame speed. Yet the turbulence is strong enough to distort and wrinkle the flame surface. Since the flame speed is not influenced by the turbulence, it can be said that the wrinkled flame front will propagate with laminar flame speed and rate of reaction directly proportionate with the multiplication of overall flame surface area and the laminar burning velocity. This regime is associated with the well-known fast chemistry assumptions which has been utilized in many combustion models like the Peter's model, since most of the combustion devices including piston engines is operating in this regime. On the other hand, a large chemical time scale ($Da \ll 1$) causes the reactants and burnt products to mix well with each other by turbulent eddies, thus mixing becomes the defining factor. This region is called the perfectly stirred reactor. Reaction rates for this region is evaluated using simplified Arrhenius type expressions [25].

Karlovitz number is the relative magnitude between the smallest turbulent time scale and chemical time scale. The value of Karlovitz number directly can be used as a guideline to determine the suitable type of combustion model for a particular case. For $Ka < 1$, chemical time scale is smaller compared with any time scales of turbulence. Thus, flame front is a thin laminar like structure having a flame thickness smaller than the Kolmogorov scale. Turbulence can make it distorted and wrinkled but cannot

influence the interior flame structure. Ratio between unstrained laminar flame speed and turbulent intensity (u'/S_l^0) is used to further divide this region [38]. Lesser u' compared to S_l^0 means that turbulence does not have the ability to distort the flame front until it crosses itself creating pockets of burnt and fresh gases. Thus, flame front will look like a continuous yet wrinkled surface, hence the name wrinkled-flamelet regime is given. Inversely, higher u' makes gas pockets by strong turbulent motion rising the name of corrugated flamelet regime. Altogether these regimes lie in the flamelet region where Norbert Peters has done a vast amount of studies. Peters [36] was able to derive an expression to find the smallest scale of the turbulent eddy which can cause the flame front to wrinkle and eventually that scale was named as Gibson scale L_G. This scale is given by following equation.

$$L_G = \frac{{S_l^0}^3}{\epsilon} \tag{4}$$

Since L_G depends on $\frac{u'^3}{L_i}$, above equation can be in the following way. C_G is a constant.

$$L_G = C_G L_i \left(\frac{S_l^0}{u'}\right)^3 \tag{5}$$

Thicken wrinkled flame regime or thin reaction zone is characterized by limits *Ka* > 1 and *Da* > 1 which implies that chemical time scale is smaller than the turbulent time scale. Thus, flame brush thickness is larger than the smallest scale of turbulence which lets the eddies of that scale to penetrate the flame brush and thicken it.

So, from the explanation above, it is obvious that the level of turbulence affects the interaction characteristics between flame and flow differently, causing it is extremely difficult to generate a global combustion model. Therefore, most models were developed are only applicable for one or few regimes. Hence assessment of combustion models for different applications is vital.

3 MODELLING PROCEDURE: RANS

A successful IC engine simulation should always have the models and sub models to calculate the physical properties of important processes like combustion, fuel spray, turbulence and spark ignition. In this chapter, a detailed description of the utilized models and their governing equations are presented. Also, for the LES formulation, modifications applied to the models are also presented. This is vital since the incorporated complex physical processes can only be predicted correctly, by using suitable formulations.

3.1 Reynolds averaged Navier-Stokes equations (RANS)

The industrial standardized method for CFD simulations over the last decades was RANS. This technique is properly formulated.These procedures are the basis on which most of the engine simulation studies are developed nowadays.

Most of the commercial CFD codes continue being developed mainly for RANS modelling. The reason for RANS methods to be so popular, is mainly in the lower spatial and temporal resolution requirements they have. Using relatively high computing time and rough meshes, can generate sufficiently accurate and detailed solutions for complex industrial flow problems maintaining acceptable accuracy levels. Taking into consideration the amount of use, RANS literature is properly documented and studies upon it are at disposal for possible reference. Still, research remains vital, taking into consideration that this method is not perfect due to the simplifying assumptions associated with the models. RANS method needs studies to exploit its full potential and correct the identified issues which are mentioned in the following section.

A given flow property, in RANS, is decomposed into a fluctuating component and a time averaged mean value. If these components are substituted in the unsteady Navier-Stokes equation, it will result a number of fluctuating unknown terms. These terms are known as Reynolds stresses. The main challenge of RANS modelling is finding an approximation for these Reynolds stresses. In order to close the Reynolds stress terms, numerous strategies have been proposed. These models have had considerable impact in the progress in CFD and similar fields, as per a wide range of evidences. Anyways, being problem dependent processes, their applicability is limited. For instance, a given model can excel in aerodynamic flows but will fail to produce a given degree of accuracy in reacting systems bounded by walls. Even though these techniques are not

considered as capable for predicting unstable phenomena in detail, taking into consideration the averaging and modelling involved [39]. Cycle-to-cycle variations in engines cannot be accessible from an ensemble averaged formulation.

Another RANS modelling drawback is its considerable use of turbulence model parameters for other calculation like combustion, species mixing etc. A significant role in the engine simulation is played by the combustion model. RANS based reacting flow modelling has undergone notable progress in the last decades. Regard to flame front description and reaction rate estimation there are different points of views. For instance, the Standard Arrhenius type models assume that the combustion process is completely chemically driven while the Eddy-Break-Up (EBU) type models assume that the combustion process is turbulence driven [25]. Furthermore, the models that are based on flamelet assumptions take both chemical and turbulence effects into consideration together.

Nevertheless, especially when working with new designs or significantly different operating conditions [29], the common weaknesses of most of the actual models is that they should tune empirically, one or more model coefficients or other input parameters referring to experimental data must be changed repetitively to obtain satisfactory quantitative predictions. There are two main factors that contribute to this; the large number of simplifying modelling assumptions associated with and the poor understanding of the actual phenomenon.

Taking as an example, the flame surface density (FSD) model that is proposed by Bray-Moss-Libby (BML) [26], involves four model constants, meanwhile the balance equation proposed by Bray & Cant [27] for FSD contains three model constants [28]. Tuning these constants in a simulation to obtain good predictions, is a time-consuming task.

Another weakness of these models is the associated wall flame acceleration (i.e. predicting extremely high unphysical reaction rate near solid boundaries). The consequences for EBU model have been reported in [29] while those of BML model, in [30]. Because of the wall flame acceleration issue, these models are barely useful without modifications in wall bounded reacting flow modelling. Both models do assume isotropic homogeneous turbulence. Their application in the core region of the flame provides satisfactory results. Meanwhile, if applied near solid boundaries, the

homogeneous assumption does not stand because of the presence of a sharp gradient of turbulence flow properties. In order to achieve accurate results, it is necessary to accept sufficient allowances for special inhomogeneity in turbulence in the different regions of the problem domain.

As a result, different elements of RANS based combustion models are yet to be researched. An important note is that, the combustion modelling concepts used in immerging LES modelling are themselves based on the ideas developed in RANS. Therefore, both the LES and RANS can be considered equally benefitted if further evaluation and improvements of RANS based flow models is done.

3.2 Conservation equations for reacting flows

Any kind of a flow problem is solved with governing equations. These equations are derived from conservation laws namely mass, momentum and energy. Combustion process is a reacting non-isothermal gas mixture composed with multiple species (hydrocarbons, oxygen, water, carbon dioxide). Those species should be tracked individually to obtain a realistic and accurate solution. Since this problem domain is a mixture of gases, transport coefficients (heat diffusivity, species diffusion, viscosity) require specific attention. Hence these equations will be different from standard Navier-Stokes equations.

Following is the equation for the conservation of mass of the system. It is same as the conservation of mass equation for a non-reacting system because mass cannot be created or destroyed.

$$\frac{\partial p}{\partial t} + \nabla \cdot [pu] = 0 \tag{6}$$

When a single species is considered, transformation from one species to another can cause a difference. For a species k, we can write down the conservation of mass equation in following manner [29],

$$\frac{\partial\, \rho Y_k}{\partial t} + \frac{\partial\left(\rho\left(u_i + V_{k,i}\right)Y_k\right)}{\partial x_i} = \omega_k \tag{7}$$

where chemical reaction source ω_k, are obtained using chemical kinetics as functions of species concentrations, temperature and pressure where Y_k is the mass fraction of species k. Here, the mass fraction of the species and its diffusion velocity V_k should also

be considered. Remaining two equations are momentum and energy. They are as follows [18].

Momentum:

$$\frac{\partial\, \rho u}{\partial t} + \nabla.(\rho u u) = -\nabla p + \nabla.\tau + \rho g \tag{8}$$

Energy:

$$\frac{\partial\, \rho E}{\partial t} + \nabla.(\rho u E) = -\nabla.q + \nabla.(\tau.u) + \omega_T \tag{9}$$

Where τ is the viscous stress tensor and E is total non-chemical internal energy, the combustion heat release is given by ω_T. In turbulent premixed combustion, major challenge is to model ω_k and ω_T which present in species mass conservation and energy equations respectively. As described in Chapter 2, there are various methods of varying complexities to tackle these terms. For the present work "C" equation approach (see section 3.3) was used where a transport equation is solved to track the flame front.

3.3 C equation model

There are several well-established ways to model the combustion process of an engine and many of them require very small spatial and temporal resolutions since resolving detailed chemical kinetics and molecular diffusion processes is needed. But such resolutions will emerge the need of large computational resources and will take long time to produce results. Also incorporating detailed chemistry will increase the accuracy of the outcome. There is a significant progress in that regard over the recent years [40], and now there is the ability to calculate theoretical burning velocities of alkanes up to octane [41].

Scientists have developed models to predict only the combustion by solving a single transport equation for a progress variable incorporating a one-step global reaction. This method gives reasonably well results while minimizing the requirement of computational power. Also, it basically tracks the flame front.

Tracking of the flame is done by solving a governing equation for a so-called scalar "*C*'. Normally the value of *C* is a normalized quantity which changes with combustion. Temperature, mixture fraction or a combustion product can be used in that sense and in Ansys fluent, normalized sum of the product species mass fractions inside the chamber has been used. Normalization is done based on burnt and unburnt temperatures which

have been provided for the common fuels being used. Here, the value of scalar variable *C* changes from 0 to 1 as the mixture get burnt where 1 represents the burnt regions. Flame brush contains the intermediate and it travels with a modeled turbulent flame speed upstream converting fresh mixture into burnt products. Governing equations for *C* is given below.

$$\frac{\partial \rho c}{\partial t} + \nabla . \rho v c = \nabla . \left(\frac{\mu_t}{Sc_t} \nabla c \right) + \rho S_c \tag{10}$$

where

c = reaction progress variable S_c = reaction progress source term

Sc_t = turbulent Schmidt number μ_t = turbulent viscosity

The governing equation of *C* evaluates the progress of the flame front in both space and time. Closing the reaction progress source term is needed to fully resolve this equation. Here the reaction progress source term calculation is done by utilizing a turbulent flame speed closure. In the present work, the combustion models of interest, namely Peters and Zimont employ same approach.

3.4 Turbulent flame speed models

3.4.1 Zimont model

The turbulent premixed combustion model, based on work by Zimont and Lipatnikov [42, 23, 24, 43] solves a transport equation for the reaction progress variable in order to track the flame front. This approach is very much efficient since it only needs one additional transport equation other than in a non-reacting flow problem [42]. The closure of this equation is based on the turbulent flame speed which is a vital parameter in combustion process. Governing equation for the progress variable is given in section 3.3. Formation of the flame front and its extinction is modeled by this S_c term where turbulent flame speed is used as the closure method. In the model, they have developed the formulation taking following physical mechanisms into consideration.

- The increment of thickness of a steady propagating flame according to the law of turbulent diffusion.
- Widening of the local reaction region due to eddies which are smaller than the flame thickness and distortion of the flame due to the large-scale eddies.

- Combustion failure due to the hydrodynamic deformations.
- Preferential diffusion [42].

Modeled equation is as follows.

$$\rho S_c = \rho_u S_t |(\nabla c)| \tag{11}$$

Here the term ρS_c represents the mean reaction rate while ρ_u is the density of unburnt mixture and S_t is turbulent flame speed. The key to the premixed combustion model is the prediction of turbulent flame speed. There are several factors which affect the value of S_t. They are,

- Laminar flame speed
- Flame front wrinkling and stretching due to the presence of turbulent eddies of various scales.
- Flame quenching near the walls.

Utilizing all these factors to develop the formulation makes the model sensitive to both turbulence parameters and properties of combustible mixture. Derivation of the formulation has been thoroughly described in [44] [23] [45]. Small scale eddies intensify the molecular exchange of heat and mass inside the reaction region thus controlling its thickness and propagation speed. These thickened flamelet are wrinkled and distorted by the larger eddies and as the thickness of the reaction zone increases, more and more eddies are immersed into the zone [44] [34] [31]. Total area of the flamelet depends on the integral characteristics of the full turbulence spectrum and the parameters of thickened flamelet. This mechanism is only valid if there is an equilibrium between heat conduction, convection and reaction processes such that it will limit the expansion of the reaction zone. Taking all these factors into consideration, following equation for turbulent flame speed has proposed.

$$S_t = A u'^{\frac{3}{4}} S_l^{\frac{1}{2}} \alpha^{-\frac{1}{4}} l_t^{\frac{1}{4}} \tag{12}$$

Where

A = model constant

u' = RMS velocity (m/s)

S_l = laminar flame speed (m/s)

α = molecular heat transfer coefficient of unburnt mixture

l_t = turbulence length scale (m)

Values for α can be found either from standard references or can be calculated using computer programs. Finding laminar flame speed U_l is done using Metghalchi and Keck model which has been described in section 3.5. Turbulence length scale l_t and u' will be determined from the turbulence model. The model constant A is taken as 0.52 in RANS context and that value has been verified for a wide range of fuels and operating conditions with good accuracy using data base of stirred bomb experiments [42] [46]. In that way, complete closure of the source term of the equation of progress variable has been achieved. Since this model contains only one modelling constant (A), empirical tuning is not much needed, making this model more ideal to use in different flow and combustion problems.

Literature and validation against experimental data related to Zimont model is somewhat limited when compared with the level set approach proposed by Peter's model. In the original paper [23] the model is verified using experimental data obtained using a gas turbine burner stand. Model predictions were well matched with experimental values of temperature and velocity distributions in that case though there were significant differences of the central recirculation zone size and location.

As explained in authors next paper [24], a model was developed to predict the characteristics of the intermediate steady propagation (ISP) flames which are usually found in industrial premixed combustion chambers operating with high levels of turbulent intensity. In 2001 [43], model was validated against the experimental results for the intermediate steady propagation regime. Here the inherent feature of such flames is their growing thickness of the flame brush which happens according to the dispersion law of turbulence. Numerical simulation results of a 2-D planner channel with parameters which replicates the actual combustors available in industrial applications have been compared. For that standard experimental data obtained from a high speed turbulent premixed flame has been used [47]. Methane air mixture is utilized for the case. Also, validating the model using spherical bomb combustion in the presence of artificially introduced turbulence, can be found in the papers [48] [46] [49]. Industrial related application of the model and an initial comparison with Moreau experiments is available in papers [23] [50]respectively.

3.4.2 Peter's model

Another advanced model for turbulent premixed combustion was proposed by N. Peter. This model [38] utilize the form proposed by Ewald [51].

$$S_t = S_l(1 + K_t)L_G = C_G L_i \left(\frac{S_l^0}{u'}\right)^3 \tag{13}$$

Where

$$K_t = -A\frac{l}{l_f} + \sqrt{\left(A\frac{l}{l_f}\right)^2 + B\frac{u'l}{s_l l_f}} \tag{14}$$

$$u' = \sqrt{\frac{2}{3}k}\,, \qquad A = \frac{a_4 b_3^2}{2b_1}, \qquad B = a_4 b_3^2$$

In this equation, modelling the effects of turbulence which determines the behavior of the flame and its propagation has been done using the integral turbulence length scale *l* and the laminar flame thickness, l_F.

$$l = \frac{a_1 u'^3}{\epsilon} \tag{15}$$

$$l_F = \frac{D}{S_l} = \frac{\lambda}{c_p \rho_u S_l} \tag{16}$$

The diffusion coefficient for the flame is computed from molecular properties of the unburnt mixture indicated by the subscript u. The default values for the model constants are listed below.

Table 1- Values of coefficients

Coefficient	Default Value
a_1	0.37
a_4	0.78
b_1	2.0
b_3	1.0

The diffusion coefficient for the flame is computed from molecular properties of the unburnt mixture indicated by the subscript u. The default values for the model constants are listed below.

Peter's model is used considerably in engine and non-engine applications due to the flamelet concept which associate fast chemistry assumption. Two of such cases for premixed flames in RANS context are presented in papers [52] and [53]. In the work of Tan and Reitz [54], Peter's model was used with some modifications to simulate combustion with exhaust gas recirculation and was validated using experimental data. In [52] and [54] even the model is validated against experimental data obtained from a SI engine, the fuel is set as propane. This is a huge concern in most validations. Octane is hardly used as the fuel source, thus making a comparison using Octane quite useful. More useful application of the model can be found in [55] where flame propagation inside of a direct injection gasoline engine was simulated and evaluated against experimental results. Here a parameter study had been carried out to check the plausibility of the model and a numerical simulation of a hypothetical DISI engine was done to check the potential of the model. Another practical evaluation of the model is presented in [56] where detailed chemistry is incorporated to yield more accurate results on fuel oxidation and pollutant formation. Experimental data was obtained from a homogeneous charge propane SI engine (cylinder pressure and NOx data) and validated.

3.5 Laminar flame speed

In the initial state of the flame, propagation is spherical in shape and rate of propagation is determined by the laminar flame speed. Also, laminar flame speed is needed to calculate the turbulent flame speed thus making it a very important parameter in turbulent premixed combustion. There are several methods to calculate this property for a given fuel and, in some situations, it is being taken as a constant. But laminar flame speed heavily depends on the temperature and pressure of the mixture thus need to be calculated in real time. Present work uses the model proposed by Metghalchi and Keck [57] which can be used with various fuels like CH_4, methanol, C_3H_8, iso-octane and is given in Following equation.

$$S_l = S_{l,ref} \left(\frac{T_u}{T_{u,ref}} \right)^{\gamma} \left(\frac{P_u}{P_{u,ref}} \right)^{\beta} \tag{17}$$

In the equation, T_u represents the unburnt reactant temperature. P_u is the pressure of the unburnt gas mixture which is present ahead of the flame, two reference values of temperature and pressure $T_{u,ref} = 298K$ and $P_{u,ref} = 1atm$.

$$S_{l,ref} = C_1 + C_2(\Phi - C_3)^2 \tag{18}$$

Calculation of reference laminar flame speed, is done using Φ, which is the equivalence ratio of the gas mixture and three fuel -specific constants C_1, C_2 and C_3. For iso-octane, fuel used in present work C_1 =0.2632, C_2 =0.8472 and C_3 =1.13. The exponents γ and β are calculated from,

$$\gamma = 2.18 - 0.8(\Phi - 1) \tag{19}$$

$$\beta = -0.16 + 0.22(\Phi - 1) \tag{20}$$

In these equations also, it can be observed that there is a big dependence on equivalence ratio. Thus one must give significant attention to the equivalence ratio when modelling.

3.6 Gas density model

Behavior of the in-cylinder gases dictates the whole combustion process in a strong manner. Changes of the vital properties like temperature, pressure governs the flow and combustion characteristics strongly. Hence prediction of those properties accurately is of greater importance. For that, a model is utilized for gas density. In an IC engine where temperature and pressure change drastically, such a model will yield unacceptable results. Thus, need of a reliable model arises. To predict the relationship between state functions, **Soave Redlich Kwong Model** was used and it is derived from the Redlich-Kwong equation of state [58] which has led to the development of several real gas models. The equation known as cubic equation of state is given below.

$$P = \left(\frac{RT}{V - b + c}\right) - \frac{a(T)}{V(V + b_0)} \tag{21}$$

P = absolute pressure (Pa)

T = temperature (K)

V = specific volume

R = universal gas constant/molecular weight

The coefficients b, c and b_0 are given for each equation of state as functions of the critical temperature, critical pressure, acentric factor and critical specific volume. Term $a(T)$ represents the Redlich-Kwong temperature function which is defined as

$$a(T) = a_0 \left(\frac{T_c}{T}\right)^n \tag{22}$$

T_c is the critical temperature and the value of exponent n depends on the species of interest and values of and for some widely used substances are given in the original paper. Following empirical equation is also used to find values of n [54].

$$n = 0.4986 + 1.1735\ \omega + 0.475\ \omega^2 \tag{23}$$

Where ω is the acentric factor defined as $\omega = -\log\left(\frac{P_v(T)}{P_c}\right) - 1$.

The Soave Redlich-Kwong real gas model was originally published in [59].

The deviation from the original Redlich-Kwong model to Soave Redlich-Kwong is that the way parameter n is calculated. This model uses the equation to calculate the parameter.

$$n = 0.48 + 1.574\ \omega - 0.176\ \omega^2 \tag{24}$$

Another two important parameters, unburnt density and thermal diffusivity all also calculate by this model.

3.7 Turbulence model

3.7.1 K-epsilon model

Since the flow process inside the cylinder is highly turbulent and its interaction between the flames determines the turbulent flame speed, modelling turbulence accurately is very important. As mentioned above, there are two main approaches to resolve turbulent flows namely RANS and LES. Both approaches were implemented in the present work and for RANS, k-epsilon turbulence model was utilized [60]. This is model consist with two turbulence parameters where following transport equations for solves both those parameters k (turbulent kinetic energy) and ϵ (dissipation rate of k) are solved.

$$\frac{\partial \rho k}{\partial t} + \frac{\partial (\rho k u_i)}{\partial x_i} = \frac{\partial}{\partial x_j}\left[\frac{\left(\mu + \frac{\mu_t}{\sigma_k}\right)\partial k}{\partial x_i}\right] + G_k + G_B - \rho\,\epsilon - Y_M + S_k \qquad (25)$$

$$\frac{\partial (\rho\,\epsilon)}{\partial t} + \frac{\partial (\rho\,\epsilon u_i)}{\partial x_i} = \frac{\partial}{\partial x_i}\left[\frac{\left(\mu + \frac{\mu_t}{\sigma_\epsilon}\right)\partial\,\epsilon}{\partial x_j}\right] + C_{1_\epsilon}\left(\frac{\epsilon}{k}\right)C_2 - C_3\rho\left(\frac{\epsilon^2}{k}\right) + S_\epsilon \qquad (26)$$

Using these values, the turbulent (or eddy) viscosity, μ_t, is computed. Value of C_μ = 0.09

$$\mu_t = \rho C_\mu (k^2/\epsilon) \qquad (27)$$

3.8 Early flame propagation speed model

Flame kernel development of a spark ignition engine depends on the properties of the ignition system: spark time, spark energy, plasma temperature distribution, gap width and heat losses to the chamber walls and electrodes; properties of the fuel mixture: fuel, Equivalence ratio, pressure, temperature, Laminar flame speed and residual gas fraction; and of the flow parameters: length and time scales, strain on flame, mean flow

In these equations, G_k represents the generation of turbulence kinetic energy due to the mean velocity gradients, G_b is the generation of turbulence kinetic energy due to buoyancy. Y_M represents the contribution of the fluctuating dilatation in compressible turbulence to the overall dissipation rate, C_1, C_2 and C_3 are constants. σ_k and σ_ϵ are the turbulent Prandtl numbers for k and ϵ, respectively. S_k and $S\epsilon$ are user-defined source terms.

velocity and turbulent intensity [61] [10] [62]. Modelling of formation of flame kernel is associated with simultaneous resolving of chemical kinetics, spark physics and flow and turbulent interactions. Modelling spark physics is in its initial stage and the number of publications available is limited [63] [64]. Treatment on chemical kinetics is usually based on a one step global reaction and first law of thermodynamics.

Studies on interactions between turbulent flow and flame kernel show that large eddies convect the flame kernel while smaller eddies wrinkle and stretch the flame increasing the area of the flame [65]. Even though it is believed that turbulence only supports the growth of flame kernel, it is only true for moderate levels of turbulence. When the turbulent levels are too high, flame will tend to quench due to the huge strain posed on its surface. Thus, predicting the turbulence is a vital part and conventional turbulent flow models are still not in a satisfactory level to produce highly accurate results in engine applications [66].

Modelling the spark related combustion is a vital part of the simulation since it determines the initial rate of combustion, transition from laminar to turbulent combustion and hence overall combustion characteristics. Typically, the size of initial spark is small, which makes the process of burning few cells at the beginning an erroneous approach. To resolve the spark accurately, it will require very fine spatial and temporal scales. That requires considerable time and computational power. Since this early flame kernel development is occurring in small temporal and spatial scales, models with spatial filtering approach were employed. Such models assume that the spark is perfectly spherical and its flame front is infinitely thin. The growth of the spark is given by following equation [67].

$$\frac{dr}{dt} = \frac{\rho_u}{\rho_b} S_t \tag{28}$$

Radius r of the spark changes with time t and the rate which it changes depend on density of the unburned fluid ahead of the flame front $\rho_{u,}$ density of the burnt fluid behind of the flame ρ_b and turbulent flame speed S_t. Densities are taken from the material properties and those densities are calculated using a PDF which depends on composition and temperature. To calculate the flame speed, several models are available in the software and they are discussed below.

3.8.1 Laminar

In this model, turbulent flame speed will be replaced with laminar flame speed which will be calculated as mentioned in Section 2.2. Since the initial state of the flame is less affected by the turbulent scales, this model is sufficiently acceptable.

3.8.2 Turbulent curvature

In this model the effects of flame curvature are considered which causes a decrease of both laminar and turbulent flame speeds.

$$S_t = \max\{S_l - \frac{2D}{r}\ , S_t(r) - \frac{2D_t}{r}\} \tag{29}$$

D and *Dt* are laminar and turbulent diffusivities, respectively which are evaluated at the location of spark. $S_t(r)$ is the turbulent flame speed which is evaluated with the turbulence length scale at the spark location. This is because the turbulence length scales larger than the spark will only convect the flame and the ones which are smaller causes the increase of flame speed and surface area of the flame. Values for S_l and *D* is gained from the material property inputs.

3.8.3 Herweg and Maly

This is a model based on the strained flamelet model [68] [26] [69] and it takes all physical and chemical parameters into consideration. Models developed earlier treated the flame kernel as a fully developed structure and neither include turbulent and ignition system characteristics nor utilized developed turbulent combustion closures.

This model has taken the importance of parameters like strain rate, characteristics time and length scales, flame front thickness and kernel radius into the derivation of model equations. Herweg and Maly [70] uses the following equation to calculate the turbulent flame speed.

$$S_t = max\{S_l, S_l[I_0 + I_0^{0.5}\frac{{u'}^{0.5}}{(u' + S_l)^{0.5}}\left(1 - ex\left(-\frac{r}{l_t}\right)\right)^{0.5}]G\} \tag{30}$$

$$G = \left(1 - \exp\frac{(t_0 - t)}{T}\right)^{0.5}\left(\frac{u'}{S_l}\right)^{\frac{5}{6}} \tag{31}$$

I_0 is a function for effect of strain on the laminar burning velocity calculated as

$$I_0 = \max\{0{,}1 - \left(\frac{\delta}{15 l_t}\right)^{0.5} \left(\frac{u'}{S_l}\right)^{\frac{3}{2}} - 2\frac{\delta}{r}\frac{\rho_u}{\rho_b}\} \quad (32)$$

Here *t* is current time, t_0 is start time, *u'* is turbulent velocity scale and δ is laminar flame thickness. Normally this is obtained from the ratio between diffusivity and Laminar flame speed. But when the Blint modifier is being used,

$$\delta = \frac{D}{S_l} B_1 \left(\frac{\rho_u}{\rho_b}\right)^{B_2} \quad (33)$$

Where B_1 and B_2 are constants with values of 2 and 0.7.

$$T = \frac{l_t}{u' + S_l} \quad (34)$$

From the earlier investigations and simulations, it was found that this model gives better results for premix SI engine cases, thus it was used for the present work.

3.8.4 Transition radius

After the early flame propagation which is laminar like, transition of the combustion to the CFD grid will happen through a representative volume of cells. The radius of this volume is called as "transition radius" and will depend on the local turbulent length scales. However, to prevent the volume being too small or too large, following equation is used.

$$r_t = max\{r_0 + 3\Delta, 3r_0, \min[0.5 l_t, r_0 + 10\ \Delta] \quad (35)$$

Here r_0 is the user-defined initial spark radius, Δ is the cell length scale and l_t is the turbulent length scale. The reason behind using turbulent length scale to determine transition radius is that when the flame becomes that much large, all the levels of turbulence will affect the speed of the flame. After reaching transition radius.Value of progress variable inside the spark volume is given by the equation below and *r* stands for the instantaneous radius of spark.

$$c = \left(\frac{r}{r_t}\right)^3 \quad (36)$$

3.8.5 Selection of numerical schemes

To meet engineering accuracy requirements, usually a second order method with moderate refined grids is enough in obtaining good results. Literature [71], [72] and [73] have already provided wide evidence on this aspect However, experiments have been made on the modelling of combustion in complex geometries [74]. Taking into consideration that it is a new research area. Therefore, best practices are still to be established.

Anyways, the literature related to engine as far as premixed combustion modelling with LES is concerned, has been limited to a number of publications [75, 76, 77, 78]. Taking into consideration that combustion is a sub-grid scale phenomenon, premixed combustion modelling is for LES a considerable challenge. LES mesh sizes are usually bigger and thicker that the reaction zone thickness of the flame front. That is why, the flame front cannot be resolved on such grids using conventional methods. Sub-grid wrinkling effects, on the other side, due to turbulent flame interaction need to be exactly estimated as far as resolved parameters are concerned. Majority of today's LES combustion models are similar to RANS combustion models in their approach and formulation. At this phase, it is not clear if these models fully extract the advantage of the resolved field, even though providing a good start ing point. As a conclusion, today strongest requisite in terms of engine simulation, is the proper re-evaluation of the actual methodology and enabling the necessary allowances to be in line with LES concepts.

4 SIMULATIONS PROCEDURE

Three dimensional simulations of the process were carried out using the commercial CFD code (Ansys Fluent). IC engine package is available in “Ansys workbench” is a dedicated package for flow and combustion modelling in engines. Simulation setup required setting up the boundary conditions, creating and setting up the dynamic mesh zones to simulate the motion of the piston and vales, selecting suitable material properties, selecting and adjusting the model constants of the relevant models for flame generation and its propagation, models to predict laminar flame speed, turbulent flame speed, gas properties and turbulence. For the calculation of aforementioned parameters, models used are Herweg and Maly [70], Metghalchi and Keck [57] and k-epsilon respectively. The reasoning behind the selection of those models are described in Chapter 3.

4.1 Preparation of the geometry

Prior to setting up the solver, preparation of the geometry and mesh was required. The 3-dimensional model of the engine geometry was imported into the design modeler where it was partitioned and named for it to be meshed properly so that mesh will have large percentage of high quality elements and suitable type of elements in desired locations. These named regions were also used in setting up of boundary conditions. The ordered and logical manner of the names was very much helpful.

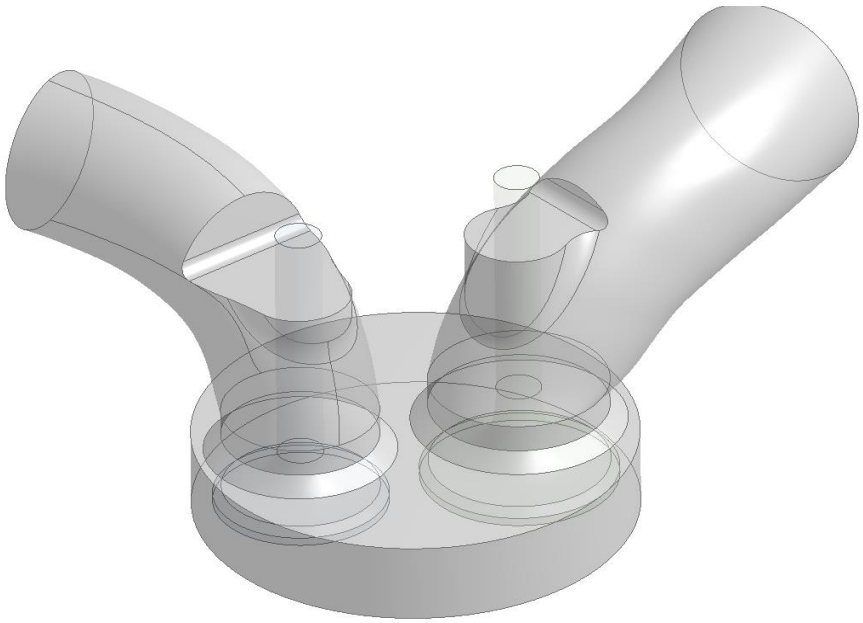

Figure 2- Engine geometry before decomposition

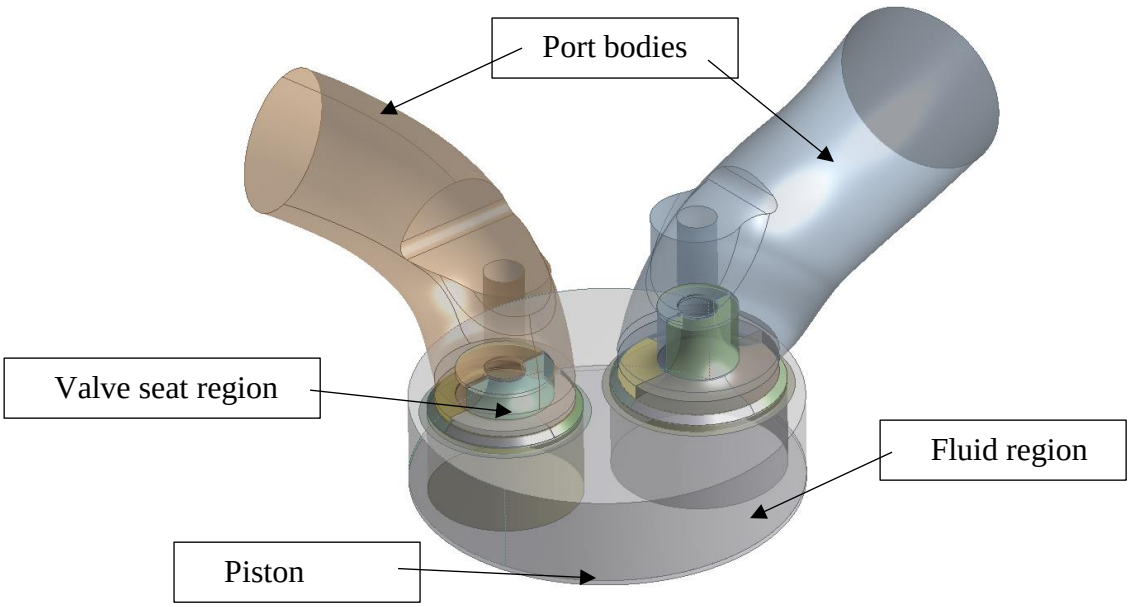

Figure 3- Engine geometry after decomposition

To make the solutions as accurate as possible, realistic boundary conditions should be applied. Also, the cell elements play a huge role in the simulation. In practices, it is very hard to employ such meshes on complex engine geometries. However highly stretched and skewed meshes will cause errors while running and will use more time to run than a structured mesh. Hence making a suitable mesh is very important to get a successful simulation as much as all the other factors.

4.2 Meshing process

Meshing was done in a manner so that it creates high portion of un-skewed elements with orthogonal quality closer to 1 over the entire domain. Sectioning the geometry was done in previous step keeping in mind that different types of elements will be needed in different sections depending on the flow and combustion processes occurring at those places.

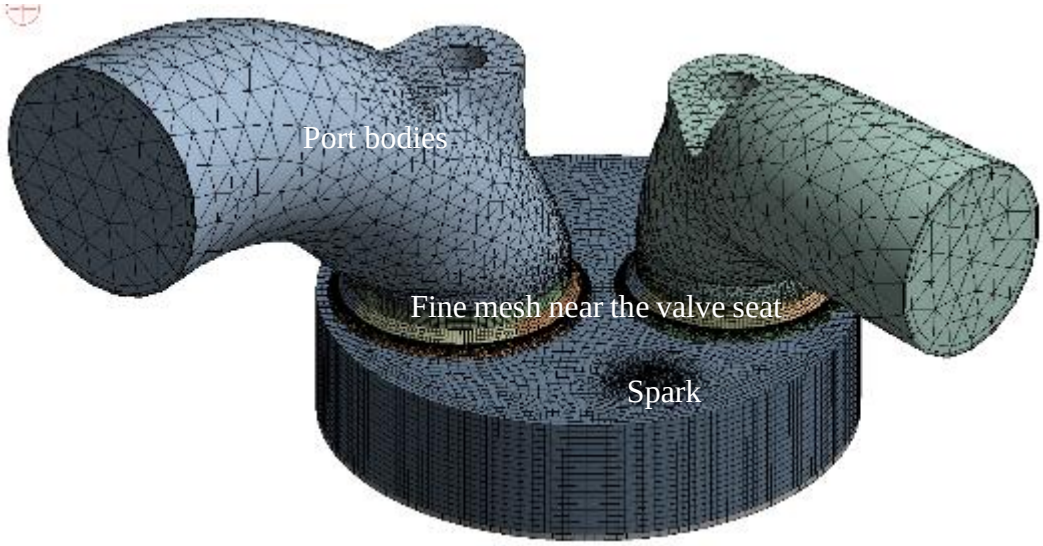

Figure 4- Meshed engine geometry

As shown in the figure, port bodies are meshed with tetrahedral elements with lesser level of refinement since inside the ports, only flow processes will occur. Boundary layer mesh with wedged elements were applied near the walls of the ports to capture the rapid velocity and pressure gradients due to the formation of boundary layer. Then regions near the valve seats were meshed with wedged elements in an ordered manner due to very high velocities occur at the opening and closing of valves. Such large values will cause divergence of the solution if not handled with care.

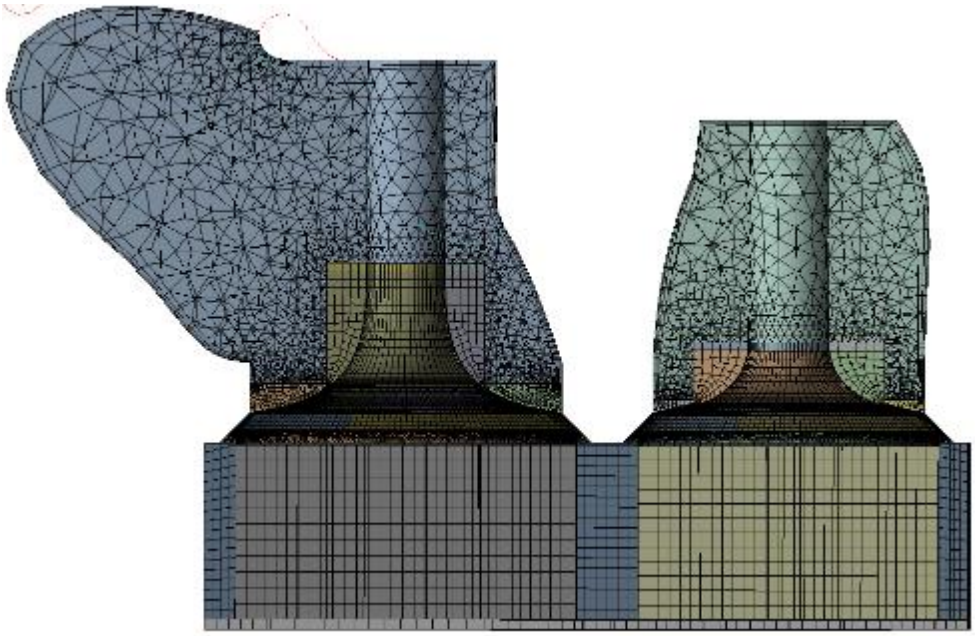

Figure 5- Sectioned view of the mesh

The combustion chamber has a hexahedral mesh which is known to yield fast and accurate results compared to any other mesh elements type [79]. Using a hexahedral mesh was possible only because the lesser complex cylindrical geometry of the chamber. Nevertheless, a much-refined mesh was applied near the spark location due to the complexity of processes happening in that region.

4.3 Test cases and engine parameters

All the engine simulations were started running from the opening of the intake valve and the initial conditions for a particular case was set up using the experimental data obtained from Loughborough University [80]. All relevant experimental data is given in the appendix. Intake valve opening is followed by an air intake which will be compressed due to the motion of the piston. Piston motion is handled with a piston motion profile which will be generated by the software itself based on the input data provided. For the motion of valves, motion profiles should be supplied by the user and the used motion profiles for present work is given below.

Then governing equations will be solved for mass, momentum, energy and for variables required by the models in use. The state relationships of the gases were obtained by the Soave Redlich Kwong Model and it is described in Section 2.4. Main reason to select a real gas model rather than using the ideal gas law was that the high temperature and pressure ranges occurring inside the chamber. Then the turbulent flow should be resolved and for that a turbulence model should be selected. For this research, two different turbulence models were employed. For RANS, k-epsilon model was used while for LES simulations, Smagorinsky-Lilly Model was utilized. Both the models were used with the default model constants.

After modelling the flow and motion, combustion process had to be modeled. First task in modelling combustion is modelling the spark initiated combustion. Since this early flame kernel development is occurring in small temporal and spatial scales where if it is needed to be resolved, very small-time step sizes and mesh elements will be needed.

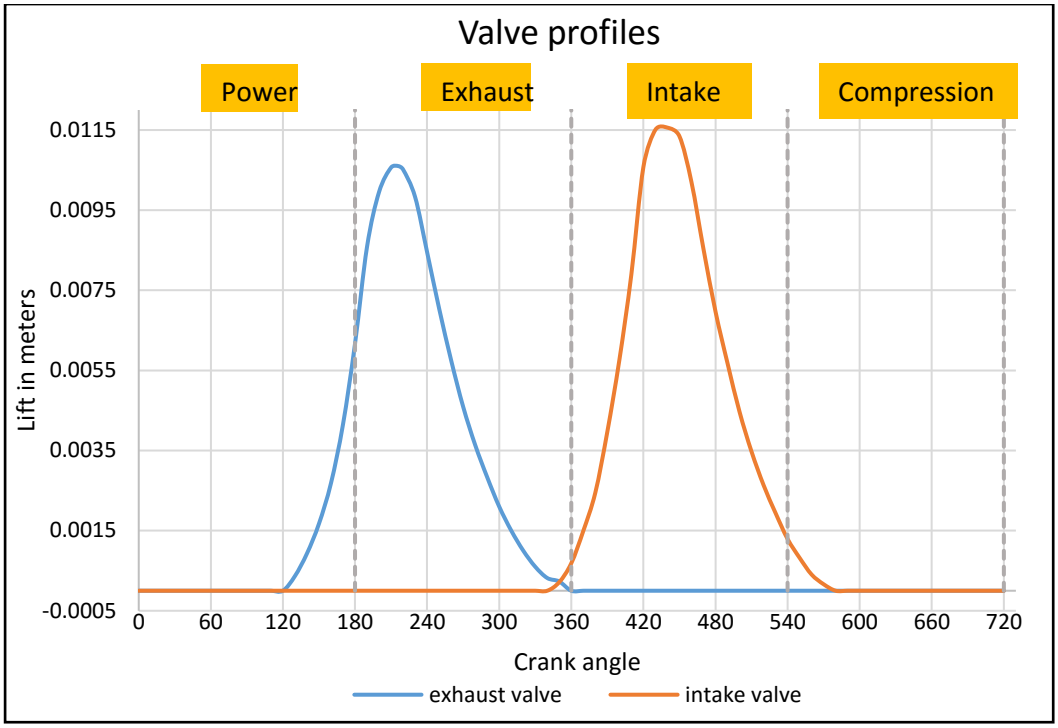

Figure 6 - Valve motion profiles

Thus, a model with spatial filtering approach was employed where the spark event is not modeled in detail, but as the initiation of combustion over a period of Crank angles. For that model, following input parameters were used.

Table 2- Input parameters for spark model

Parameter	**Value/model**
Initial radius	0.5 mm [81]
Spark energy	10 mJ [33]
Spark duration	0.222 ms [82]
Early flame propagation speed model	Herweg-Maly [70]

Here the shape of the spark is assumed to be spherical with a thin flame front. Early propagation of the spherical flame is decided by equation 28. As it implies, rate of propagation is determined by the density ratio between burnt and unburnt gasses and the turbulent flame speed S_t. There are several methods to calculate the turbulent flame speed and they have been described in detail in prior sections. For this research,

turbulent flame speed is calculated by the model Herweg and Maly [70] which uses equation **30** to calculate the turbulent flame speed.

This sub grid scale representative volume will grow in time while it reaches to a certain radius called as transition radius where it will be transferred into the computational mesh. Determination of the value for transition radius is done by using the following equation. This radius of the propagating flame will reach the transition radius which then will transfer the turbulent flame speed calculation to the main turbulent combustion model.

$$r_t = max\{r_0 + 3\Delta, 3\mathrm{r}_0, \min[0.5l_t, r_0 + 10\ \Delta]\} \quad (37)$$

The engine used to obtain the experimental data is a single cylinder, variable compression and four stroke research engine [80]. The experimental pressure and heat release rate data obtained from this engine is used to evaluate the predictability of the combustion models mentioned above. Four different cases were selected and their relevant properties and details of the engine geometry are mentioned in detail in "Table 1" and "Table 2". CA represents crank angle while 0 CA means that the piston is at top dead center in the power stroke.

Table 3- Ricardo e6 engine specifications

Ricardo E6 Engine	
Bore	76.2 mm
Stroke	111.1 mm
Connecting rod length	241.3 mm
Intake valve opens	351 CA
Intake valve closes	577 CA
Exhaust valve opens	139 CA
Exhaust valve closes	550 CA

From "table 3" it is evident that the differences in the selected cases are their equivalence ratios, compression ratios and the engine rpm. This will lead into different heat release rates and pressure plots.

Table 4- 4 Cases and their details

	Case 1	**Case 2**	**Case 3**	**Case 4**
Spark position	704 CA	704 CA	700 CA	704 CA
Compression ratio	8.7	8.7	8.7	7.5
Equivalence ratio	1.089	0.936	0.967	0.953
Engine rpm	1500	1500	1800	1500

Side view of the meshed engine geometry is shown in “Figure 7”

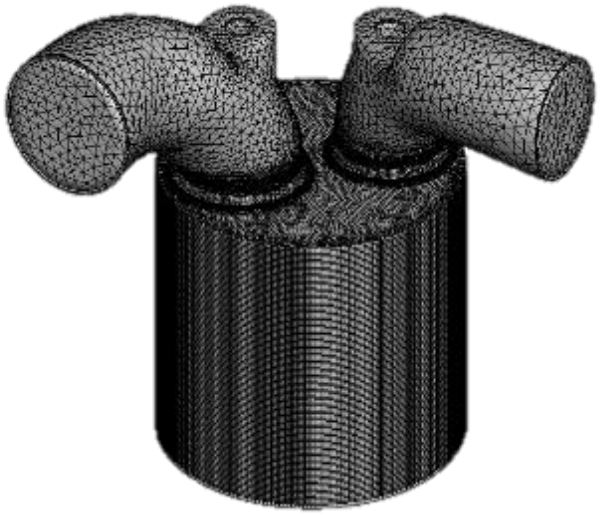

Figure 7- Meshed engine geometry

To assess the applicability of the combustion models, to understand the underlying issues with computational modelling techniques related to IC engine problems and to validate the developments of the models, computational results should be compared with experimental data. In the present work, experimental data for heat release rate and in cylinder pressure of a laboratory engine was used to evaluate the results at first. Qualitative comparison of the numerical results against published literature was also carried out. For the Present work, experimental data from the Ricardo E6 engine in the Loughborough University engine laboratory was used. They were originally measured for the work of [80] and was used in this work with the permission of the author.

This engine is a single cylinder, four stroke variable compression engine with following specifications.

Ricardo E6 Engine

Bore	76.20 *mm*
Stroke	111.1 *mm*
Compression ratio (CR)	Variable
Squish at 8.7 CR	1.4428 *mm*
Connecting rod length	241.30 *mm*
Spark advance	Variable
Valve timing	
Intake valve opens	9° BTDC
Intake valve closes	37° ABDC
Exhaust valve opens	41° BBDC
Exhaust valve closes	10° ATDC
Valve lift	
Maximum lift - intake valve	11.56 *mm* @ 85° ATDC
Maximum lift - exhaust valve	10.60 *mm* @ 52° ABDC
Valve diameter	
Intake valve max. diameter	34.37 *mm*
Exhaust valve max. diameter	29.62 *mm*

Figure 8- Ricardo E6 engine specifications [80]

The experimental pressure curves presented in this Section is averaged over 100 consecutive cycles to get more sensible results. Heat release rate was calculated by considering the combustion chamber as a closed thermodynamic system during the combustion period. Several thermodynamic models are available to evaluate the heat release rate either using many simplifying assumptions or modelling the processes like heat loss to the surrounding and spark plug and prescence of a crevice volume [10]. The model adapted in this work and the model used by Ansys fluent are discussed brifely in the next Chapter.

$$PV^n = Constant \tag{38}$$

Where n is closer to 1.3. In cylinder pressure rise can be devided into two parts: due to change in volume and due to consumption of fuel. Pressure rise due to the volume change can easily be calculated using the above relationship and since the total pressure

change can be measured, increase of pressure due to heat release can be calculated. This can be used to determine the heat release rate. But the shortcomings of this method are powerful enough to cause reasonable amount of errors. Hence following adjusted form of heat release rate equation is used.

$$AHRR = \frac{\gamma}{\gamma-1} P\frac{dv}{dA} + \frac{1}{\gamma-1} V\frac{dP}{dA} + V_{cr}\left[\frac{T'}{T_W} + \frac{T}{T_W(\gamma-1)} + \frac{1}{bT_w} \ln\frac{\gamma-1}{\gamma'-1}\right]\frac{dp}{dA} + Sh_c(T-T_W) \quad (39)$$

$AHRR$ - Heat release rate into the mixture due to chemical reactions

$Sh_c(T-T_W)$ - Heat release rate from cylinder walls due to convection

γ - Specific heat ratio for in cylinder mixture

γ'- Specific heat ratio for crevice gas

V_{cr} - Crevice volume

T'- Crevice gas temperature

T - Mean gas temperature

T_W - Mean cylinder wall temperature

A - Crank angle

S - Combustion chamber surface area

h_c - Convective heat transfer coefficient averaged over the chamber surface area

this method gives much realistic values with respect to the model used in the software which has the following form.

$$AHRR = \frac{\gamma}{\gamma-1} P\frac{dv}{dA} + \frac{1}{\gamma-1} V\frac{dP}{dA} \quad (40)$$

Since this equation has neglected the last two terms it yields lesser values for heat release rate which will be seen in next chapters. Thus heat release rate results has been compared with a qualitative focus.

5 RESULTS AND DISCUSSION: RANS

Analysing the results generated from the RANS simulations is vital to understand the pros and cons of the formulation and to lay a foundation to describe the need of a advanced formulation like LES. Mainly, pressure and heat release rate data were taken for the analysis since they are comperativly easier to be measured experimentaly. The results and discussion section is arranged in the following manner. First the predictability of the initial stage of combustion by the early flame propagation speed models in association with two turbulent flame speed closure models was evaluated. In that section, the user inputs needed at the early stage flame modelling and the influence of those are also discussed. These analysis was used as a basis to identify the most suitable values and models. Then full cycle simulations were carried out for each 4 cases with the use of both turbulent flame speed models namely Peter's and Zimont. Those models solves the flame in fully developed phase and using the results generated, their benefits, drawbacks and suitability are analysed. Finally, the importance of a formulation with mesh independence, less uer interaction and ability to give more insight is discussed.

5.1 Flow inside the chamber

Flow characteristics inside the chamber plays the biggest role in propagation/extinction of the flame. The level of turbulence, swirl and tumble ratio and the magnitude of velocity determines the regime which the flame belongs hence its behavior and structure. Figure 9 shows the velocity distribution on a plane across the intake valve at a crank angle of 11.63 degrees after BDC of the suction stroke. It clearly shows the high-speed jet of charge mixture coming into the engine chamber. The incoming flow collides with the engine walls generating a rotating tumble flow. This thumbing flow feature enhances the mixing of trapped gas with the incoming fresh gases while making a desirable level of turbulence for the generation and propagation of a stable flame.

Figures 10 and 11 reveals the behavior of the velocity field along the longitudinal direction of the piston. Three locations were selected such that they contain top, middle and bottom sections of the cylinder

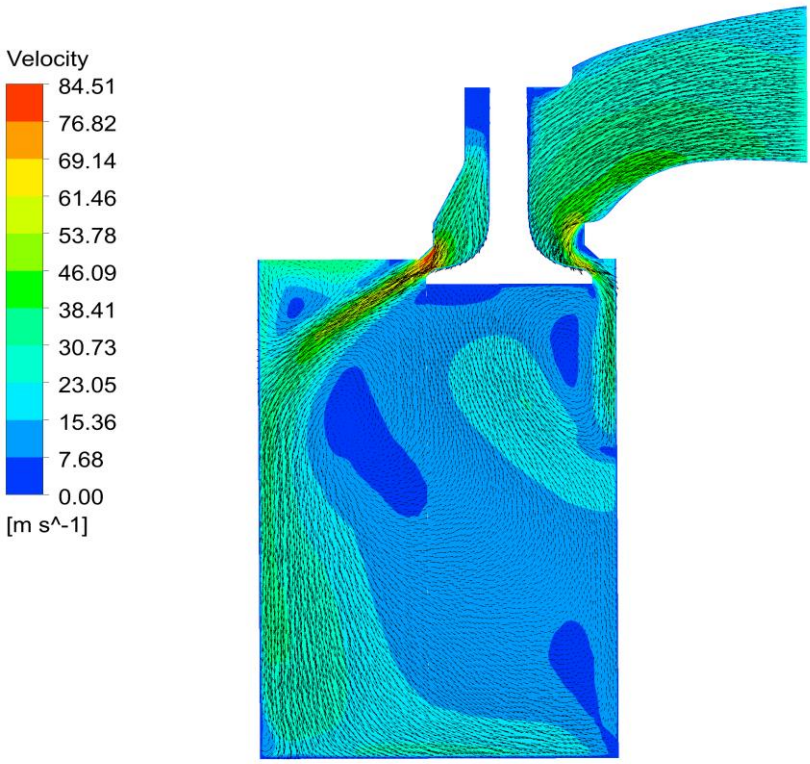

Figure 9- Velocity contour plot with velocity vectors
on a plane through intake valve at crank angle 11.63 after BDC of suction stroke

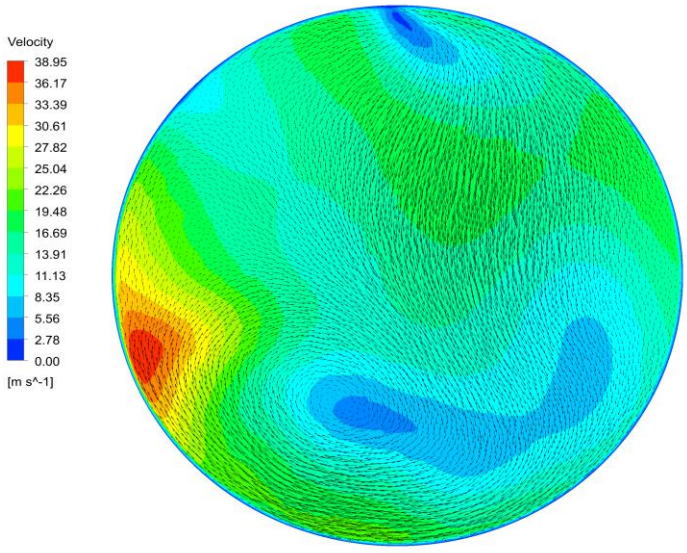

Figure 10- Velocity contour plot with velocity vectors at Z = 4.5 cm
at crank angle 11.63 after BDC of suction stroke. Z= 0 is the BDC

.

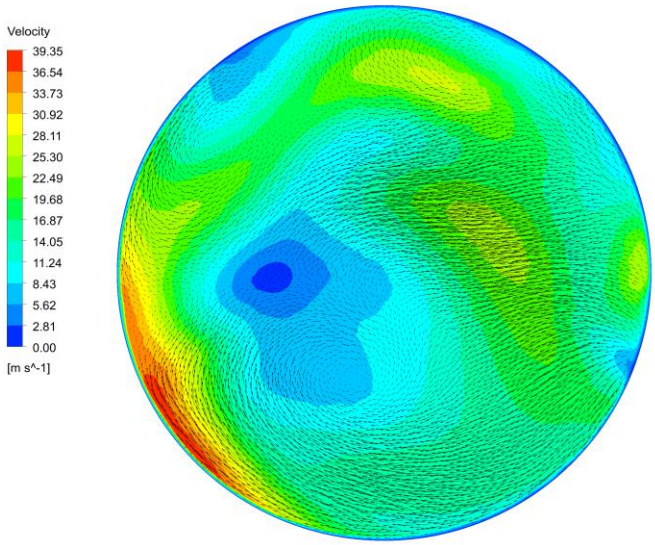

Figure 11- Velocity contour plot with velocity vectors at Z = 8.0 cm at crank angle 11.63 after BDC of suction stroke

These figures reveal the inherent behavior of the velocity field during the intake stoke. Near the TDC, large velocity magnitudes can be observed with high levels of turbulence. As it moves down along the chamber, number of flow structures get reduced and the velocity also drops considerably. Also, swirling motion of the flow is visible even closer to the BDC and this swirling motion is helpful for mixing.

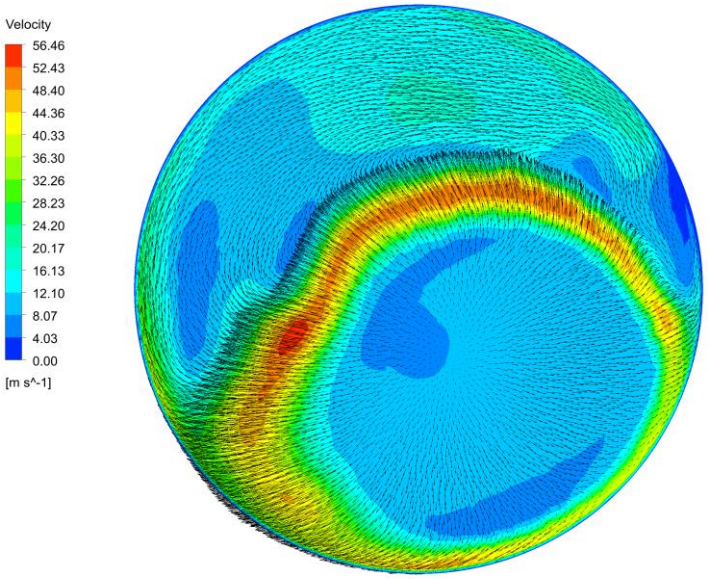

Figure 12- Velocity contour plot with velocity vectors at Z = 11.5 cm at crank angle 11.63 after BDC of suction stroke

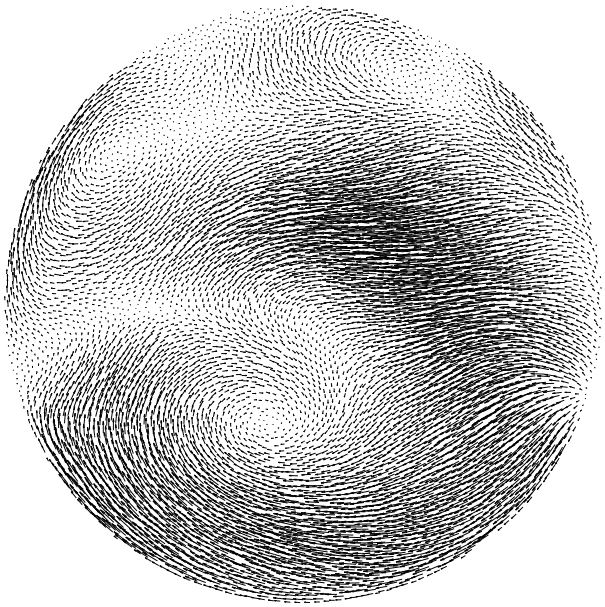

Figure 13- Velocity vectors at Z = 8.0 cm at crank angle

11.63 After BDC of suction stroke

Figure 13 which shows the velocity vectors closer to the TDC, shows many flow structures even this being a RANS simulation. This is an evidence for the highly unsteady and turbulent nature of the flow and resolving this accurately is a challenge using RANS techniques.

From the above figures, a strong jet of premixed charge is entering the chamber creating both tumble and swirl. Since it is still in the intake stroke, few isolated swirling and tumbling eddies are present across the chamber. As the piston moves to the TDC during the compression stroke, those eddies transformed into a strong swirling upward flow. Upward flow is induced due to the motion of the piston. Figures 14 and 15 which were taken few degrees before spark ignition show that clearly.

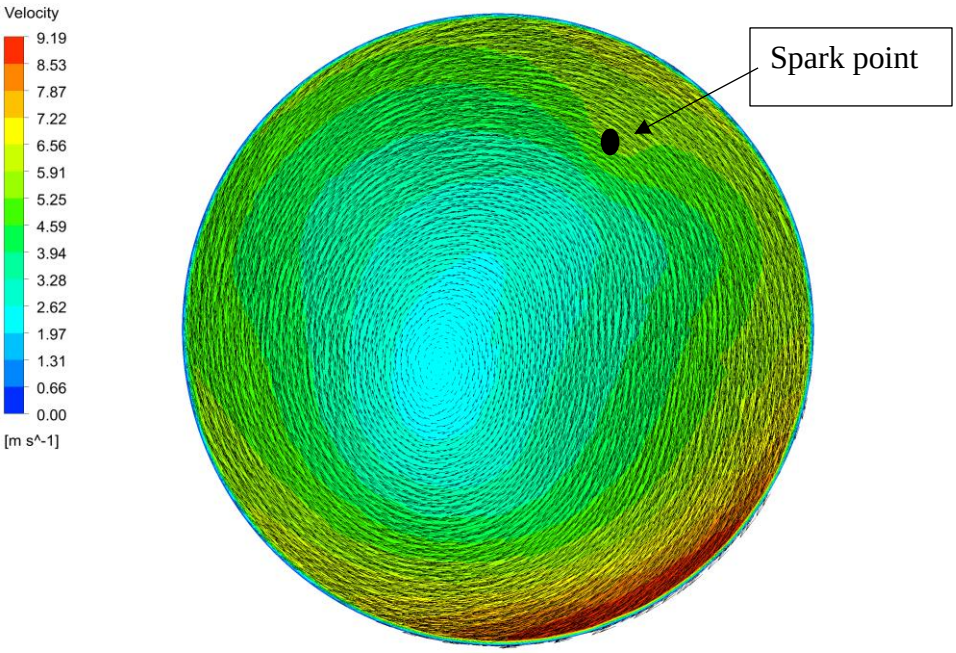

Figure 14 - Swirling flow near the spark point
At crank angle 1.5 degrees before the ignition. Velocity contour plot with vectors are shown here

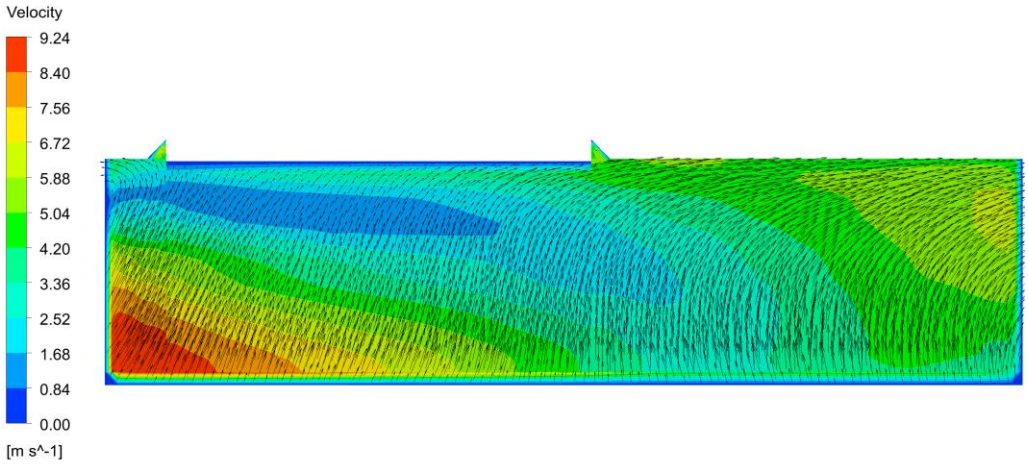

Figure 15- velocity contours on cross sectional plane through the intake valve

From figure 16, it can be noted a region where velocity is somewhat smaller than the other regions. This is near the spark location. This characteristic is an important thing since large velocities will tend to either extinguish the flame or will convect flame kernel away.

Another important aspect to look at is the behavior of the parameters like temperature, pressure and turbulent kinetic energy before and after the ignition. Following figures shows the velocity, temperature and turbulent kinetic energy distribution on a plane across the spark point, 2 crank angles before and after the ignition.

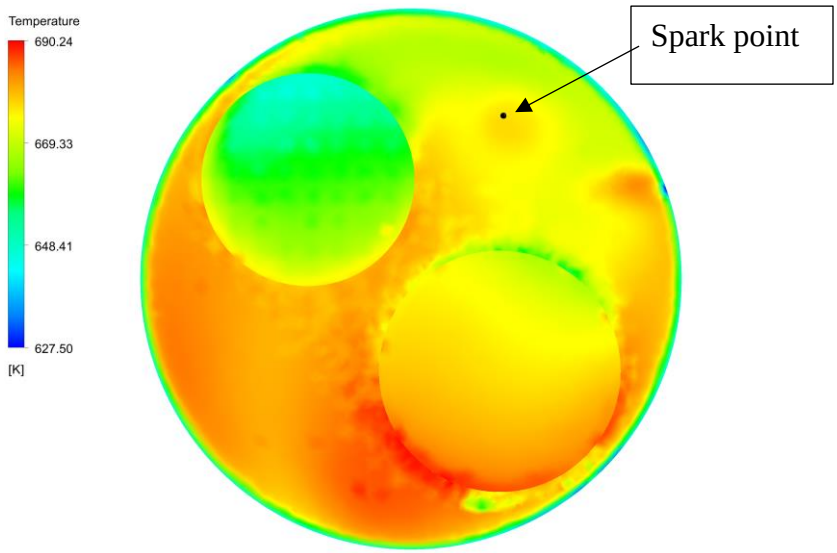

Figure 16- Temperature variation near the spark point before ignition

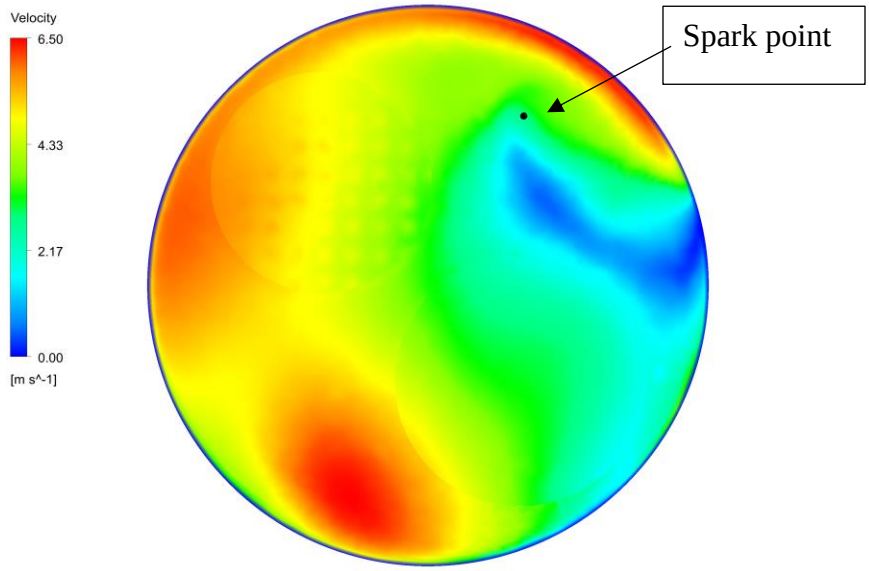

Figure 17- Velocity variation near the spark point before ignition

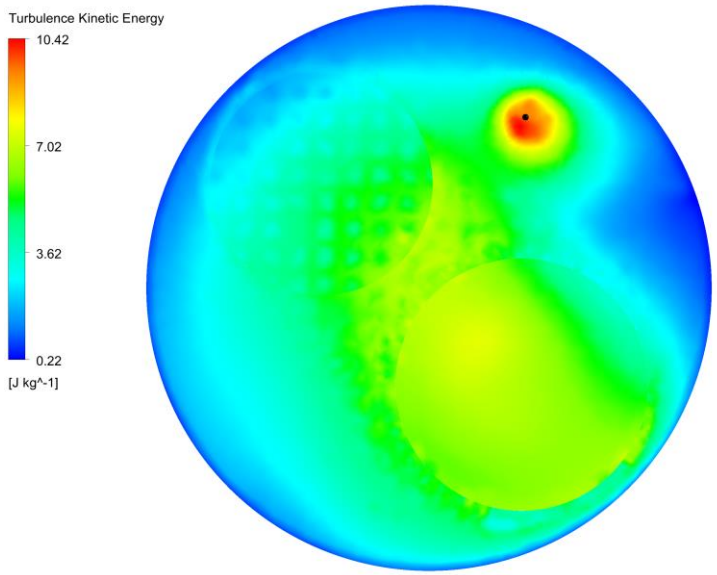

Figure 18- Turbulent kinetic energy variation near the spark point before ignition

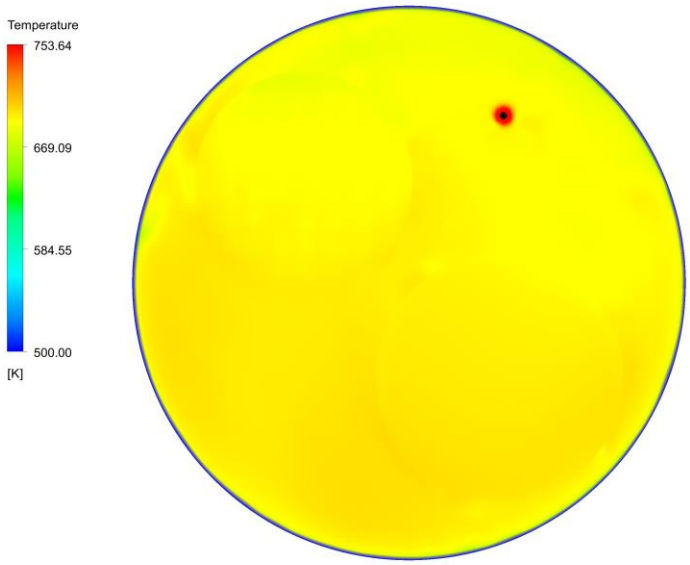

Figure 19- Temperature variation near the spark point after ignition

Here the black dot indicates the location of spark point. Before the ignition, temperature inside the chamber looks almost the same and it helps for a homogeneous combustion. Turbulence kinetic energy looks much higher closer to the spark point but this may be due to the higher mesh density closer to that point. This high mesh sensitivity can also be noted as a drawback of the RANS simulations and this can be reduced using LES with a reasonable SGS formulation.

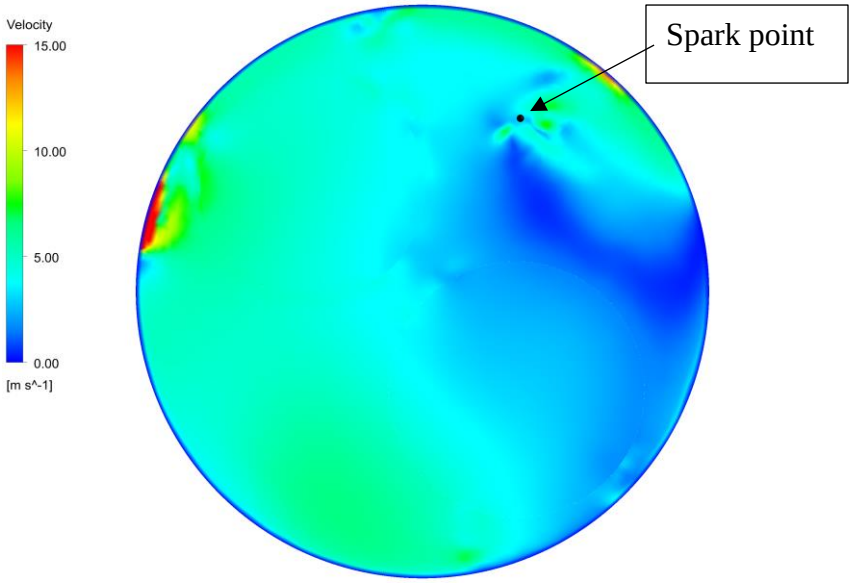

Figure 20- Velocity variation near the spark point after ignition

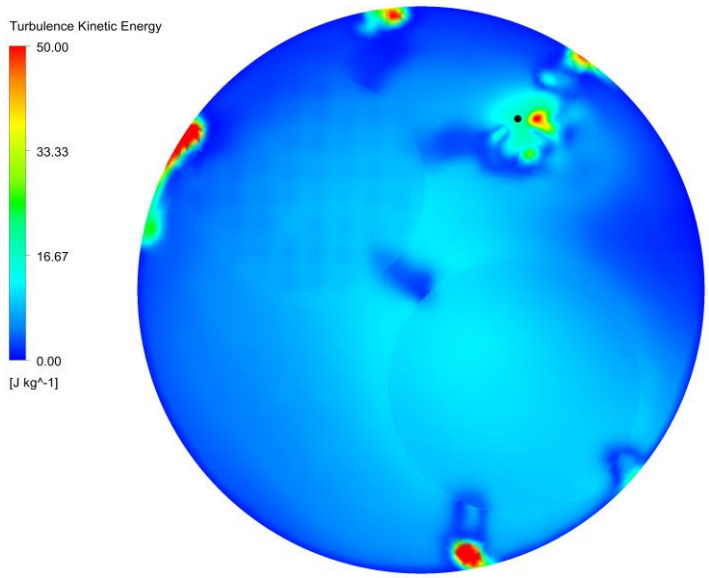

Figure 21- Turbulent kinetic energy variation

Near the spark point 4 CA after ignition

After the ignition, localized high temperatures and velocities can be observed near the spark location. This is the expected behavior and some locations with high values of the concerned parameter can be seen which is unexpected. This may be due to modelling and numerical errors and can be avoided with an advanced formulation like LES.

5.2 Heat release and pressure at spark

Flame development in SI engines has two stages: initial spark associated flame development and the fully developed stage. In the first stage, modelling the initial flame is done. For this initial radius, spark input energy and spark duration must be given as user inputs. It is very difficult to find exact values for the parameters mentioned above since they are hard to be measured. Also, the Behavior of pressure and heat release rate strongly depends on these inputs. Thus, a study was carried out to observe the response of pressure and heat release rate when initial radius, transition radius and the early flame propagation speed model were changed. The ignition energy and the spark duration were taken to be 60 mJ and 1.2 ms respectively. These values represent typical magnitudes of ignition parameters of a transistorized coil ignition system (TCI) [80].

5.2.1 Initial radius

First the impact of initial radius was investigated using experimental results of case 1 as the reference test case. Basically, initial radius of the flame kernel depends on the power input from the spark, heat losses to the spark plug and surrounding and energy consumption due to molecular dissociation and ionization [63]. This makes it an unfixed value which should be evaluated for every case of interest in the expense of computational time. Nevertheless, several studies have suggested 0.5 mm as a good initial value for radius and in this study, validity of that claim was first evaluated to use it for the Present work [83] [63].

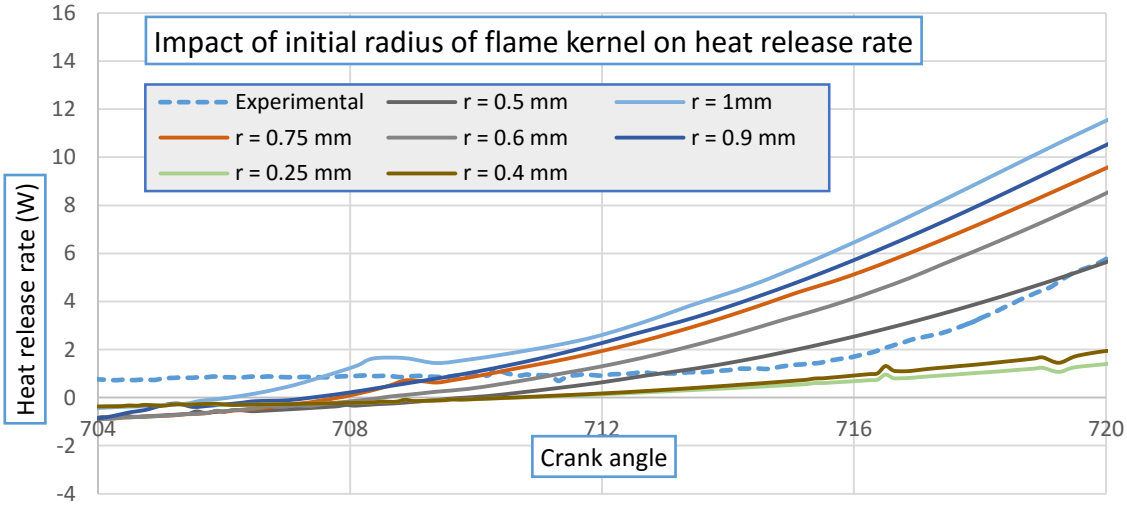

Figure 22- Change in heat release rate vs. crank angle when the initial radius is changed. Dashed line shows the experimental heat release rate for case 1.

As shown in Figure 24, as the radius of flame kernel is increased, heat release rate is also increased causing more and more fuel burn at the flame development stage. 0.5 mm for initial radius yields a heat release rate curve which is much closer to the experimental values. Values less than 0.5 mm gives lesser heat release rates. This will cause the combustion process to last longer since more fuel must be burnt by the fully developed flame. This will yield lesser peak heat release rates due to the comparatively high combustion times and consequently less peak pressures. The reasons for long lasting combustion are twofold. One is as explained above, since it starts small it takes time to grow and develop. But most importantly lesser the size of the kernel, strain and the curvature affect the flame speed causing it to slow down. Vice versa is applicable for radii higher than 0.5 mm. Hence 0.5 mm was taken as the initial radius for the Present work.

5.2.2 Early flame propagation speed model

For each combustion simulation, two flame speed models are employed for the two stages. Identifying the model to determine the flame kernel growing speed to be associated with both Zimont model and Peter's model was very much important since it make sure a smooth transition between two models. That is vital because if a mismatch between speeds and heat release rates at the transition is present, that will cause the flame growth to either slow down drastically or speed up rapidly generating large deviations between experimental and simulation values. Both turbulent flame speed models were checked with following early flame propagation speed models and their results are presented below.

Early flame propagation speed models:

1. Turbulent curvature 2. Herweg and Maly

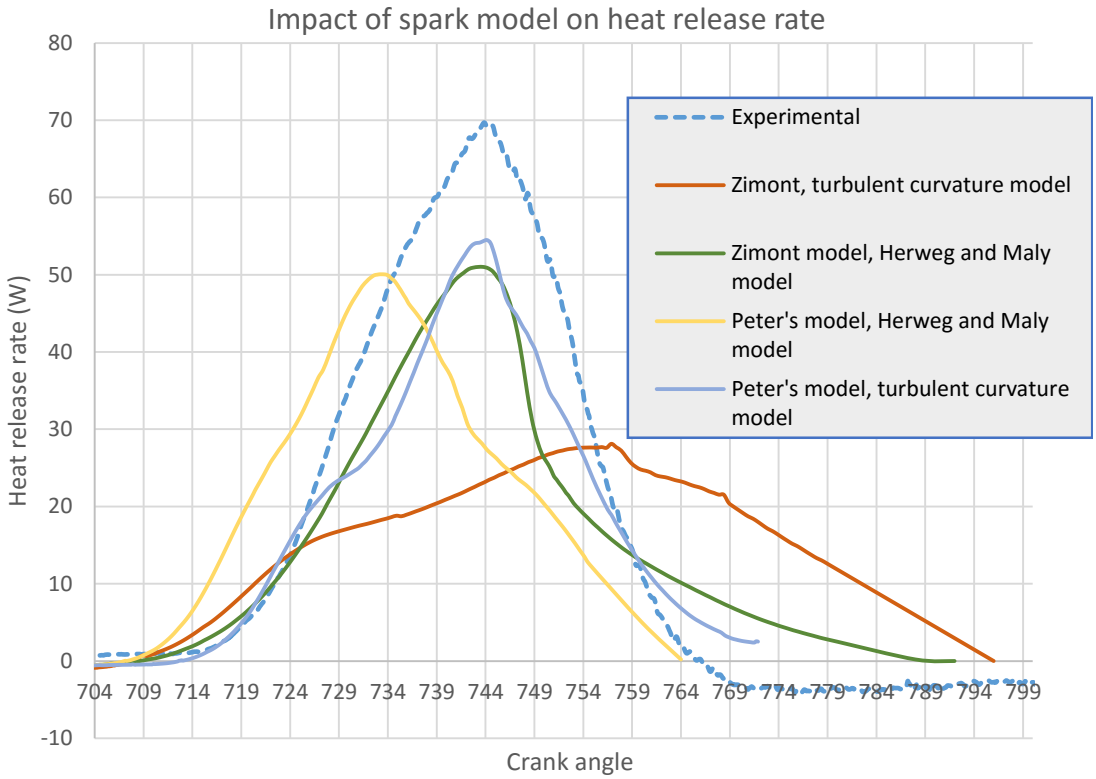

Figure 23- Heat release rate vs initial radius

From fig. 23, it can be observed that with turbulent curvature model, heat release rates from turbulent flame speed model and early flame propagation speed model at the transition has different gradients. This is mainly because turbulent curvature model only considers curvature effects for calculating flame speed. But Herweg and Maly model uses a much-advanced formulation where many factors involve the calculation. Thus, it gives a smooth transition between models. Since Peter's model gives much faster heat release rates and consequently high peak pressures, Zimont model was seen to provide good predictions for fully developed combustion phase.

A significant role in the engine simulation is played by the turbulent combustion model for the fully developed phase. Regarding the flame front description and reaction rate estimation there are different point of views. For instance, the Standard Arrhenius type models assume that the combustion process is completely chemically driven while the Eddy-Break-Up (EBU) type models assume that the combustion process is turbulence driven [25]. Instead, the models that are based on flamelet assumptions take into consideration chemical and turbulence effects altogether.

The model of interest in this paper utilize turbulent flame speed closure to model the combustion with one step global reaction.

5.3 Fully developed combustion (RANS)

Further simulations were done to assess the applicability of the Zimont model [43] [24] [42] and Peters model [52] [38] to predict the heat release rate and in cylinder pressure, and effects of modelling constants and simulation parameters on the final outcome. Several modelling parameters were changed and simulations were done for the combustion part. Among the parameters which were changed, Schmidt number and flame speed constant A were the notable ones. Four different cases were simulated and pressure and heat release rate data were obtained.

RANS based model's inability to solve the turbulent properties accurately in a universal manner was evident when the turbulent Schmidt number (Sc) was changed. This non dimensional constant shows the ratio between mass diffusivity to turbulent diffusivity. Since Zimont model was originally developed for high turbulent combustion, it was suitable to use 0.7 as the default value for Sc. But when it was used with present work, where turbulence is moderately intense, results were not upto a satisfactory level. Hence Unity Schmidt number was utilized for RANS cases as suggested in few literatures [79] [84] to balance out the turbulent diffusion term. Such situations would have been avoided using LES simulations since they only model a small portion of the turbulence spectrum.

Results obtained from the simulations for the 4 different cases are presented below.

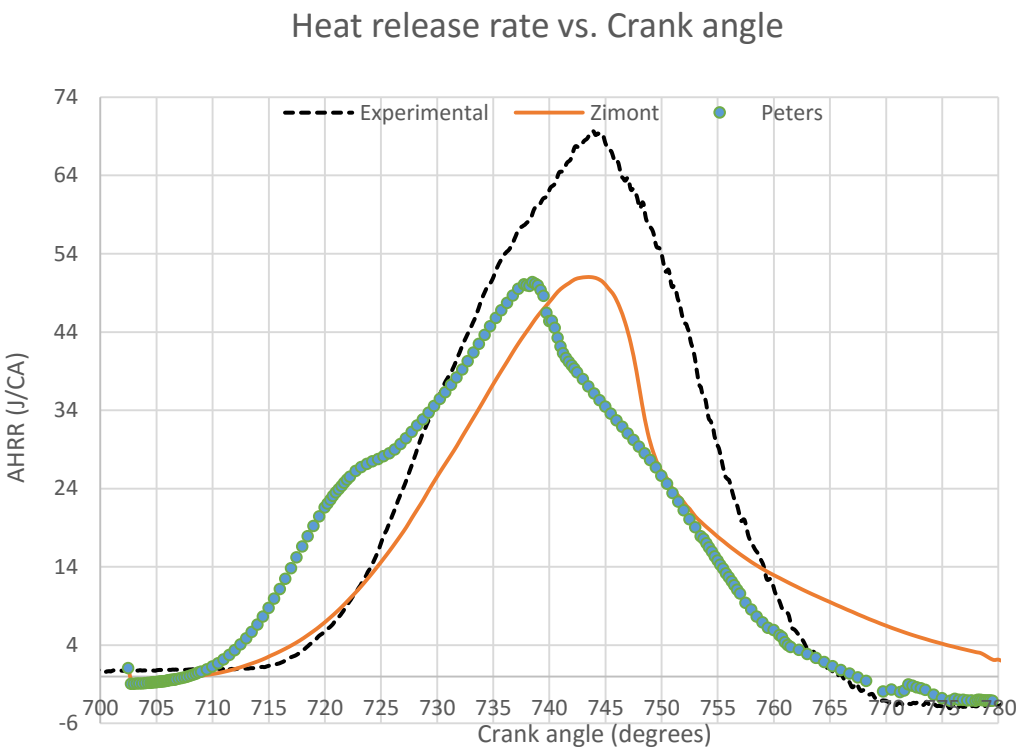

Figure 24- Case 1 heat release rate comparison

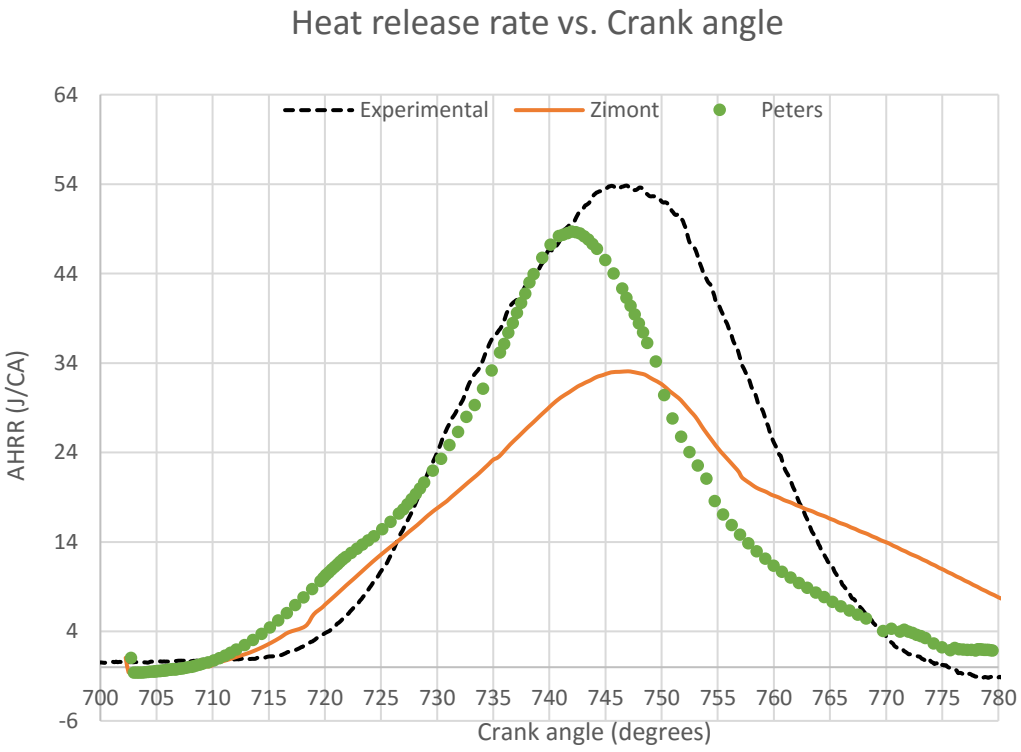

Figure 25- Case 2 heat release rate comparison

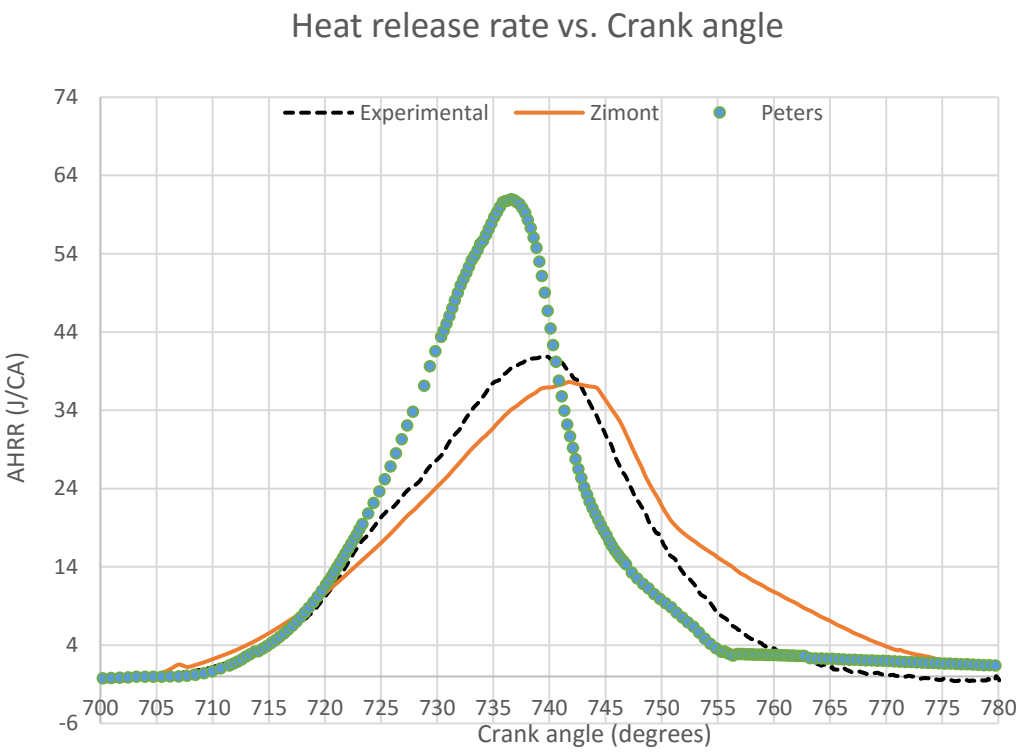

Figure 26- Case 3 heat release rate comparison

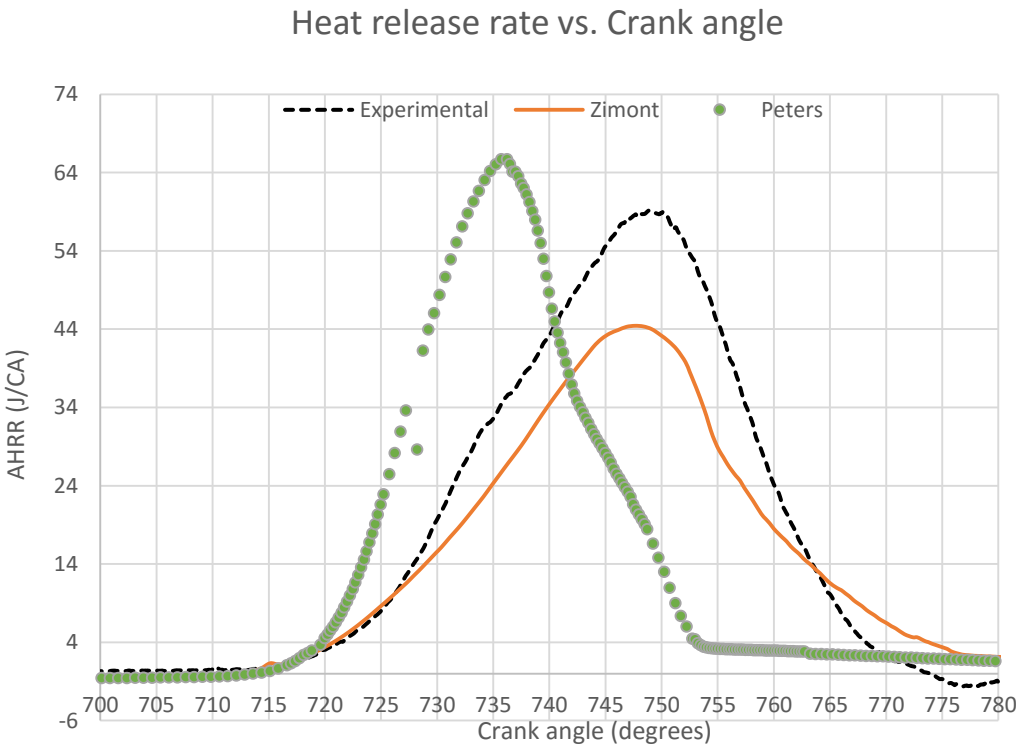

Figure 27- Case 4 heat release rate comparison

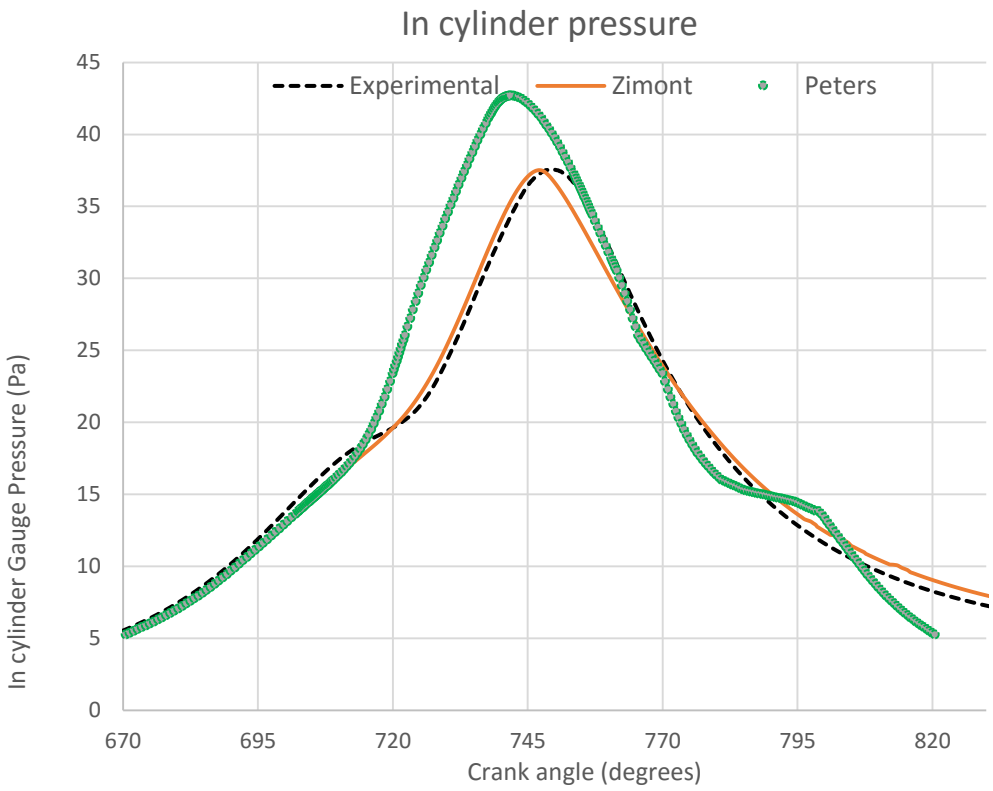

Figure 28- Case 1 In cylinder pressure vs. crank angle comparison

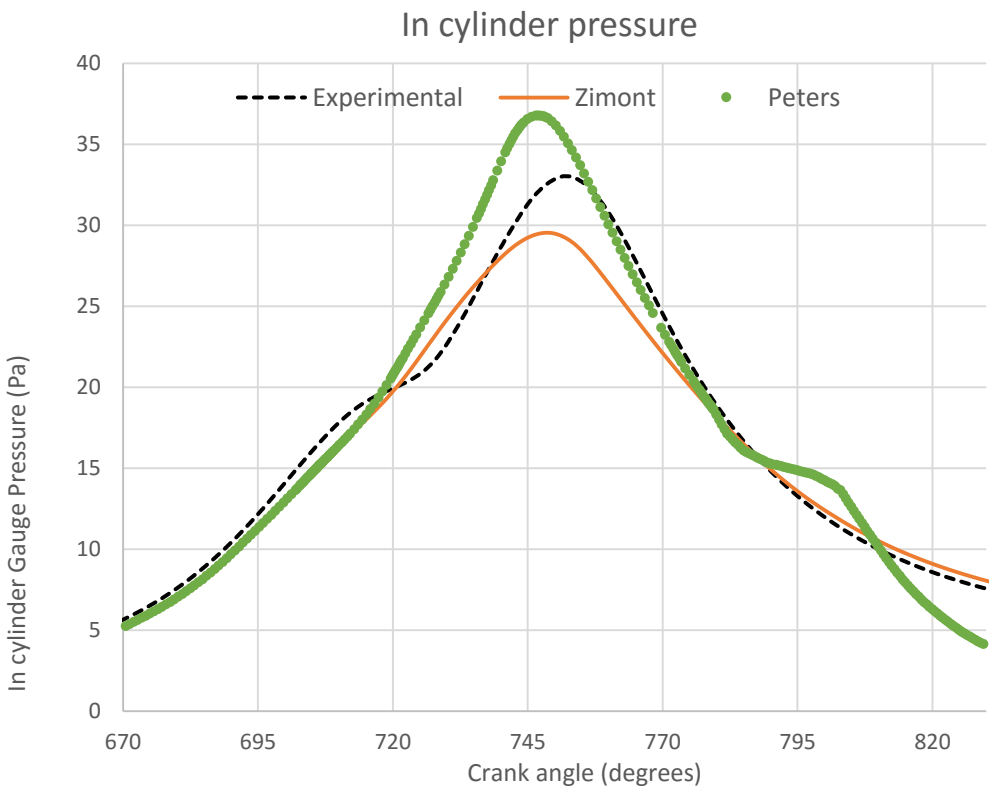

Figure 29- Case2 In cylinder pressure vs. crank angle comparison

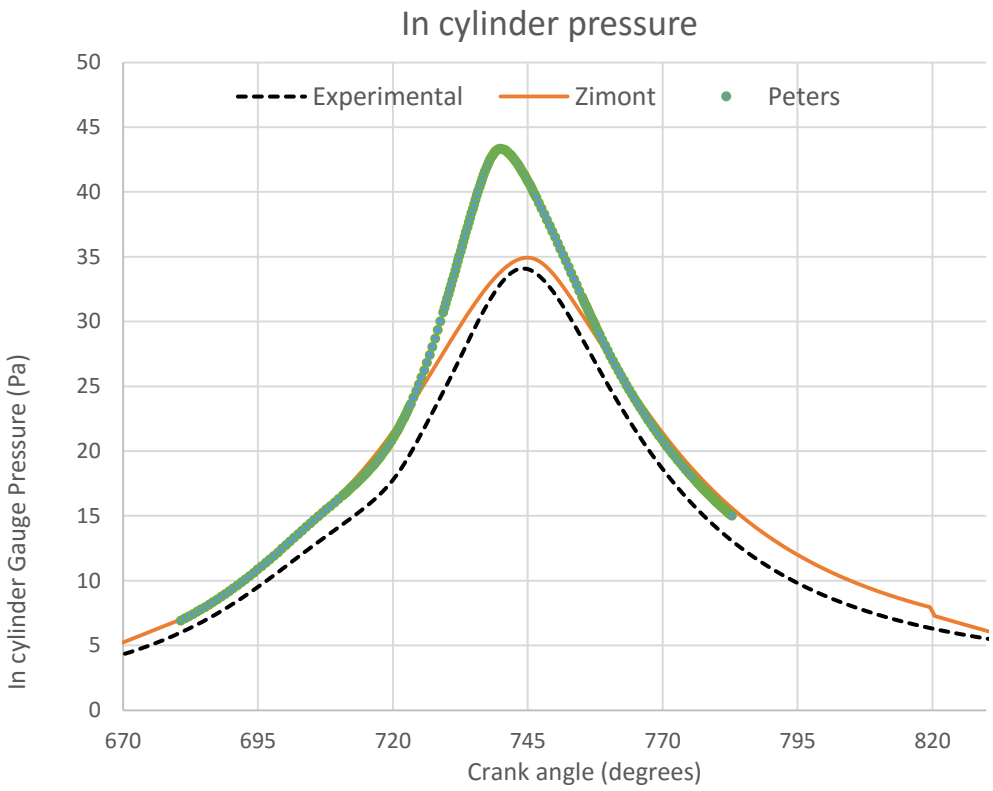

Figure 30- Case 3 In cylinder pressure vs. crank angle comparison

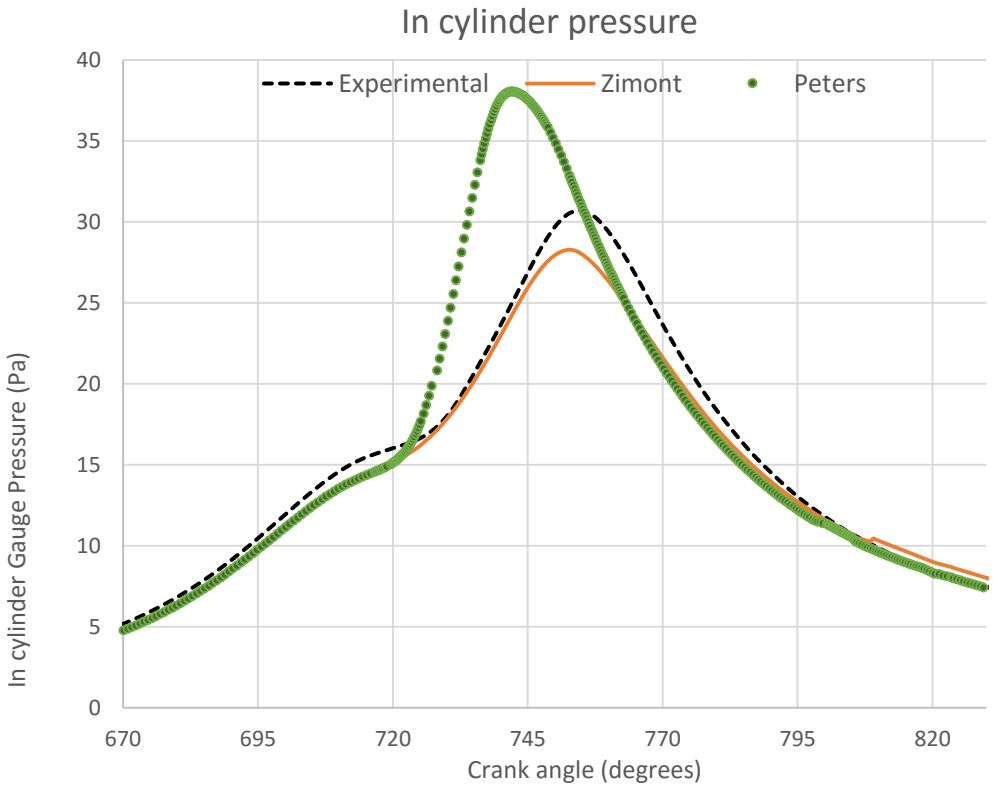

Figure 31- Case 4 In cylinder pressure vs. crank angle comparison

From the comparison of data for pressure and heat release rate, it can be observed that the pressure prediction from the simulation gives values very much closer to the experimental ones when Zimont model was utilized. But a small offset of the peak pressure location can be seen and experimental position occurs after the numerical one in exception of case 3. This can be described by looking at the heat release rate graph.

In heat release rate graphs, at the beginning, a quicker rate for numerical ones can be observed than the experimental ones. This leads the occurance of peak location to happen early.This early prediction of heat release makes the temperature to increase inside the chamber at low volumes, making the in cylinder pressure higher than the experimental value. That issue is much more evident from the results for Peter's model. This over prediction is considerably large and need to be corrected if the Peter's model to be used with engine simulations where turbulence is not that much intense.

In the heat release rate graph, peak values in simulations are smaller than the ones in experimental while the combustion last long in the simulation. That is evident by the spread of heat release rate plot over many crank angles than the experimental one. These mismatches between experimental and numerical values can be due to several reasons. Heat release rate is directly associated with all the parameters: volume of the combustion chamber, in cylinder pressure, crank angle and specific heat capacity ratio of the working fluid. Pressure depends on temperature while progress variable plays a role in prediction of temperature. Therefore, slight change in any parameter affects the outcome. This reason alone causes to put a big weight on each modelling parameter.

Another major reason for this is the formulation used by the software to calculate the AHRR and it has been explained in detail at the beginning of the chapter. Also, Prediction of laminar flame speed plays a vital role in everywhere the flame speed is calculated. Rate of reaction is directly proportional to the laminar flame speed thus errors in its prediction can lead into wrong heat release rate values. This again emphasis the need for an accurate formulation to resolve turbulence properties since they play important roles in governing equations. Also, unavailability of dynamic formulation for significant parameters like Lewis number, Schmidt number was identified as another reason as descried at the beginning of the chapter.

To get the results even up to this level, many number of simulations had to be carried out and lot of fine tuning of modelling parameters had to be done. All these things emphasize the need of a developed combustion model with LES capability, which is the last goal of this study.

HRR results shows that with Peters model, location of the peak is occurred early with respect to the experimental data. This happens due to the over prediction of combustion rate by the model. Since this model is originally developed to use with situations with high levels of turbulence, moderate turbulence in the engine where the data was recorded can be a reason to this mismatch.

But with Zimont model, this problem is somewhat diminished. But still the peak value of heat release is far small than the experimental one. Peak pressures and shape of the heat release rate graph looks reasonable.

6 MODELLING PROCEDURE: LES

6.1 Large eddy simulation (LES)

LES, is generally accepted as the tool of next generation for turbulence modelling [85]. To a certain degree it has enabled bridging the gap between classical RANS modelling and DNS. LES uses a spatial filtering procedure instead of time averaging, where the large-scale motion is calculated exactly and only modelling the effect of sub-filter scale (often called sub-grid-scale (SGS)). That is why, there is preservation of the information of larger eddies than a given cut-off filter scale. Lost is only the sub- filter details. SGS motion's effect on the large scale is found to be universal. As per Kolmogorov theory of turbulence regarding the energy cascade concept, energy is transferred from larger anisotropic eddies to smaller eddies, which remain in equilibrium. The smaller eddies in the bottom range or the inertial sub range are locally isotropic. The eddy characteristics are believed to be universal and not related to the flow geometry [86]. When the modelled SGS part of LES lies within the inertial sub range, this universality belief of the small-scale turbulence is advantageous. The theory itself leads to a possible generic simulation and modelling strategy, where predictions in use do not impact the employed SGS model. Due to above mentioned, LES has become increasingly popular as a more reliable prediction tool than RANS when modelling complex flow configurations usually encountered in engineering [87].

The ability to predict the characteristics of large scale eddies has become a big advantage of LES especially when it comes to IC engines. It enables to study the cyclic variability of engines, make the results more sensitive on design changes and generates more detailed results with high accuracy. The inherent characteristics of an IC engine, like the unsteady nature, moderately high Reynolds numbers and the mid-sized computational domain makes the situation perfect for LES to be used. But still user must put that extra effort to determine which LES models are well suited for his application to get accurate results as quickly as possible. Nevertheless, increasing computational powers have reduced the computational time considerably. These facts have led many people to utilize LES on their studies and creating a best practice is vital in that sense. This paper addresses that need and will provide a support to the researchers to select the best models and sub models for a multi cycle IC engine simulation.

The flow physics in IC engines is well suited for LES method. The moving pistons and valves make the flow to change rapidly in time creating flow structures varying in size. That unsteady nature of the flow can be obtained from a LES solution rather than from a RANS solution because of the time averaging techniques involved in RANS. Large scale flow structures (integral scale) are also a very important part in IC engines. They determine the bulk motion of the flame and plays a big part in constructing the small-scale flow geometry. LES has the profound ability to solve large scale flow structures without employing any modelling thus making those results more reliable. Reynolds numbers have modest values of the engine flows. Generally, they vary in between 10,000 to 30,000 [85]. This means that the flow will not be highly intense in a turbulence point of view and will not require high end computational resources. Hence realistic computational times can be achieved using LES for-engine flows. Finally, the domain size of the interested case is a wall bounded one with a moderate size. This makes the grids employed to have less number of mesh elements which makes using LES a strong possibility. Thus, researches claim that they are reaching DNS (direct numerical simulation) state [88].

6.1.1 Pros and cons of LES

There are several expectations of the research community regarding LES simulation results. Those expectations are the main force driving research communities towards LES for IC engine applications. First is the expectation of more flow structures. As LES simulations only model a portion of the turbulent spectrum, some portion of eddies are solved on computational grid. Also, the lesser values utilized for turbulent viscosity makes LES models less dissipative hence preserving more flow structures [78]. This is verified by Fig. 1 shown below. It shows the velocity vectors at a middle plane along the axis of the combustion chamber obtained 80 degrees before TDC at compression stroke. On the left a vector field with less eddies can be seen which an outcome from a RANS simulation. On the right the LES flow field is more detailed with more vectors and eddies.

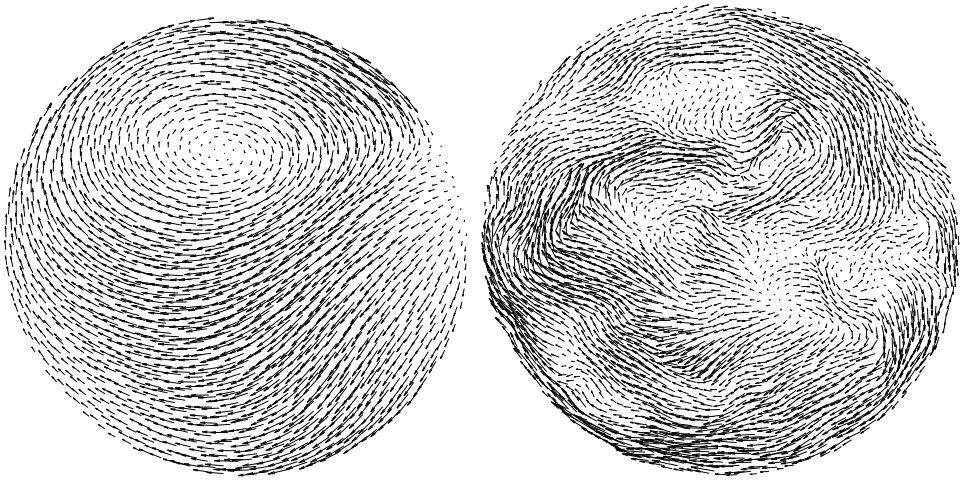

Figure 32- Comparison of velocity vectors from RANS and LES simulations

Often, success of a simulation depends on the empirical tuning of a set of constants. Compared to RANS, LES requires only a low level of empirical input. In fact, there are dynamic LES formulations, where fine tuning does not occur at all. Necessary model parameters are calculated based on the local flow conditions automatically. This way, LES results provide a more complete information on the flow structures, as it produces a direct solution without time averaging [89]. As a result, there are more eddies and vortex structures resolved, in a rather realistic flow field. This enables users to analyze previously inaccessible unstable phenomena, such as cyclic variability in engines [90]. Knowing only the mean characteristics is not always enough for the rapid progress of a field. Three-dimensional turbulence characteristics and effects of combustion instabilities are of particular importance.

These heavily unstable flow behaviors however, cannot be properly predicted with conventional RANS techniques. That is why the one practical possible solution would be to use some form of LES. On the other hand, the predictability of LES is considered to be better since it resolves more of the flow rather than modelling. Since uncertainty of turbulence models are much higher, this claim is believed by many in the scientific community. Yet this is not universally true due to the fact of uncertainty found in boundary conditions, initial conditions and grid resolutions [91]. Even though there are added advantages in a LES simulation, there are some drawbacks to be understood [67]. Since LES uses a spatial filtering technique, validating against experimental results which are

usually averaged values over few cycles will arise the need to run multiple engine cycle simulations. Those results will have to be averaged and compared with experimental data. This is much time consuming additionally to the inherent feature of LES to consume more time. But selection of good LES models enables the user to use coarse meshes which reduces the time considerably. Therefore, selection of the suitable models and sub models plays a vital role in the outcome [9].

When it is considered in IC engine applications, LES has two major beneficial features compared to RANS modelling approach. As the first one, its ability to give more detailed results yield the opportunity to study new phenomena. Not like in RANS, LES utilizes a filtering approach and thus unsteadiness of flow and combustion more accurately captured. This enables to examine many unsteady phenomena which was unable to be accessed using RANS. Next one is the increased design sensitivity. As in flow structures, LES's ability to observe slight changes enables to capture effects from design changes like fuel injection angles for direct injection, small changes in operation (spark timing, injection timing, valve timing) and changes in combustion chamber shape, pistons bowls and port design.

On the other hand, to obtain a cycle averaged result, multiple full engine cycles must be simulated. This is time consuming and expensive since moving parts should also be modeled to run a full cycle. Moving meshes usually slows down the simulation and inherently unstable [92]. Also, since LES can capture complex nature of the processes like spark ignition, fuel spray and emissions, it is needed to have a good knowledge not only to interpret the results, but to use suitable models and formulations to represent those complex processes [74].

6.2 Turbulent premixed combustion in LES context

Due to various benefits provided by LES modelling approach, as described in previous sections, it is considered to be the tool of next generation in IC engine simulations. But still the approach needs to be developed to a state where the flow and combustion problems can be solved efficiently and accurately. On that purpose scientists have developed and assessed various combustion and flow models in LES context. But combustion and flow models alone cannot resolve the whole process inside an IC engine.

There is a need for suitable sub models to solve phenomena like fuel injection, soot formation and spark ignition [93]. In this section, details on such useful models and their experimental and numerical assessments will be discussed.

Flow structures in a solution of a simulation generally occurs due to the non-linear terms present in the momentum equation. Turbulence models do not generate flow structures and what they do is modelling the impact of eddies in unresolved scales. To obtain more flow structures, user have to incorporate denser grids and less dissipative numerical schemes so that more kinetic energy will be present in the resolved scale. The role of the turbulence models can be vital in determining the total computational time when the user want to get more flow structures out from the simulation [86]. Using a simple turbulence model should be done with a denser grid. Denser grids allow more eddies to be solved in a wide range of length scales. The role of turbulence model would be to provide numerical dissipation at smaller scales thus more users tend to use much simpler turbulence models. But this will sometimes cause dissipation over a wide range of length scales making denser grid requirements which ultimately increases the computational time [85].

To use a less dense grid, one must utilize a good turbulence model which has enough dissipation ability to keep the numerical stability of the solution. Such models will dissipate more energy at the sub grid scales which is present due to the coarse meshes employed. In the present work, Smagorinsky-Lilly Model was used to model the turbulence. The reasoning behind the selection was that this model is simple and stable as described above [94] [95]. Major drawback of the model which is its high dissipative nature was countered by using a denser grid. But the grid was not very much denser to maintain reasonable computational times. This dissipative nature of the model does not significantly affect the flow structures resolved by the simulation since the sub grid energy available in an IC engine application is comparatively large to the dissipation done by the model [96] [85].

Nicoud and Ducros [97] developed a variation of Smagorinsky-Lilly Model which is called wall adapting local eddy (WALE) viscosity model. This model had indicated that it can solve flow at near wall regions precisely with coarser meshes. But this claim yet to be verified completely.

Several studies have used WALE model to simulate both engine and non-engine flows with different success [39] [98]. Scale similarity modelling approach is another promising one which was originally proposed by Bardina29 and further developed by Meneveau and Katz [99]. This approach is utilizing the smallest resolved scale to represent the unresolved sub grid scale parameters. In a sense it is logical to use this smallest resolved scale when the grids become denser since it provides much closer approximation to the unresolved scale. But this model is unstable since it does not utilize a turbulence viscosity term. This model has been implemented by several research groups including Lund University group where the work has mainly been focused on homogeneous charge compression ignition (HCCI) combustion. Even though they managed to get satisfactory results, denser grid requirements and unstable nature of the model have posed difficulties. Additionally, there are models much complex with one or more transport equations to resolve sub grid scales which found to produce better results at high computational expense. They are not discussed here since a main objective of the present study was to identify an approach which is simple and computationally inexpensive yet provide good results.

6.2.1 Smagorinsky-Lilly Model

This is a simple model to evaluate the turbulence at sub grid scale which was first proposed by Smagorinsky [100]. In this model eddy-viscosity is modeled using the following equation

$$\mu_t = \rho L_s^2 \sqrt{2 S_{ij} S_{ij}} \tag{41}$$

Where *Ls* is the mixing length for sub grid scales and is computed using the equation below by fluent. *K* and *d* stands for Von Karman constant and distance to the wall, *Cs* is the Smagorinsky constant, and Δ is the local grid scale.

$$L_s = \min(kd, C_s \Delta) \tag{42}$$

$$\Delta = V^{\frac{1}{3}} \tag{43}$$

Δ is computed according to the volume of the computational cell. Lilly derived a value of 0.23 for *Cs* for homogeneous isotropic turbulence in the inertial sub range.

However, this value was found to cause excessive damping of large-scale fluctuations in the presence of mean shear and in transitional flows as near solid boundary and has to be reduced in such regions. In short, *Cs* is not a universal constant, which is the most serious shortcoming of this simple model. Nonetheless, a value of around 0.1 has been found to yield the best results for a wide range of flows, and is the value used in Present work.

Celik [101]was one of the first to use this type of model to simulate LES IC engine. They were able to obtain satisfactory results in their work [102] where they implemented this model on a KIVA code. Simulated intake and compressing flow of a diesel type engine provide accurate results even though the model was developed for RANS. These facts encouraged the author to use Smagorinsky-Lilly Model in present work.

When it comes to modelling combustion, most of the models utilized are extensions of RANS models. This is a clear evidence of the similarity in both modelling approaches and it can be used to develop more efficient computational models. Models with direct integration approach use temperature and species concentrations at the resolved grid scale to model the reaction rate terms. They ignore the influence of sub grid scale flow properties thus making these models better to be used with homogeneous flows and with detailed chemical kinetics. Denser grids are also a suitable way with such models due to the lesser variance in sub grid scale values. Several studies have used these models with LES successfully to simulate low temperature combustion in direct injection diesel engines. Bu with the stringent computational requirements associated with detailed chemical kinetics and denser grids have made the use of such models in LES nearly impossible. There are several identified ways to reduce run times by using improved load balancing techniques and high order advanced numeric. Yet those should be closely monitored due to the presence of approximation errors, especially for events where results are sensitive to kinetic details.

Time scale approach most originally intended for SI engines and afterwards it was adopted for diesel engines in RANS context 75, 76. This model provides good results when their experimental data to fine tune the model coefficients. But difficult is obtaining experimental data for SI engines has become a draw back. Nevertheless, this model drives species concentrations to local equilibrium values in combination with flamelet approach.

This model has provided satisfactory results for LES simulations in diesel engines applications 78. It is yet to be used with LES simulations for SI engines.

Flame sheet approximation to represent premixed flames is been used in to major approaches. One is the famous C-equation approach which has been used in present work. It has already been described in previous chapter. Other one is G- equation approach and has also been described previously in RANS context. For LES, C- equation approach associated with a Smagorinsky-Lilly model type turbulence model has been used and provided good results in the studies conducted by the group at Lund University 83- 85. They have mainly focused on HCCI engine applications and the results have been compared against experimental pressure values which has shown good predictions. This success of C equation models is partly because the transformation of progress variable approach into LES from RANS is based on a simpler formulation which is known as thickened flame model [86]. It artificially increases the thickness of the flame and consequently computational times are reduced. Thus, utilizing denser grids become economical and more scales are resolved in the grid giving access to more details. Hence is was encouraged to use this approach in present work.

6.2.2 Zimont in LES

Since the theoretical details and practical implementations of the model has already been discussed, only the adaptations of the model formulation to be suited in LES use will be presented here. The equation for integral length scale in RANS formulation is replaced by the following formula where is C_s the Smagorinsky constant and Δ is the characteristics length scale of the grid.

$$l_t = C_s \Delta \tag{44}$$

Sub grid velocity fluctuation calculated by following equation is used in place of RMS velocity and T_{sgs}^{-1} the mixing rate at sub grid scale is calculated from the inverse of sub grid time scale.

$$u' = l_t T_{sgs}^{-1} \tag{45}$$

7 RESULTS AND DISCUSSION: LES

The multi-scale modelling approach of LES naturally provides a better understanding of large scale unstable phenomena and that is why, it bears a high potential in predicting the engine instability. But LES would be problematic at sometimes, since, to obtain a statistically converged mean solution in engine applications it requires hundreds of continuous cycle simulations. But still this makes LES much more suited for engine applications since large number of cycles helps to identify the cyclic variability of IC engines thus enabling developers to check their novel geometrical and operational conditions. Even though LES techniques have been used for non-reactive flow modelling widely, its use on combustion simulations, specifically on engine applications are somewhat limited. In this section, the applicability of LES techniques on an IC engine with moderate turbulence level was assessed.

LES and RANS both assume that the effect of the modelled part of turbulence on the resolved part is diffusive. This is being considered by introducing an eddy viscosity, often called as the turbulent viscosity [103]. Importance degree of the eddy viscosity in a simulation is compared to the level of modelled portion of the energy spectrum. Therefore, eddy viscosity role is much persuasive in RANS, taking into consideration that the entire energy spectrum is modelled. In LES, it is only utilized for the sub grid scale turbulence, but still need of a robust and accurate turbulence model is vital. Main goal of a LES turbulence model is to resolve more flow structures and it can be done in two ways. One is to use a lesser dissipative turbulence model and other is to use a denser grid. In present work, the used LES turbulence model: Smagorinsky-Lilly, which is known to be a much dissipative model, was utilized since much denser grid was used for the simulations in the presence of high performance computers and its simple and stable nature. Also, it was needed by the author to assess the predictability of the Smagorinsky-Lilly model in the context of engine applications.

.

Bulk motion of the flow inside the cylinder is a predominant factor in deciding the duration of the combustion and macro flame structure. Ability of LES to capture the unsteady nature of flow and flame has enabled studying the cyclic variations and possible causes for those variations. Opening of intake valve occurs at the latter stage of the closing of exhaust valve where piston is closer to the TDC. Since the pressure inside the chamber is relatively high due to compression, initially the burnt gases start to move out through the intake valve mixing with the fresh charge. As the piston goes down, pressure inside the chamber drops below the intake manifold pressure making the fresh charge to come inside. Small valve lift in the order of 0.2mm and the rapid downward motion of the piston generates a high-speed jet of fuel air mixture through the valve opening which later strongly contributes to the turbulence inside the chamber [22] [104]. Following set of figures depicts the evolution of the flow during the intake and compression strokes and the specific features associated with the flow are discussed.

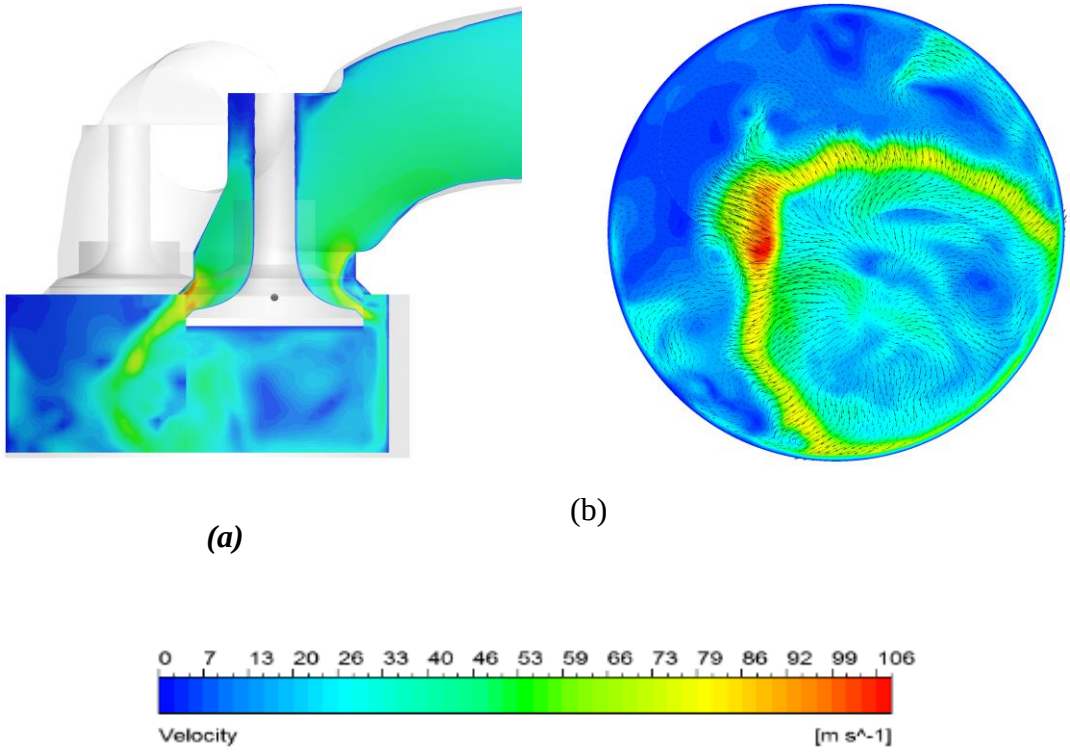

(a) (b)

Figure 33- Evolution of the flow in the cylinder

During intake stroke at 41 CA after TDC in intake stroke

(a) Flow across the intake valve plane (b) Z = 11.5 cm above the BDC

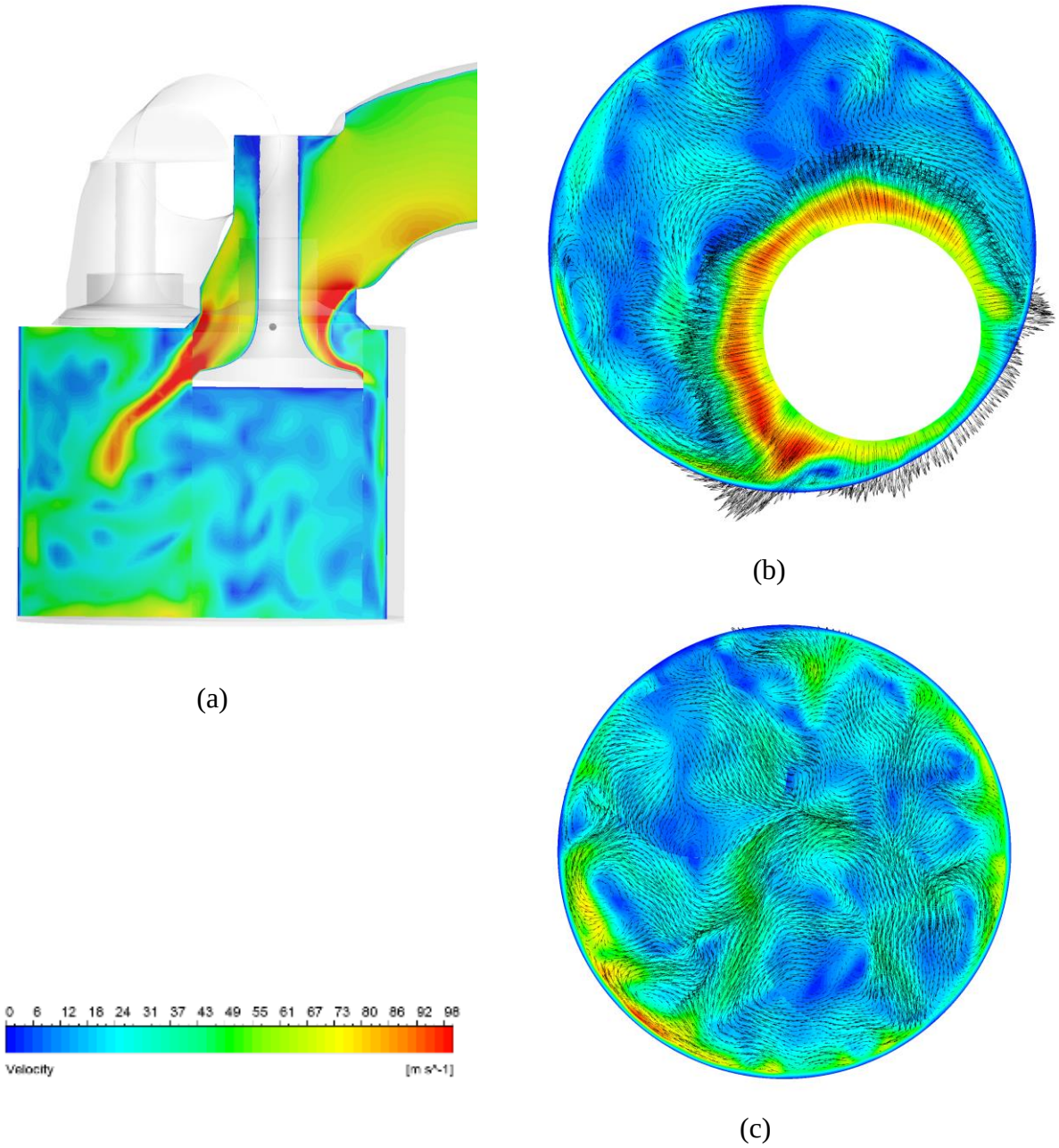

(a)

(b)

(c)

Figure 34- Flow in the cylinder during intake stroke

At 71 CA after TDC in intake stroke

(a) Flow across the intake valve plane (b) Z = 11.5 cm above the BDC

(c) Z = 8.0 cm above the BDC

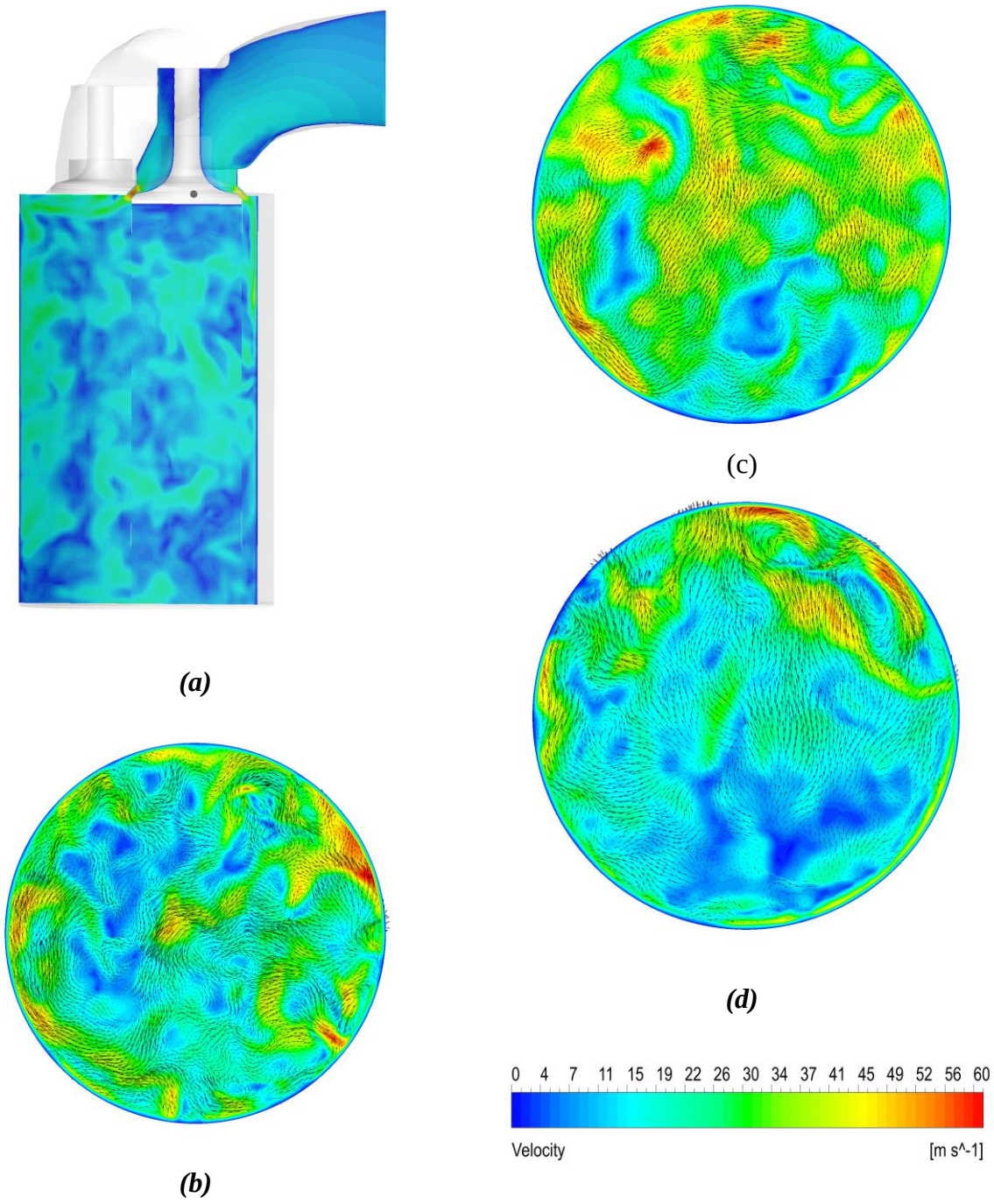

Figure 35 - Evolution of the flow in the cylinder during intake stroke

At 19 CA before BDC in intake stroke

(a) Flow across the intake valve plane (b) 11.5 cm above the BDC

(c) 8.0 cm above the BDC (d) 4.5 cm above the BDC

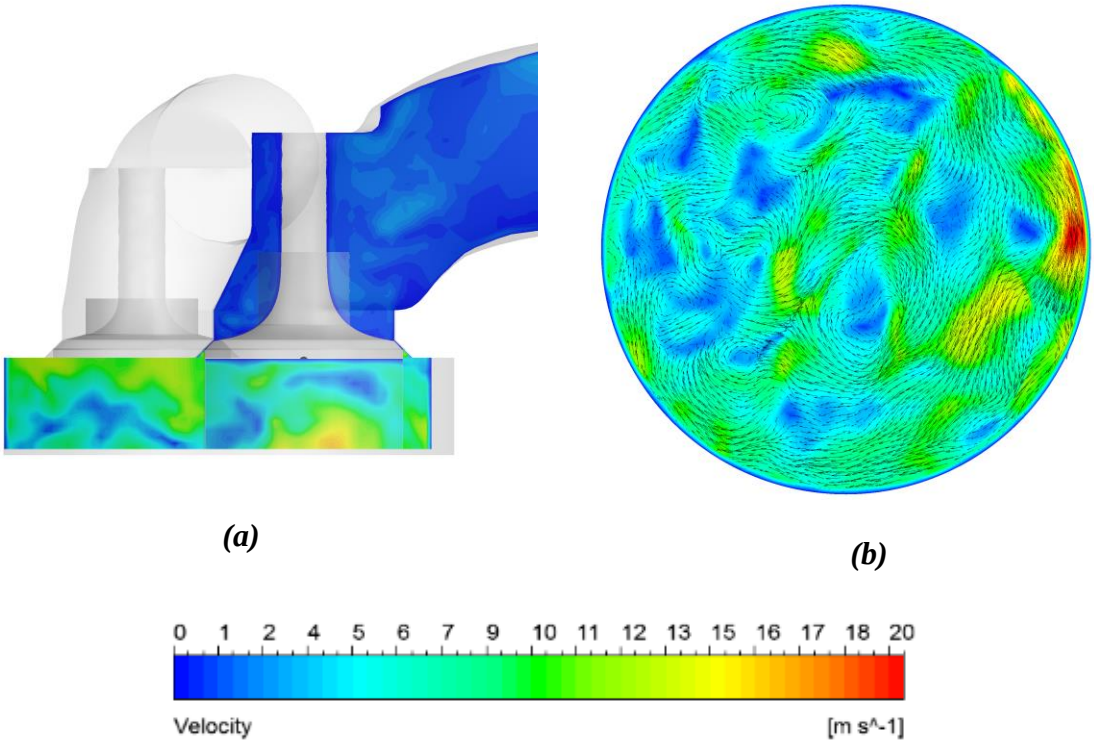

Figure 36- Flow structures inside the cylinder during compression stroke

At 14 CA before TDC

Flow velocity variation across the intake valve plane for several crank angles in the intake stroke and compression stroke are shown here with the same for few planes normal to the cylinder axis. Tangential velocity vectors are also shown in the normal planes as vector plots by arrows. Selected normal planes are located at 11.5 cm, 8 cm and 4.5 cm above the bottom dead center (BDC). As depicted in the above figures, high speed jet of fresh charge collides with the cylinder wall generating high turbulence levels with complex flow structures. Also, interaction of the flow with the moving piston creates tumbling flow which enhances the mixing of fresh charge with the trapped burnt gases inside the chamber. Usually, the valves and the motion of the piston are configured to generate large scale of tumble motion which has an axis of rotation perpendicular to the cylinder axis. In this E6 engine arrangement the tumbling motion is not that much strong compared to an actual automobile engine yet considerable. Even though there are many flow structures in various sizes can be identified from the figures, no strong swirl motion can be identified. If many LES cycles are averaged, swirl can be seen as seen in RANS. But many eddies can be seen which make highly complex flow patterns around the cylinder axis.

Figure 37 shows the flow velocity at a crank angle of 19 degrees before BDC in suction stroke and in that figure, large reduction of flow velocities can be observed. This happens due to the dissipation of energy at the walls and the reduction of intake pressure gradient. At this stage, fresh charge is almost completely mixed with the trapped air and only small region under the intake valve shows no mixing.

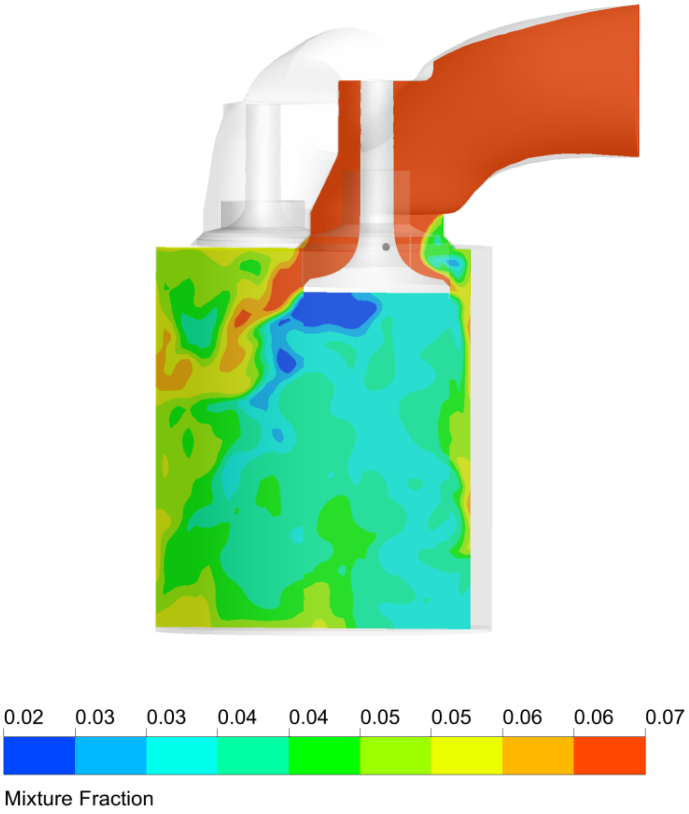

Figure 37 - Variation of mixture fraction across the intake valve plane

At 19 crank angles before BDC in suction stroke

When the piston moves closer to TDC during the compression stroke, flow velocity is reduced significantly and the flow structures has become more arranged and less strong compared to the initial stages. Yet localized flow structures can be observed which later will help for the propagation of the flame kernel from spark and the propagation of the turbulent flame.

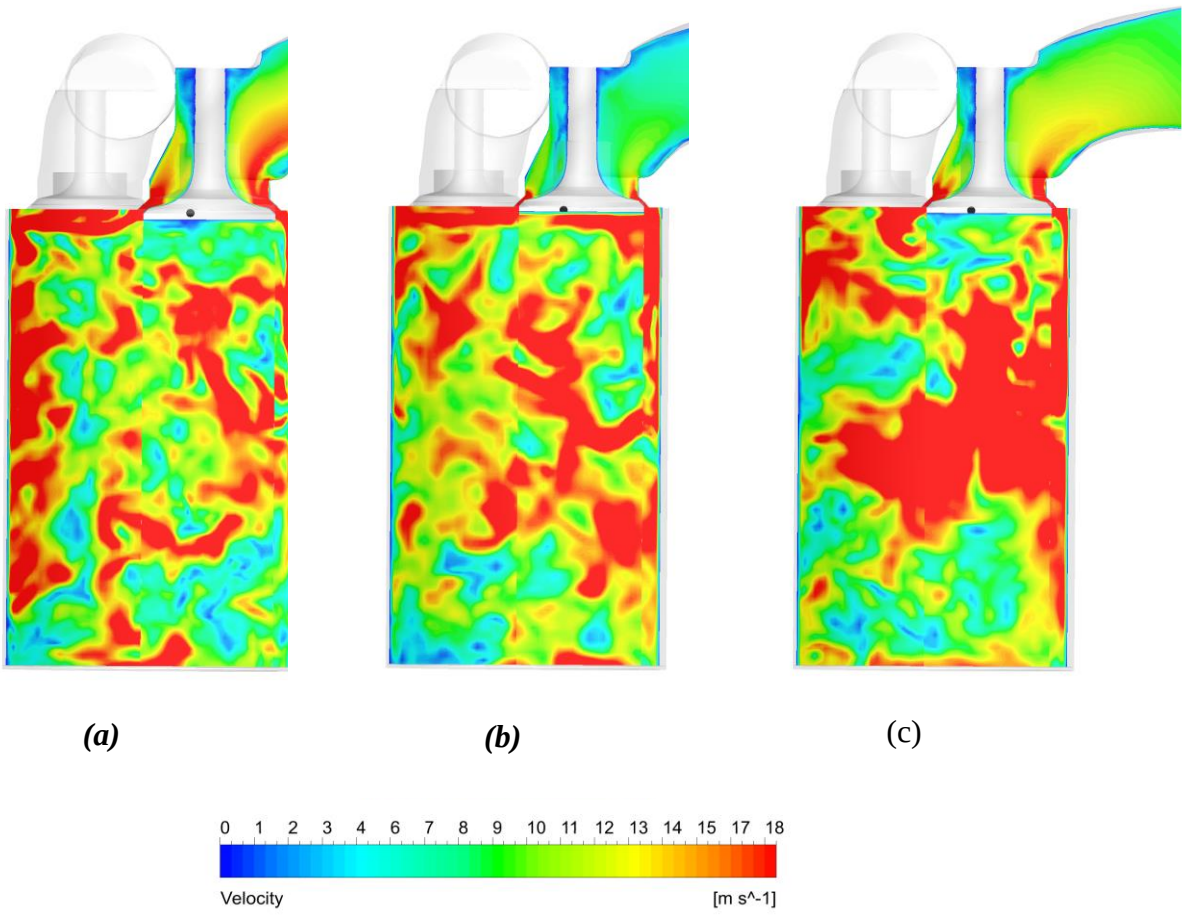

Figure 38 – Variation of magnitude of velocity across the intake valve plane

When the piston is near to BDC for 3 consecutive engine cycles for case 1

As described in previous chapters, cycle by cycle variation of the flow inside the chamber is an inherent feature of IC engines. From the figures 36 and 37 a significant difference in flow structures and its movement can be identified. Above figures were taken at 3 consecutive engine cycles across the intake valve plane when the piston is at the BDC during intake stroke. A substantial difference in flow structures is visible between the cycles, yet on a macro scale, the distribution of velocity magnitudes looks same. Local flow still looks significantly different and these differences causes uneven fuel air mixing inside the engine. These dissimilarities are one major reason for the cyclic variations since uneven mixing affect the effectiveness of the combustion process. Variation of convective bulk flow motion between the cycles are also visible in these figures. These differences affect the flame propagation characteristics and it causes the pressure and heat release rate be different in each consecutive cycle.

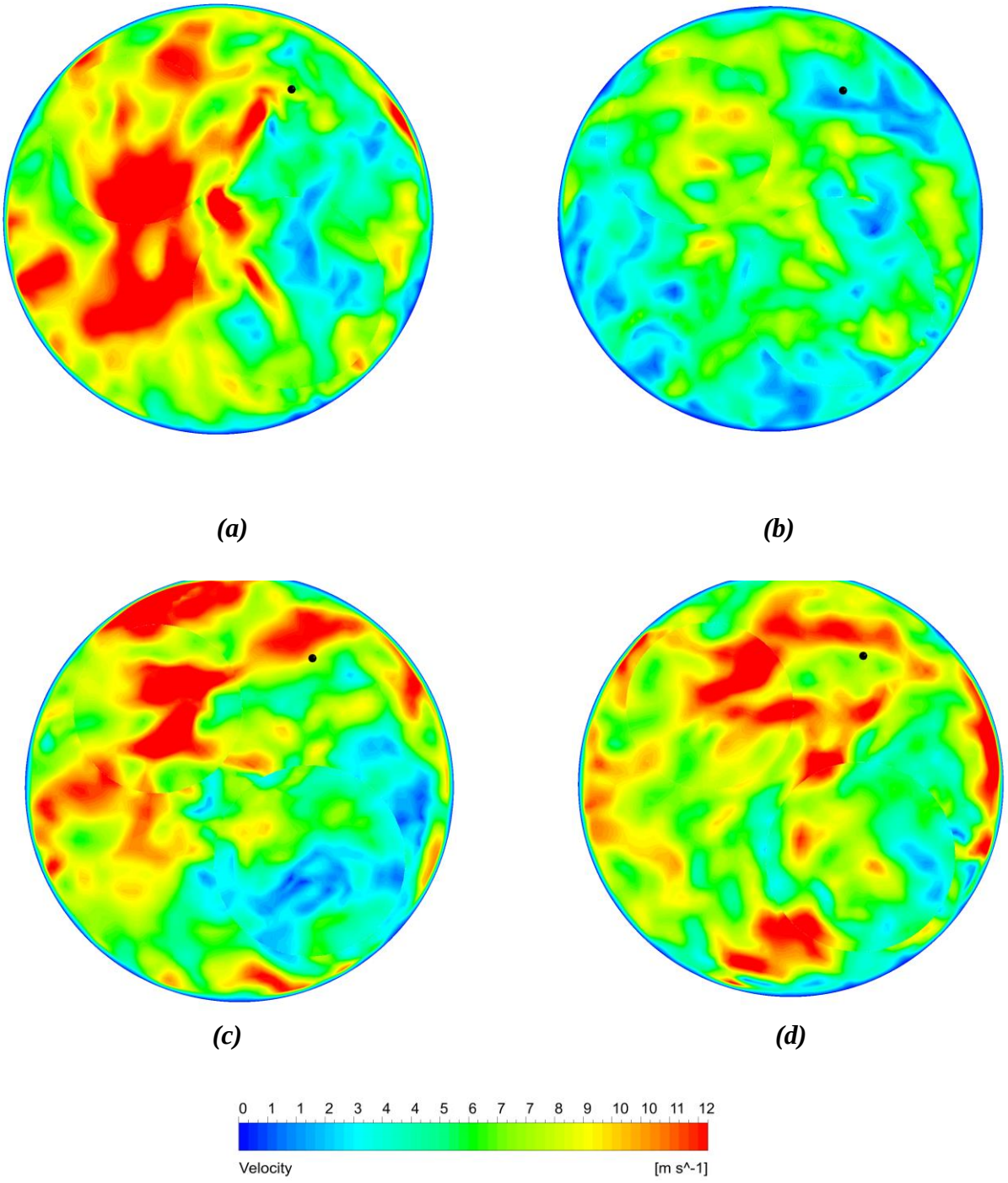

***Figure 39– Variation of magnitude of velocity across a plane located closer to* Spark point Few degrees before the occurrence of spark for 4 consecutive engine cycles for case 1**

Plots to have different shapes. Differences in bulk flow motion also affect the spark formation and propagation since intensive bulk flows tend to move flame kernels. Figure 39 show the variation of flow velocity near the spark location prior to the ignition.

Variations of the flow velocity and structures are significant and it is expected in this type of engines. These variations cause the flame to be propagated differently in different engine cycles and as a result pressure and heat release rate predictions will be different from each other. Furthermore, it is visible from these results at the spark location the magnitude of velocity is smaller than the rest of the domain. This is somewhat expected since lesser velocities does not quench the flame prematurely. Ability to capture more flow structures by LES is also visible from these velocity predictions. What is significant is that even the mesh employed in this case being a coarser one, the prediction of flow structures is up to the mark and it shows the potential that LES possess to become the standard in engine computations. The resolved flow features are not just some arbitrary structures. They represent some of most influences flow features which are expected in engine cylinder flows prior to ignition. These flow features have a big say on engine performances. Employed SGS model plays a vital part in determination of this solution.

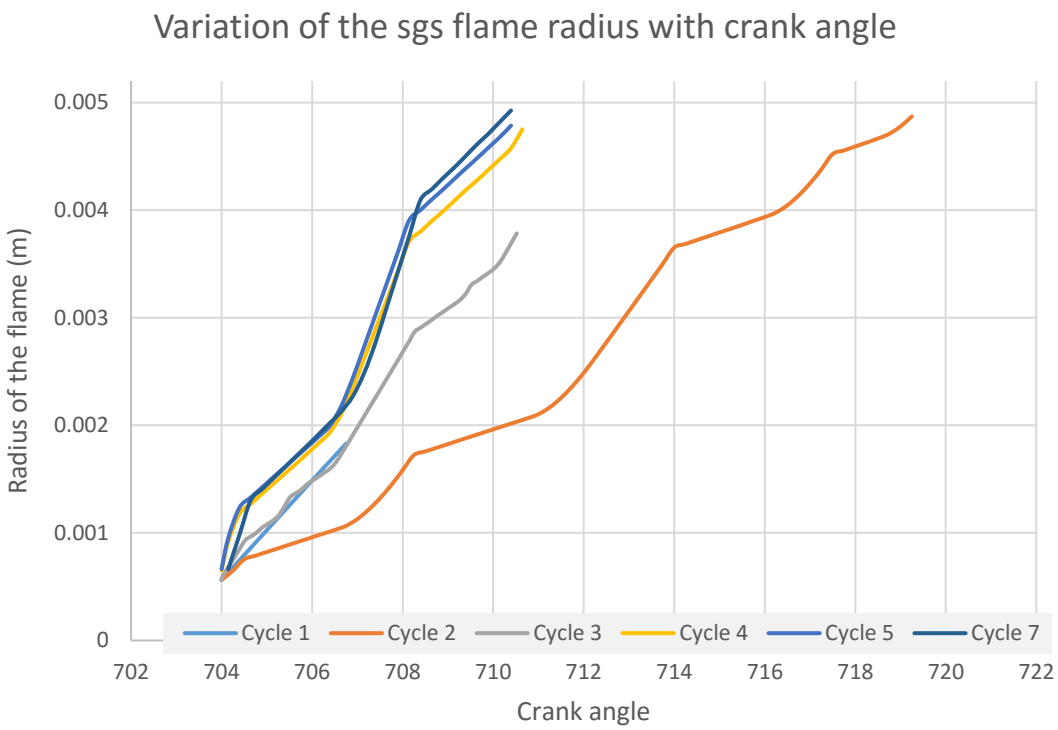

Figure 40 - Variation of the sub grid scale flame radius with crank angle.

End point of the plot represents the transition point.

Figure 40 shows the variation of flame kernel radius with crank angle up to the transition point after which the main combustion model takes control of the flame propagation calculations from the spark speed model.

It can be observed that even in the early stage of the flame, there are significant differences in flame kernel growth and transition radius in consecutive engine cycles. Additionally, no direct relationship between the transition radius and flame area can be observed from these results. This emphasis the fact that the transition point depends on the local turbulence and thermodynamic properties rather than only on the flame properties. It is suggested to study further about the dependency of pressure and heat release rate on the transition point. Observation of the flame surface for 3 consecutive cycles like in following figures, reveal the considerable differences between shapes and sizes of flame kernel. It can be observed the distortion and deformation of the flame surface and deviation of the kernel from the location of the spark. This is an evidence for the significant variation of local turbulence properties cycle by cycle.

But to interpret these variations more qualitatively and quantitatively, further experimental data is needed. Also, it is noticeable from these figures the spherical shape of the flame kernel in its initial state. This is an experimentally observed detail and a duration of 10 crank angles after ignition has been identified.

Crank angle	**Crank angles are given taking ignition crank angle as the reference point**	
	cycle 3	**cycle 4**
7 degrees after ignition	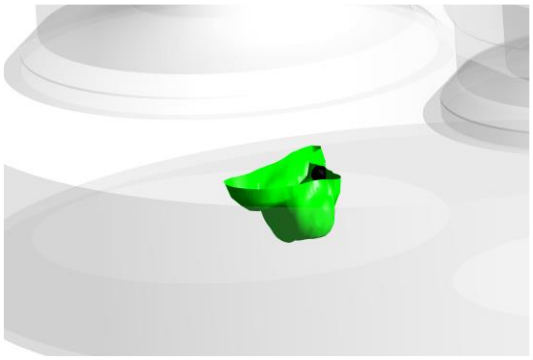	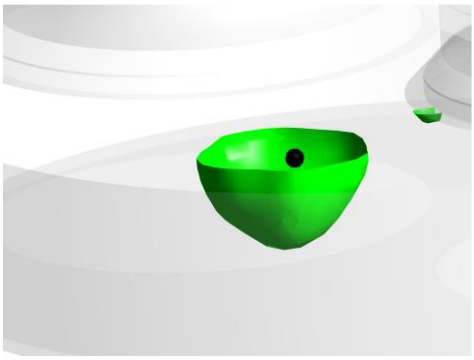
12 degrees after ignition	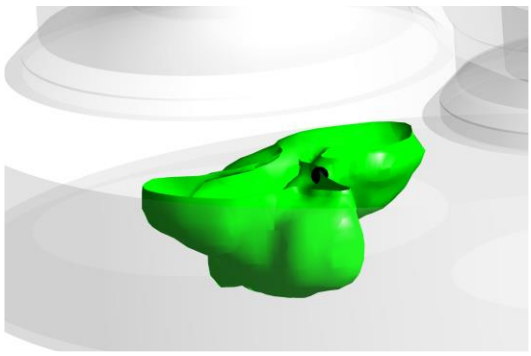	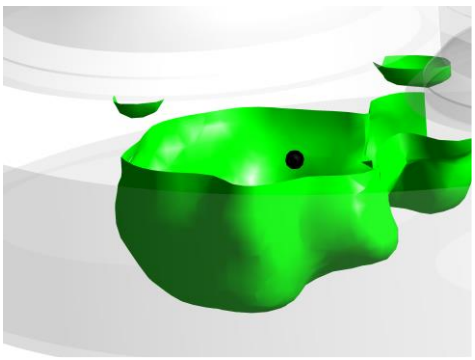
17 degrees after ignition	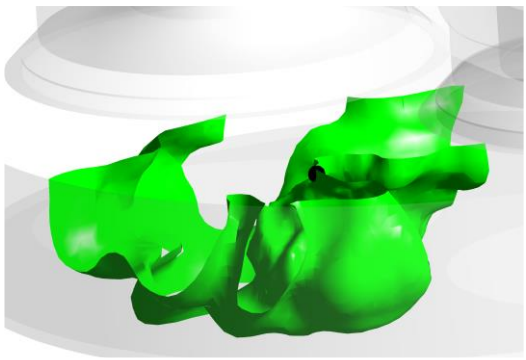	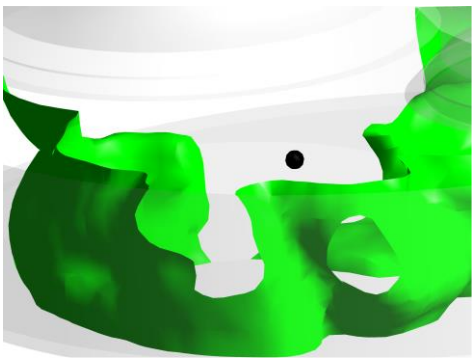

As the common period for the flame kernel to have a spherical shape [10]. Present simulations verify the above fact and effect of turbulence can only be observed after 10 crank angles from ignition.

CA **Crank angles are given taking ignition crank angle as the reference point**

7 degrees after ignition

12 degrees after ignition

17 degrees after ignition

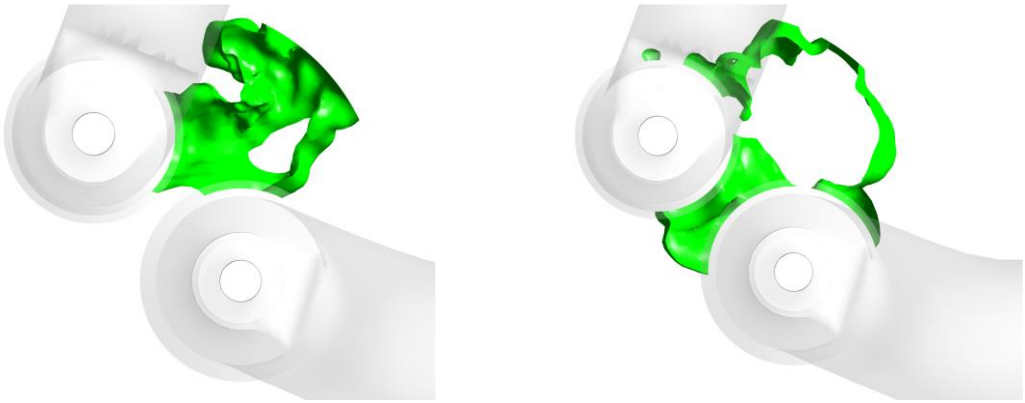

22 degrees after ignition

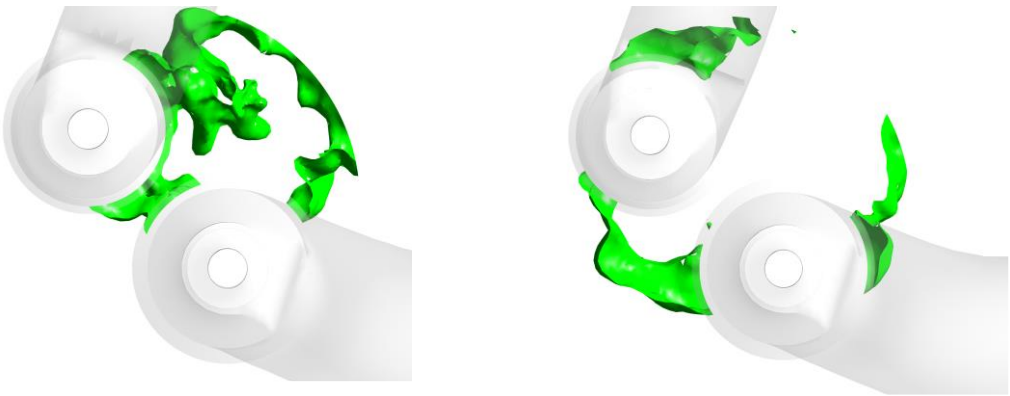

As shown in sets of figures above, significant differences of flame geometry between consecutive cycles for the full developed stage was also identified. Progress variable was used to represent Even though the instantaneous profile of the flame surface shows vast differences, its global direction of propagation and the enclosed volume seems to behave in the same manner for all cycles. Availability of a wide spectrum of turbulence inside the engine cylinder configuration is verified by the highly wrinkled nature of the flame even at the early stages of flame development.

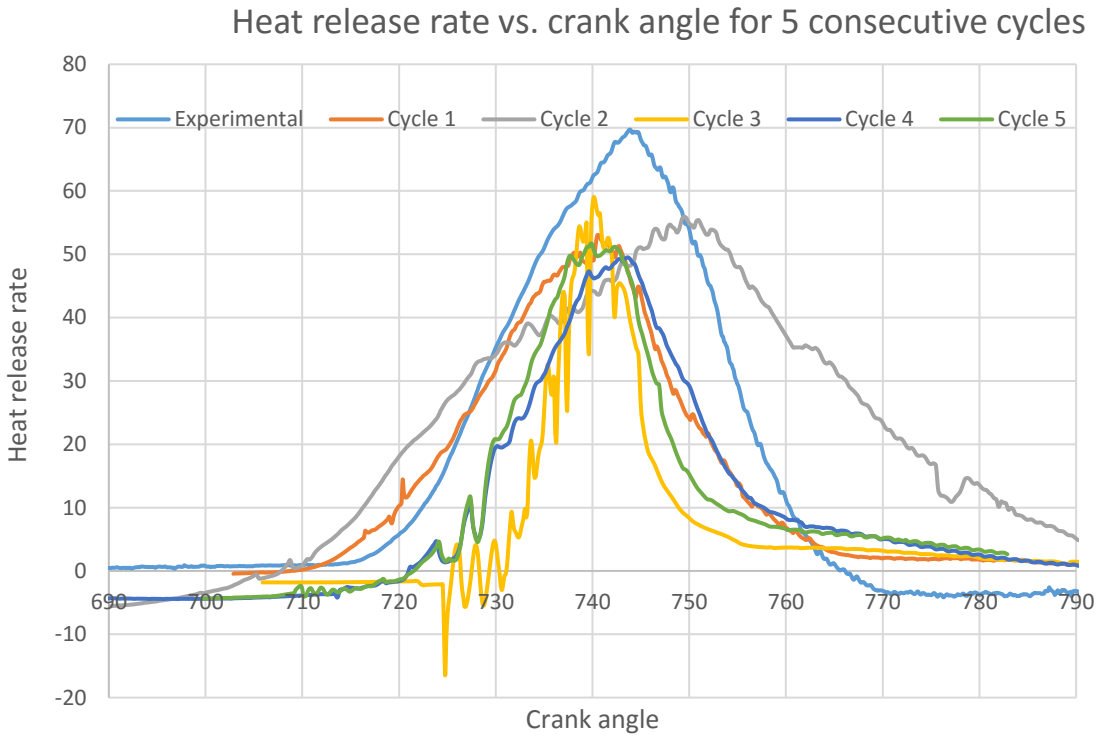

Figure 41 – Variation of heat release rate for 5 consecutive engine cycles

In the graph, significant variation from the average shape can be observed for cycle 2 and 3. Since the 1st cycle starts few degrees before intake valve opening, it does not accurately generate the residual gas properties inside the engine chamber as expected in an actual full cycle engine combustion. Thus, the simulation needs some time to adjust and this may be the reason for the difference of those plots. As in heat release rate plots, pressure plots also differ from one another in consecutive cycles. Pressure directly depends on the heat release rate; hence these variations are expected.

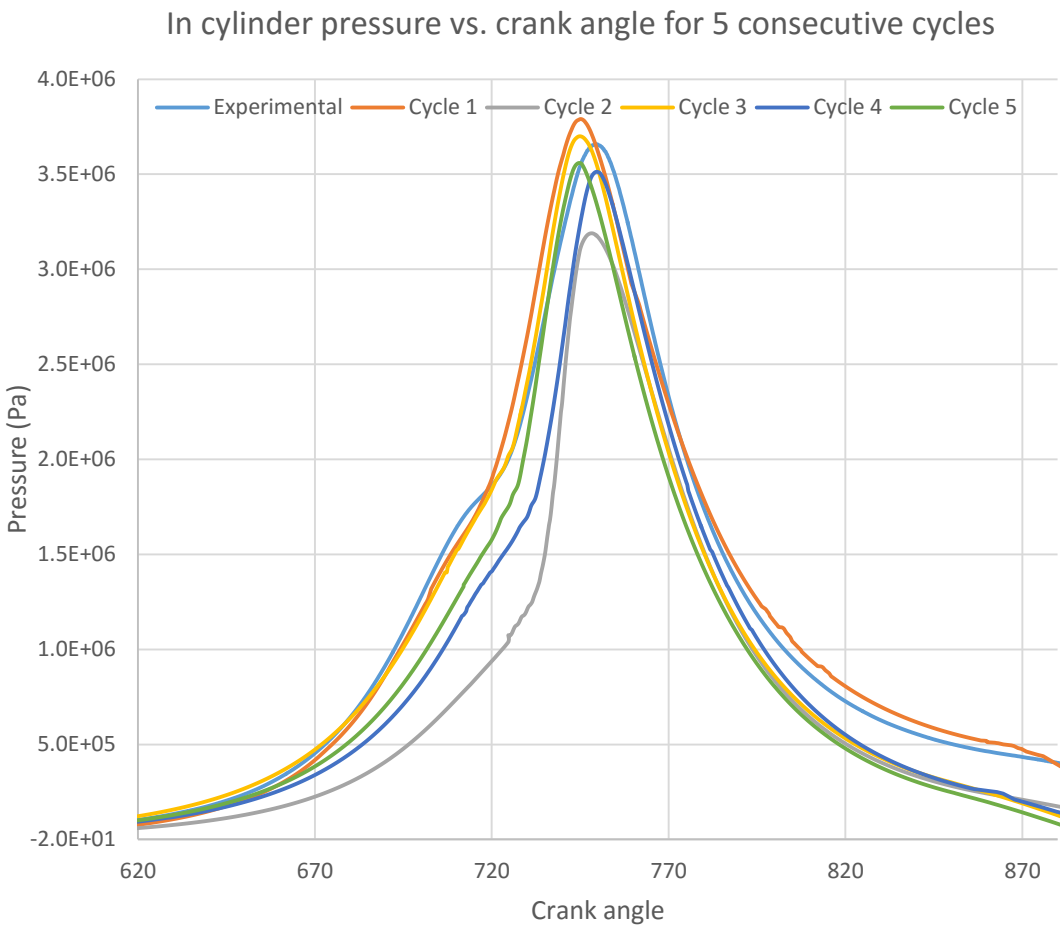

Figure 42 - Variation of in cylinder pressure for 5 consecutive engine cycles

Since there are significant variations in heat release rate graph, considerable variations in the pressure plot was also expected. From figure 42, it can be observed that there are some changes in peak pressure and peak pressure location in each engine cycle but they are not high as it was in the heat release rate plot. This may be because the heat release rate directly involve with the rate of combustion due to the formula being used and pressure has much more allowance given to stabilize in the formulation. Also these cyclic changes in pressure and heat release rate is a good indication of the potential of LES techniques to identify cycle to cycle variations and their underlying physics. Still there is room for improvement in both formulation and modelling techniques to obtain more accurate results.

8 CONCLUSION AND RECOMMENDATIONS

The main objectives of present work were to evaluate the applicability of two well-known turbulent combustion models (Peter's model and Zimont model) in premixed SI engine applications. At first stage, both models were used in RANS context to resolve the flow fields with 4 benchmark test cases and based on those results Zimont model was identified as the most suited model out of both to be used in simulations when the turbulence levels are moderate. The pressure and heat release rates predicted by the Peters model was higher than the experimental values and it tends to transfer the combustion flame speed calculations to the fully developed combustion speed model earlier. Hence, at the second stage, Zimont model with LES techniques were used to simulate multiple cycles.

From the results, it can be concluded that the Zimont model has some issues in predicting the heat release data for a gasoline fueled premixed SI engine with moderate level of turbulence. At the beginning, predicted pressure and heat release rate values differ from experimental values considerably. This may be because of simulation taking time to stabilize the interior conditions of the engine chamber. Since the first cycle starts from the beginning of intake stroke and others run a full cycle, these differences were expected. But still with tuning up modelling constants and refining boundary conditions will yield desirable results. But that is a tedious and time-consuming task as experienced by the author. Hence present work proves the need of improvement in Zimont model.

Furthermore, as the simulation progresses for several cycles, results vary by a small amount and this shows that the system is somewhat exhibiting steady kind of an operation. This is not a desired situation since a major goal of LES simulations is to identify the cyclic variability. This stagnation may be due to non-utilization of proper allocations for intake and exhaust port systems and proper evaluation of varying intake and exhaust conditions. Thus, to obtain more accurate results modelling those portions are recommended. But that will considerably increase the computational time and therefore modelling the port bodies separately and running a motored cycle simulation to determine the boundary conditions are recommended.

Another fact identified is the high dependence of the model on modelling constants. Especially if dealing with new designs or significantly different operating conditions [11], the weaknesses of the models is that it should tune empirically, one or more model coefficients or other input parameters referring to experimental data to obtain satisfactory quantitative predictions. There are two main factors that contribute to this; there should be a consequence associated with the large number of simplifying modelling assumptions or due to the poor understanding of the actual phenomenon.

At the early stages of the flame kernel formation, unavailability or the inaccessibility of data related to spark discharge and early flame geometry is a major concern since the fully developed flame characteristics depend on the features and behavior of the early flame. Therefore, more studies should be done to identify the ways to minimize the influence of these inputs on fully developed flame.

9 REFERENCES

[1] F.Charlette, C.Meneveau and D.Veynante, "A Power-Law Flame Wrinkling Model for LES Of Premixed Turbulent Combustion Part I: Non-Dynamic Formulation And Initial Tests," *Combustion and Flame,* pp. 151-180., 2002.

[2] D.A., North G.L. and Santavicca, "The Fractal Nature of Premixed Turbulent Flames,Combustion Science and Technology, 72:," 1990, pp. 215-232.

[3] D.C.Haworth, "Large-Eddy Simulation of In-Cylinder Flows," *Oil & Gas Science and Technology,* vol. 54, pp. 175 - 185, 1999.

[4] E.G.Groff and Sinnamon, "The Effect of Ignition Location in a Swirl Field on Homogeneous Charge Combustion," *SAE,* p. 821221, 1981.

[5] D.Goryntsev, A.Sadiki and J.Janicka, "Cycle-to-Cycle Variations Based Unsteady Effects on Spray Combustion in Internal Combustion Engines by Using LES," *SAE Paper,* pp. 2012-01-0399, 2012.

[6] B.H.Hjertager and B.F.Magnussen, "On Mathematical Modeling of Turbulent Combustionwith Special Emphasis on Soot Formation and Combustion," in *Sixteenth Symposium(International) on Combustion,* 1976.

[7] K.N.C.Bray, R. Britter and T.C.Chew, "Spatially Resolved Flamelet Statistics for Reaction Rate Modelling," *Combustion and Flame,* pp. 65-82, 1990.

[8] K.R., Sreenivasan, "On the Scaling of the Turbulent Energy Dissipation Rate, Physics of Fluids,27:," 1984, pp. 1048-1051.

[9] A.Leonard, "Energy Cascade in Large-Eddy Simulations of Turbulent Fluid Flows,," *Advances in Geophysics,* vol. 18, pp. 237-248, 1974.

[10] J.B.Heywood, Internal Combustion Engine Fundamentals, New York: McGraw-Hill, 1988.

[11] A.D.Gosman, "State of the Art of Multi-Dimensional Modeling of Engine Reacting Flows," *Oil & Gas Science and Technology,* pp. 149-159, 1999.

[12] K.Kim and S.Kim, "Measurement of Dynamic TDC in SI Engines Using Microwave Sensor,Proximity Probe and Pressure Transducers," *SAE Paper,* p. 891823, 1989.

[13] A.S., Palipana, "CFD Modelling of Natural Gas Combustion in Spark Ignited Engines, PhDthesis, Loughborough University, UK.," 2000.

[14] J.Abraham, F.V.Bracco and R.D.Reitz, "Comparisons of Computed and Measured Premixed Charge Engine Combustion," *Combustion and Flame,* pp. 309-322, 1985.

[15] R.G.Abdel-Gayed, D.Bradley and A.K.C.Lau, "The Straining of Premixed Turbulent Flames," in *Twenty-Second Symposium (International) on Combustion,* 1989, pp. 731-738.

[16] J.B.Heywood, Internal Combustion Engine Fundamentals, New York: McGraw-Hill, 1988.

[17] D.Bradley, M.Z.Haq, R.A.Hicks, T.Kitagawa and Law, "Turbulent Burning Velocity," in *Burned Gas Distribution and Associated Flame Surface Definition*, Combustion and Flame, 2003, pp. 415-430.

[18] V. H. W.Malalasekera, An Introduction to Computational Fluid Dynamics; TheFinite Volume Method, 2nd Edition,, Pearson, 2007.

[19] T.Poinsot, D.Veynante and S.Candel, "Quenching Processes and Premixed TurbulentCombustion Diagrams," *Journal of Fluid Mechanics*, vol. 228, pp. 561-605, 1991.

[20] P.Bailly, D.Garreton, O.Simonin, P.Bruel and Cham, "Experimental and Numerical Study of a Premixed Flame Stabilized by a Rectangular Section Cylinder," in *Twenty-Sixth Symposium (International) on Combustion*, Combustion Institute, 1996, pp. 923-929.

[21] A.Chen, A.Veshagh and S.Wallace, "Intake Flow Predictions of a Transparent DI Diesel Engine," *SAE*, pp. 981-1020, 1998.

[22] M.Weclas, A.Melling and F.Durst, "Flow Separation in the Inlet Valve Gap of PistonEngines," *Progress in Energy and Combustion Science*, vol. 29, pp. 165-195, 1998.

[23] V.Zimont, W.Polifke, M. Bettelini and Weisenstei, "An Efficient Computational Modelfor Premixed Turbulent Combustion at High Reynolds Numbers Based on a Turbulent Flame," *Journal of Gas Turbines Power*, vol. 120, pp. 526-533, 1998.

[24] V.Zimont, "Gas Premixed Combustion at High Turbulence. Turbulent Flame Closure Model Combustion Model," *Experimental Thermal and Fluid Science*, vol. 21, pp. 179-186, 2000.

[25] T. D.Poinsot, Theoretical and Numerical Combustion, Edwards, ISBN: 1-930217-10-2, 2005.

[26] K.N.C.Bray, M.Chmapion and P.A.Libby, "Turbulent Reacting Flows (Borghi R. and Murthy S.N.B. Eds),," Berlin, Springer, 1989, pp. 541-563.

[27] R.S.Cant, S. Pope and K.N.C.Bray, "Modelling of Flamelet Surface-to-Volume Ratio in Turbulent Premixed Combustion," in *Twenty-Third Symposium (International) on Combustion*, The Combustion Institute, 1990, pp. 809-815.

[28] X.Zhao, R.D.Matthews and J.L.Ellzey, "Numerical Simulations of Combustion in SIEngines: Comparison of Fractal Flame Model to the Coherent Flame Model, International," 1994.

[29] H.G.Weller, S.Uslu, A.D.Gosman, R.R.Maly, B.Herw, R.eg and Heel, "Prediction o fCombustion in Homogeneous-Charge Spark-Ignition Engines," in *COMODIA International Symposium*, 1994.

[30] A.P.Watkins, S.P.Li and R.S.Cant, "Premixed Combustion Modelling for Spark engineApplications," *SAE*, no. 961190, 1996.

[31] N.Peters, "Length Scales in Laminar and Turbulent Flames," pp. 155-182, 1991.

[32] M.Barrera, in *Models de Combustion. Revue Generale de Thermique*, 1974, pp. 295-308.

[33] K.N.C.Bray, "Turbulent Flows in Premixed Reactants in Turbulent Reacting Flows," in *Topics in Applied Physics*, Springer Verlag, 1980, pp. 115-183.

[34] R.Borghi, "ise Au Point Sur La Structure Des Flames Turbulents," *Jounal de Chimie Physique,* pp. 361-370, 1984.

[35] F.A.Williams, "Combustion Theory, Benjamin Cummings.," 1985.

[36] N.Peters, "The Turbulent Burning Velocity for Large-Scale and Small-Scale Turbulence," *Journal of Fluid Mechanics,* vol. 384, pp. 107-132, 1999.

[37] Dr.R.A.C.P.Ranasinghe, "Large Eddy Simulation of Premixed Combustion in Spark Ignited Engines Using a Dynamic Flame Surface Density Model," 2013.

[38] N.Peters, "Turbulent Combustion, Cambridge University Press. ISBN: 0521660823.," 2000.

[39] V.Moureau, I.Barton, C.Angelberger and T.Poinsot, "Towards Large Eddy Simulation inInternal-Combustion Engines: Simulation of a Compressed Tumble Flow," *SAE,* 2004.

[40] J.Warnatz, "Resolution of gas phase and surface combustion chemistry into elementery reactions," in *21st symp on combustion*, 1992.

[41] J.Warnatz, Numerical simulation of combustion phenomena, New York: Springer, 1985.

[42] Lipatnikov, V. L.Zimont and N. A., "A Numerical Model of Premixed Turbulent Combustion of Gases," *Chem. Phys. Report,* vol. 14, no. 7, pp. 993-1025, 1995.

[43] F. B. a. K. J. S. V. L. Zimont, "Modelling Turbulent Premixed Combustion in the Intermediate Steady Propagation Regime," *Progress in Computational Fluid Dynamics,* vol. 1, no. 1, pp. 14-28, 2001.

[44] V.L.Zimont, "Theory of Turbulent Combustion of a Homogeneous Fuel Mixture at High Reynolds Numbers," *Combustion explosion and shock waves,* vol. 15, pp. 305-311, 1979.

[45] R.Borghi, "Turbulent Combustion Modelling," *Progress in energy and combustion science,* vol. 14, no. 1, 1988.

[46] V.P.Karpov, A. Lipatnikov and V.L.Zimont, *Archivum Combustionis,* vol. 4, no. 3-4, pp. 125-141, 1994.

[47] P.Moreau, "Turbulent £ame development in a high velocity premixed flow," in *15th Aero-space Science Meeting*, 1977.

[48] V.L.Zimont and A.N.Lipatnikov, "A numerical model of premixed turbulent combustion of gases," *Chem. Phys. Reports,* vol. 14, no. 7, pp. 993-1025, 1995.

[49] V. P.Karpov, A. N.Lipatnikov and V.L.Zimont, in *Twenty-Sixth Symposium (Int.) on Combustion*, *Combustion Institute*, Pittsburg, 1996.

[50] L.Maciocco and V. L.Zimont, in *20th Annual Meeting of the Italian Section of the Combustion Institute*, 1997.

[51] J.Ewald, "A Level Set Based Flamelet Model for the Prediction of Combustion in Homogeneous Charge and Direct Injection Spark Ignition Engines," Aachen University, 2006.

[52] J.Ewald and N.Peters, "On Unsteady Premixed Turbulent Burning Velocity Prediction in Internal Combustion Engines," *Proceedings of the Combustion Institute,* pp. 3051-3058, 2007.

[53] E.Schneider, A.Sadiki and J.Janicka, "Modeling and 3D-simulation of the kinetic effects in the post-flame region of turbulent premixed flames based on the G-equation approach," *Flow Turbul. Combust.*, vol. 75, pp. 191-216, 2005.

[54] Tan.Zhichao and R. D. Reitz, "An ignition and combustion model based on the level-set method for spark ignition engine multidimensional modeling," *Combustion and Flame*, vol. 145, pp. 1-15, 2006.

[55] N.Dekena, Peters and M, "Combustion Modeling with the G-Equation," *Oil Gas Sci. Technol.*, vol. 54, no. 2, pp. 265-270, 1999.

[56] L.Liang and R.Reitz, "Spark Ignition Engine Combustion Modeling Using a Level Set Method with Detailed Chemistry," *SAE Technical Paper*, p. 15, 2006.

[57] M.Keck, Metghalchi and J. C., "Burning velocities of mixtures of air with methanol, isooctane and indolene at high pressures and temperatures," *Combustion and Flame*, vol. 48, pp. 191-210, 1982.

[58] B. E.Poling, The properties of Gases and Liquids, McGraw-Hill, 2007.

[59] G.Soave, "Equilibrium constants from a modified Redlich-Kwong equation of state," *Chemical Engineering Science*, vol. 27, no. 06, pp. 1197-1203, 1972.

[60] Spalding, B. E. Launder and D. B., Lectures in Mathematical Models of Turbulence, Academic Press, 1972.

[61] G. v. E. B.Lewis, Combustion, flames and explosion of gases, New York: Academic press, 1961.

[62] G. S. J.C. Hilliard, fuel economy of road vehicles powered by spark ignition engines, London: Plenum press, New York.

[63] E.Sher, J. Ben-Yaish and T.Kravchik, "On the Birth of Spark Channels," *Combustion andFlame*, vol. 89, pp. 186-194, 1992.

[64] K. N. T. T. Y. U. M.Kono, "Mechanism of flame kernel formation produced by short duration sparks," in *The combustion institiue*, 1988.

[65] F. L. D.Bradley, "Spark ignition and the early stages of turbulent flame propagation," *Combustion and Flame*, vol. 69, pp. 71-93, 1987.

[66] S. J.R., Flows in internal combustion engines, Uzkan, 1983.

[67] J.Bardina, J.H.Ferziger and W.C.Reynolds, in *Improved Subgrid Scale Models for Large-Eddy Simulations*, AIAA, 1980, pp. 80-1357.

[68] K.N.C.Bray, "Studies of the Turbulent Burning Velocity, Proceedings of the Mathematical and Physical Science," pp. 315-335, 1990.

[69] N.Peters, "Laminar flamelet concepts in turbulent combustion," in *21st symposium on combustion*, 1986.

[70] R. H. R.R.Maly, "A Fundamental Model for Flame Kernel Formation in S.I. Engines," *SAE*, pp. 1947-1976, 1992.

[71] D.C.Haworth and K.Jansen, "Large Eddy Simulation on Unstructured Deforming Meshes towards Reciprocating IC Engines," *Computers & Fluids,* vol. 29, pp. 493 - 524, 2000.

[72] K.Sone, N.Patel and S.Menon, "Implementation of Large-Eddy Simulation in to the KIVAcode-Part1: Theory and Formulation, Technical Report," CCL-2001-008, Georgia Institute ofTechnology, Atlanta, GA., 2000a.

[73] K.Liu and D.C.Haworth, "Large Eddy Simulation for an Axisymmetric Piston-Cylinder Assembly with and without Swirl," *Flow Turbulence and Combustion,* vol. 85, pp. 297 - 307, 2010.

[74] H.Pitsch, "Large Eddy Simulation of Turbulent Combustion," *Annual Review of Fluid Mechanics,* vol. 38, pp. 453-482, 2006.

[75] K.Naitoh, T.Itoh and Y.Takagi, "Large Eddy Simulation of Premixed-Flame in Engine Basedon the Multi- Level Formulation and the Renormalization Group Theory," *SAE Paper,* p. 920590, 1992.

[76] K.Truffin and O.Colin, "A Spark Ignition Model for Large Eddy Simulation Based on an FSD Transport Equation (ISSIM-LES)," *Proceedings of the Combustion Institute,* vol. 33, no. 2, pp. 3097-3104, 2011.

[77] B.Enaux, V.Granet, O.Vermorel, C.Lacour, C.Pera, C. Angelberger and T.Poinsot, "LES Study of Cycle-to-Cycle Variations in a Spark Ignition Engine," *Proceedings of the Combustion Institute,* pp. 3115-3122, 2011.

[78] B.Franzelli, E.Riber, L. Gicquel and Poinsot, "Large Eddy Simulation of Combustion Instabilities in a Lean Partially Premixed Swirled Flame," *Combustion and Flame,* pp. 621-637, 2012.

[79] D.C.Haworth and T.J.Poinsot, "Numerical Simulations of Lewis Number Effects in Turbulent Premixed Flames," *Journal of Fluid Mechanics,* pp. 405-436, 1992.

[80] R.A.C.P.Ranasinghe, "Development of combustion models for RANS and LES applications in SI engines," R.A. Chathura Prasad Ranasinghe, 2013.

[81] A.A.Amsden and P.J.O'Rourke, "Implementation of a Conjugate Residual Iteration in theKIVA Computer Program, Technical Report," Los Alamos National Laboratory, 1986.

[82] K.N.C.Bray, P. and J.B.Moss, in *Flamelet Crossing Frequencies and Mean Reaction Rates in Premixed Turbulent Combustion,*, Combustion Science and technology, 1984, pp. 143-172..

[83] J.B.Heywood, "Combustion and its Modelling in Spark-Ignition Engines," in *International Symposium*, COMODIA, 1994.

[84] P, Rogallo R.S. and Moin, "Numerical Simulation of Turbulent Flows, Annual Review of FluidMechanics, 16:," 1984, pp. 99-137.

[85] C.J.Rutland, "Large Eddy Simulation for Internal Combustion Engines-A Review," *International Journal of Engine Research,* vol. 2, pp. 1-31, 2011.

[86] B.Geurts and D.Schoore, "Large-Eddy Simulation for Advanced Industrial Design: Proposal for a new COST Action, Technical Report," 2005.

[87] A.Uddin, C.Kato, Y.Yamade, N.Ohsima, T.Tanahasi and M. Miyauchi, "Large Eddy Simulation of Homogeneous Isotropic Turbulent Flow Using the Finite Element Method," *JSME International Journal,* vol. 49, pp. 102-114, 2006.

[88] H. Y. K.Niatoh, "Large eddy simulation of premixed-flame in engine based on the multi-level formulation and the renormalization group theory," *SAE,* p. 920590, 1992.

[89] M.Germano, U.Piomelli, P. Moin and W.H.Cabot, "A Dynamic Subgrid-Scale Eddy Viscosity Model," *Physics of Fluids,* pp. 1760-1765, 1991.

[90] Haworth, "Large-Eddy Simulation of In-Cylinder Flows, Oil & Gas Science and," (1999).

[91] E.Garnier, N.Adams and P.Sagaut, "Large Eddy Simulation for Compressible Flows," 2009.

[92] K.C., Brunt M.F.J. and Platts, in *Calculation of Heat Release in Direct Injection Diesel Engines*, SAE, 1999, pp. 1999-01-0187.

[93] S.Richard, O.Colin, O.Vermorel, A. D.Benkenida, C. Angelberger and Veynante, "Towards Large Eddy Simulation of Combustion in Spark Ignition Engines," *Proceedings of theCombustion Institute,* vol. 31, pp. 3059-3066, 2007.

[94] J.H.Ferziger, "Simulation of incompressible turbulent flows," *Journal of computational physics,* vol. 69, no. 1, pp. 1-48, 1987.

[95] J.Janicka and A.Sadiki, "Large Eddy Simulation for Turbulent Combustion," in *Proceedings of the Combustion Institute*, 2005, pp. 537-547.

[96] C.J.Rutland and S.Chumakov, "Dynamic Structure Models for Scalar Flux and Dissipation in Large Eddy Simulation," *AIAA*, vol. 42, no. 6, pp. 1132-1139, 2004.

[97] F.Nicoud and F.Ducros, "Subgrid-scale stress modelling based on the square of the velocity gradient tensor," *Flow turbulance and combustion,* vol. 62, pp. 183-200, 1999.

[98] F.Brusiani and G.M.Bianchi, "LES simulation of ICE non-reactive flows in fixed grids," *SAE paper,* 2008.

[99] C.Meneveau and J.Katz, "Scale-invariance and turbulence models for large-eddy simulation," *Annual revision of fluid mechanics,* vol. 32, no. 1, pp. 1-32, 2000.

[100] J.Smagorinsky, "General Circulation Experiments with the Primitive Equations, part I: TheBasic Experiment," *Monthly Weather Review,* vol. 91, no. 3, pp. 99-152, 1963.

[101] L.Celik and I.Yavuz, "Prediction of in-cylinder turbulence for IC engines," *Combustion science and technology,* vol. 153, no. 1, pp. 339-368, 2000.

[102] A.Amsden, "KIVA-3V: a block-structure KIVA program for engines with vertical or canted valves.," Los Alamos Report, 1997.

[103] J.Ferziger and M.Peric, "Computational Methods for Fluid Dynamics," Springer, 2002.

[104] S.Dinsdale, A. Roughton and N.Collings, "Length Scale and Turbulence Intensity Measurements in a Motored Internal Combustion Engine," *SAE,* p. 880380, 1988.

[105] W.Malalasekera, H.K.Versteeg, J.C.Henson, Jo and J. nes, "Calculation of Radiative HeatTransfer in Combustion Systems," *Clean Air,* vol. 3, pp. 113-143, 2002.

[106] V.Granet, O.Vermorel, C.Lacour, B.Enaux, V. Dugué and T.Poinsot, "Large-Eddy Simulation and Experimental Study of Cycle-To-Cycle Variations of Stable and Unstable Operating Points in a Spark Ignition Engine," *Combustion and Flame,* pp. 1562-1575, 2012.

[107] R., Maly, "State of the Art and Future Needs in S.I. Engine Combustion, Twenty-FifthSymposium (International) on Combustion, The Combustion Institute, 25:," 1994, pp. 111-124.

[108] N.Peters, Turbulent Combustion, Cambridge : Cambridge University Press, 2000.

[109] Misegades and P.Kent, "Extraction of Boundary Layer Characteristics from Fluent Results," 2005.

[110] M.Weclas, A.Melling and F.Durst, "Flow Separation in the Inlet Valve Gap of Piston," 1998.

[111] M.Jia and M.Xie, "A Chemical Kinetics Model of Iso-Octane Oxidation for HCCI Engine," in *Fuel*, 2006, pp. 2593-2604.

[112] M.Boger, D.Veynante, H. Boughanem and A.Trouvé, "Direct Numerical SimulationAnalysis of Flame Surface Density Concept for Large Eddy Simulation of Turbulent Premixed Combustion,," in *Proceedings of the Combustion Institute*, 1998, pp. 917-925.

[113] K.Naitoh, T.Itoh and Y.Takagi, "Large Eddy Simulation of Premixed-Flame in Engine Based on the Multi- Level Formulation and the Renormalization Group Theory," *SAE Paper,* vol. 920590, 1992.

[114] K.Lee, M.Yoon and M.Sunwoo, "A Study on Pegging Methods for Noisy Pressure signal," *Control Engineering Practice,* vol. 16, pp. 922-929, 2008.

[115] K. J.B.Moss, in *A Unified Statistical model for Premixed Turbulent Flame*, Acta Astronautica, 1977, pp. 291-319.

[116] F.C.Gouldin, "An Application of Fractals to Modelling Premixed Turbulent Flames," *Combustion and Flame,* pp. 249-266, 1987.